GEOPHYSICAL IMAGING:

AN OVERVIEW OF TWELVE COMMONLY EMPLOYED METHODS

Content

- What is "**Geophysical Imaging**"
- **Tabular** and **descriptive** summaries of twelve geophysical methods commonly used for highway-related investigations
- **Non-uniqueness** of interpretations
- **Ground truth**: constraint and verification

Geophysical Imaging

Geophysical imaging is used to map variations in the **physical properties** of the subsurface.

If constraints (e.g. borehole control) are available, **geophysical data** can be used to generate 1-D, 2-D or 3-D **geologic models** of the subsurface.

Twelve Commonly Employed Geophysical Methods

gravity	**magnetics**
resistivity	**induced polarization (IP)**
self potential (SP)	**electromagnetics**
refraction seismic	**seismic tomography**
reflection seismic	**cross-hole seismic**
ground-penetrating radar (GPR)	**multichannel analysis of surface waves (MASW)**

Gravity Method

↓

Measures spatial variations in the strength of the earth's gravitational field

↓

Maps spatial variations in the density of the subsurface

↓

Geologic model based on external constraints and mapped density variations

GRAVITY

Gravity is not uniform. It is a function of the mass of the earth, the mean radius of the earth, the angular velocity of the earth, the elevation of the observation location and surface topography in proximity to the observation location

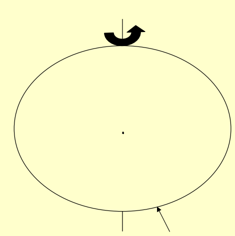

g directed towards center of mass

The mean value of gravity at the earth's surface is about 9.80 m/s^2.

Basic gravitational equation:

$$g = GM/R^2$$

G - gravitational constant
M - mass of the Earth
R - radius of Earth

GRAVITY

It also varies because of small-scale density variations within the earth's crust (variable depth to bedrock, presence of voids, lateral lithologic variations, etc.)

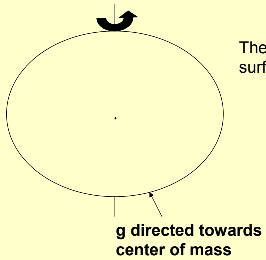

The mean value of gravity at the earth's surface is about 9.80 m/s^2.

Basic gravitational equation:

$$g = GM/R^2$$

G - gravitational constant
M - mass of the Earth
R - radius of Earth

GRAVITY

Gravimeters are generally used to measure relative variations in the earth's gravitational field.

Normally, we're only interested in variations that are caused by subsurface geological features of interest (variable depth to bedrock, presence of voids, etc.).

So we go to great lengths to isolate the residual gravity anomalies associated with the subsurface features of interest from those that are due to changes in latitude, elevation, etc.

We do this by applying reduction corrections and filters to our recorded field data, thereby isolating the anomalies caused by features of interest.

GRAVITY

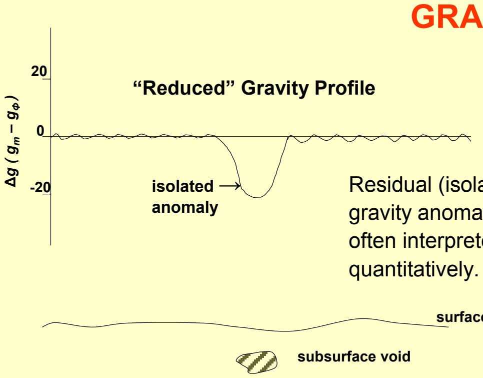

Residual (isolated) gravity anomalies are often interpreted quantitatively.

GRAVITY

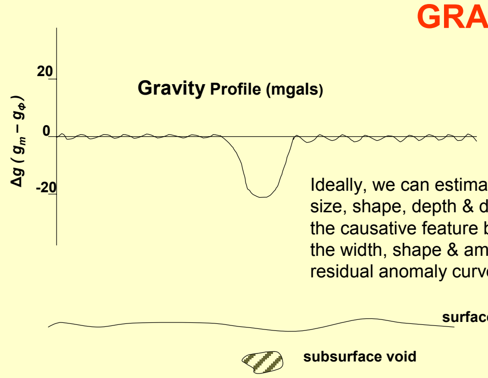

Ideally, we can estimate the size, shape, depth & density of the causative feature based on the width, shape & amplitude of residual anomaly curve.

GRAVITY

Residual gravity anomalies are generally interpreted quantitatively, and used to generate model images of the causative subsurface feature of interest.

The user must remember that the interpretation of gravity data is non-unique!

Physical constraints (depth, density contrasts, volume, etc.) are necessary to ensure the output model images are reasonable.

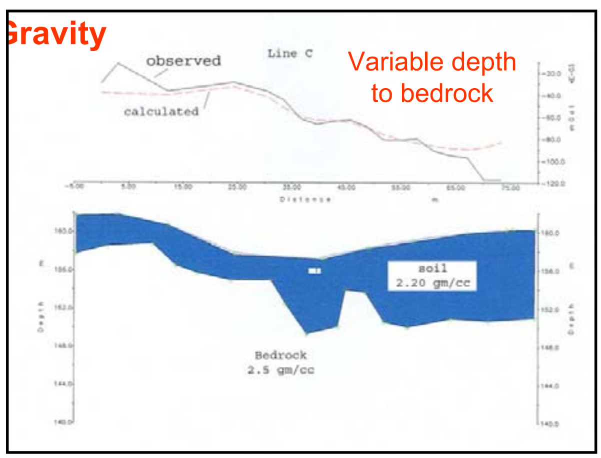

Gravity

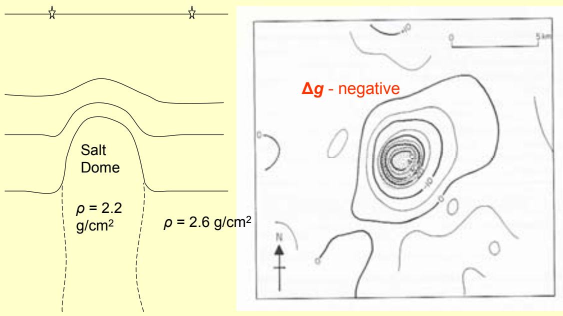

Gravity anomaly over the Grand Saline Salt Dome, Texas, USA

Strengths

- Gravimeters respond to density variations
- Data can be acquired anywhere gravimeter can be placed and survey data acquired
- Data can be interpreted quantitatively
- Model (depth, shape, size, density) of target can often be generated

Limitations

- Gravimeters respond to density variations – only!
- Very precise surveying control is required so that elevation and latitude corrections can be applied
- Gravity signatures are superposed!
- Inversions are non-unique!
- External constraints are required
- Signatures are superposed

Significant Applications

- Mapping air-filled cavities in kart terrain
- Mapping abandoned underground mines
- Estimating tonnage of ore
- Estimating depth to bedrock
- Determining volume of organic material in filled-in lakes or karst features
- Determining in-situ rock/soil densities
- Determining volumes of available fill

TWELVE COMMONLY EMPLOYED GEOPHYSICAL METHODS

gravity	**magnetics**
resistivity	**induced polarization (IP)**
self potential (SP)	**electromagnetics**
refraction seismic	**seismic tomography**
reflection seismic	**cross-hole seismic**
ground-penetrating radar (GPR)	**multichannel analysis of surface waves (MASW)**

Magnetic method

↓

Measures spatial variations in the strength of the earth's total magnetic field ($\mathbf{B}_T$)

↓

Maps spatial variations in the concentration of magnetically-susceptible material in the subsurface

↓

Geologic model based on external constraints and variable concentration of magnetically-susceptible material

MAGNETIC METHOD

The earth's **primary magnetic field** (B_E) is caused by the circulation of charged particles in coupled convective cells within the outer, fluid, part of the earth's core.

To a certain extent, the earth's **primary magnetic field** (B_E) can be modeled as though it was generated by a large dipole bar magnet located in its interior.

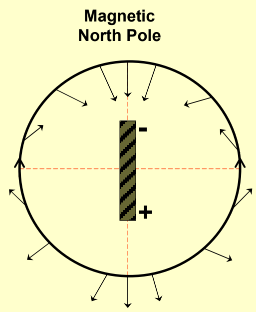

MAGNETIC METHOD

The earth's **primary magnetic field** (**B_E**) is not nearly as uniform as its gravitational field (~25,000 nT in equatorial regions and ~70,000 nT at the poles).

B_E also varies in direction, being perpendicular to the earth's surface at the poles and parallel at the equator.

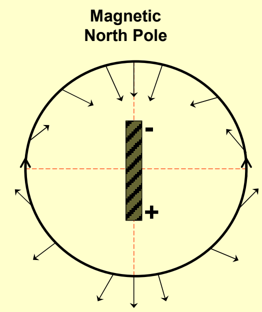

MAGNETIC METHOD

The **total magnetic field (B_T)** at any observation point on the earth's surface is the sum of the earth's **primary magnetic field (B_E)** and any proximal **secondary magnetic fields (ΔB)**.

The **secondary magnetic fields (ΔB)** are generated by materials that have become slightly magnetized in the presence of the earth's magnetic field (mostly iron-bearing or magnetite-bearing material).

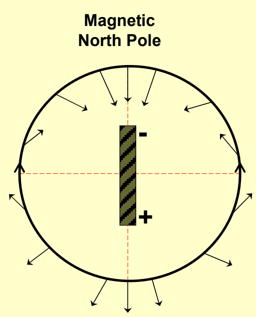

$$\Delta B = B_T - B_E$$

MAGNETIC METHOD

Magnetometers are designed to measure the total magnetic field of the earth **(B_T)**.

Normally, we're only interested in the secondary magnetic fields (**ΔB)** associated with subsurface features of interest (buried pipelines, steel drums, etc.).

So we isolate and interpret spatial variations these secondary magnetic fields (**ΔB**), where:

$$\Delta B = B_T - B_E$$

Secondary magnetic fields (**ΔB**) associated with man-made iron-based materials are usually very easy to identify, because they are relatively high magnitude and "stand out".

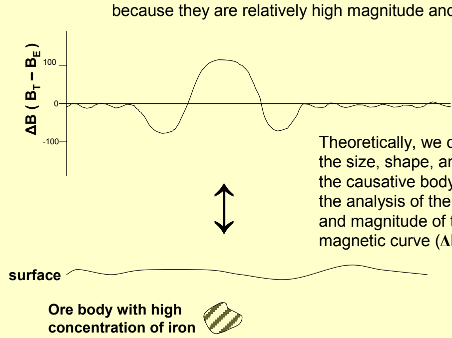

Theoretically, we can estimate the size, shape, and depth of the causative body based on the analysis of the width, shape, and magnitude of the residual magnetic curve (**ΔB**).

However, secondary magnetic field anomalies (**ΔB**). are usually interpreted qualitatively – as opposed to quantitatively. This is because secondary magnetic field anomalies are often very complex.

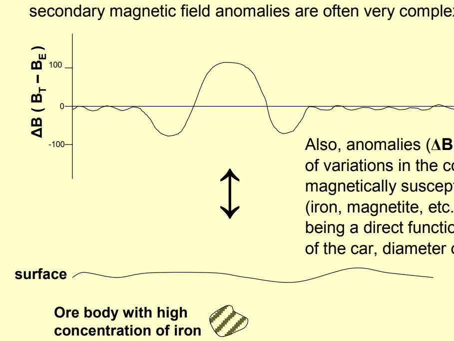

Also, anomalies (**ΔB**). are indicative of variations in the concentration of magnetically susceptible material (iron, magnetite, etc.) as opposed to being a direct function of the make of the car, diameter of pipe, etc.

MAGNETIC METHOD

The magnetic signature (ΔB) of the sulfide body is a function of magnetite concentration.

Vertical field ground magnetic anomaly profile over a massive sulfide ore body. The shaded area represents the location of the ore body inferred from EM measurements.

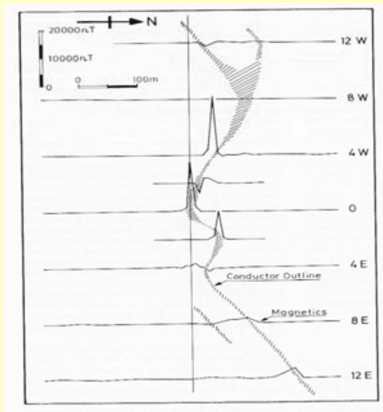

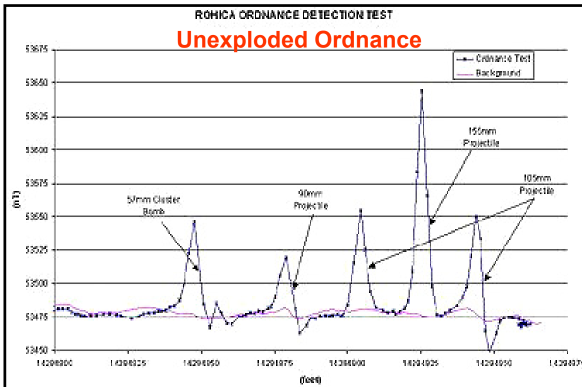

The magnetic signature of man-made material is a function of iron concentration.

Strengths

- Magnetometers respond to the presence and concentration of magnetically-susceptible material (almost exclusively man-made iron-based materials or magnetite)
- Data can be acquired rapidly and inexpensively (1-person crew)
- Data are usually interpreted qualitatively and therefore require minimal post-acquisition processing
- Precise surveying is not required

Limitations

- Magnetometers respond to presence and concentration of magnetically-susceptible material only!
- Magnetic signatures are superposed!
- Anomalies are generally very complex and may be extremely difficult to interpret quantitatively
- It is often difficult to generate a realistic model of the target (but usually no one cares!!!)
- Interpretations are non-unique
- External constraints are required

Significant Applications

- Locating sand and gravel deposits (that contain heavy minerals)
- Locating underwater ferromagnetic objects
- Locating fault contacts
- Regional geologic mapping
- Locating buried well casings
- Locating buried drums, pipelines and other ferromagnetic objects
- Archeological investigations
- Rebar in concrete
- Locating/mapping landfills

TWELVE COMMONLY EMPLOYED GEOPHYSICAL METHODS

gravity	**magnetics**
resistivity	**induced polarization (IP)**
self potential (SP)	**electromagnetics**
refraction seismic	**seismic tomography**
reflection seismic	**cross-hole seismic**
ground-penetrating radar (GPR)	**multichannel analysis of surface waves (MASW)**

Resistivity Method

↓

Measures spatial variations in potential differences in response to induced current

↓

Map spatial variations in the resistivity of the subsurface

↓

Geologic model based on external constraints and mapped variations in subsurface resistivity

RESISTIVITY METHOD

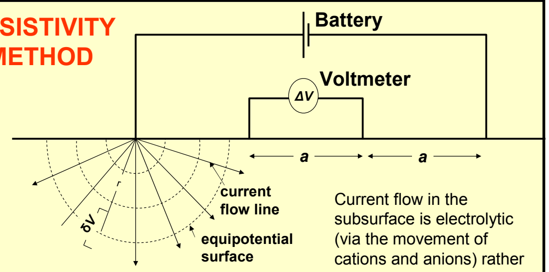

Current flow in the subsurface is electrolytic (via the movement of cations and anions) rather than electronic

Resistivity surveying is relatively straightforward. A known **AC current (I)** is input into the ground using a battery or a generator, and **potential differences** (**ΔV**) are measured using a voltmeter.

RESISTIVITY METHOD

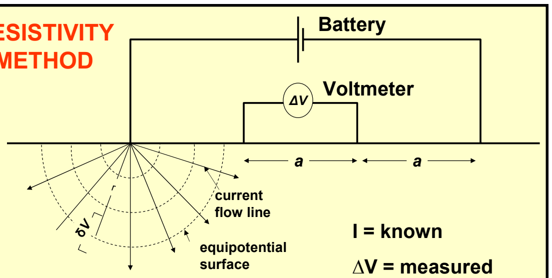

I = known

ΔV = measured

The **resistance (R)** of the subsurface can be calculated using the well-known formula:

$$\Delta V = IR$$

RESISTIVITY METHOD

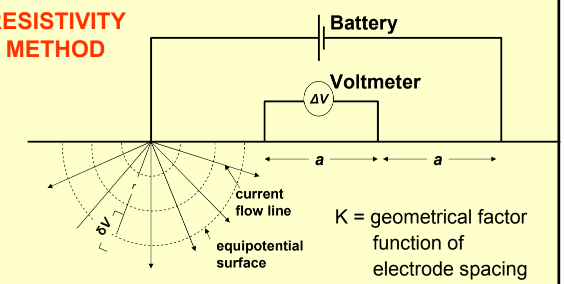

K = geometrical factor function of electrode spacing

The **resistivity** (**ρ**) of the subsurface can then be calculated using the formula:

$$\rho = K(\Delta V/I)$$

The **resistivity** (**ρ**) of the subsurface at different locations and at different depths can be measured by shifting the array laterally and varying the electrode spacing.

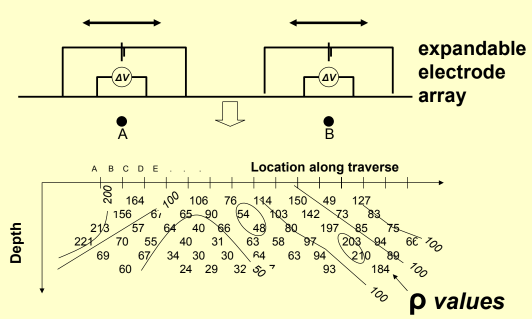

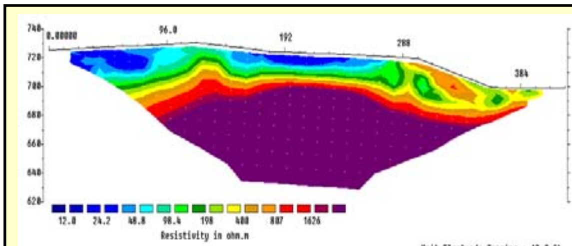

Resistivity (**ρ**), like density, is an intrinsic property of a material.

ρ is mostly a function of lithology, porosity, clay content, permeabilty and fluid saturation salinity.

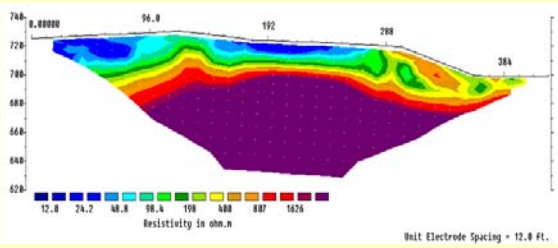

Hence, a 2-D resistivity **(ρ)** profile can often be transformed into a realistic 2-D geologic/hydrologic model of the subsurface.

The accuracy of such models will be increased if external constraints (borehole control) is available.

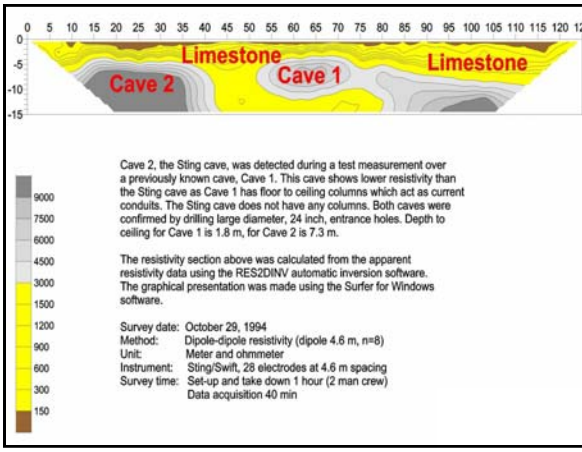

Strengths

- 1-D, 2-D or 3-D geologic/hydrologic images of the subsurface
- interpretations, if constrained, can be remarkably accurate
- reconaissance tool used to optimally locate exploratory boreholes
- cost-effective means of establishing control between boreholes
- acquisition is relatively straightforward
- processing is automated
- interpretation is generally relatively straightforward (if constrained)

Limitations

- relatively slow, as electrodes must be coupled to ground surface
- coupling can be a problem (rock or dry sand)
- limited depth penetration (typically 100 ft)
- resolution diminishes with depth
- depth to top of void $\leq$ diameter
- cultural features can create problems (metal fences, buried pipelines, electric power lines, etc.)
- all you ever end up with is an interpretation
- interpretations are non-unique
- ground truth is needed to constrain interpretations

Significant Applications

- variable depth to bedrock
- variable depth to water table
- variations in porosity,
- variations in salinity
- locate voids, abandoned mines and tunnels
- mapping clay layers and lenses
- mapping sand and gravels
- differentiate/map rock units
- mapping faults, fractures, weathered zones
- mapping contaminants
- mapping lithologic contacts

TWELVE COMMONLY EMPLOYED GEOPHYSICAL METHODS

gravity	**magnetics**
resistivity	**induced polarization (IP)**
self potential (SP)	**electromagnetics**
refraction seismic	**seismic tomography**
reflection seismic	**cross-hole seismic**
ground-penetrating radar (GPR)	**multichannel analysis of surface waves (MASW)**

<u>Time Domain</u> Induced Polarization (IP)

↓

Measures spatial variations in polarization voltages after induced current is terminated

↓

Map spatial variations in the capacitive properties of the subsurface

↓

Geologic model based on external constraints and mapped variations in electrical capacitance

TD IP METHOD

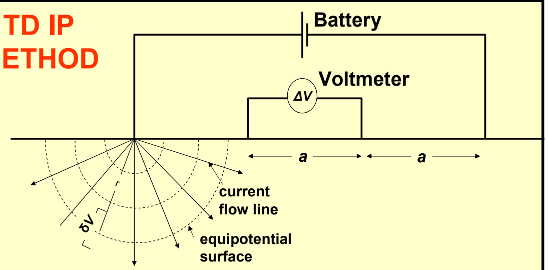

When DC current flows through ground under an external voltage, ions become effectively "log-jammed" in narrow pore throats and in pore throats blocked by clays and metallic minerals.

TD INDUCED POLARIZATION

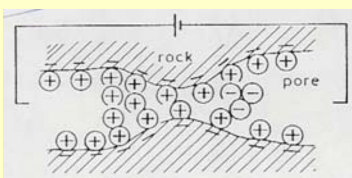

Membrane polarization

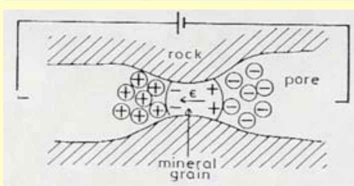

Electrode polarization

TD INDUCED POLARIZATION

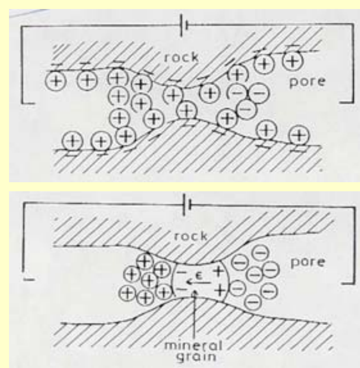

When the external voltage source is shut off, current continues to flow as these ions gradually move to re-establish equilibrium, and potential differences (**ΔV**) continue to be recorded by the voltmeter.

TD INDUCED POLARIZATION

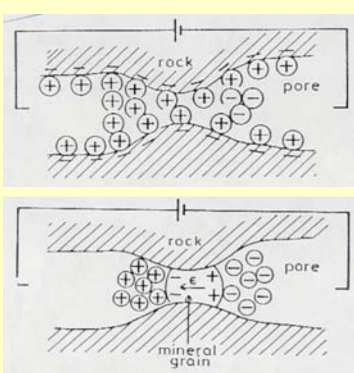

The magnitude and duration of the potential differences (**ΔV**) measured after the external voltage source is shut off, provide an estimate of combined clay and metallic mineral concentration in the subsurface.

TD INDUCED POLARIZATION

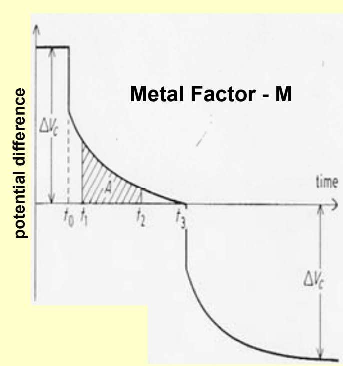

At time t_0 the current is switched off. The measured potential difference, after an initial large drop from the steady state value ΔV_c, decays gradually to zero. *"A"* represents the area under the decay curve for the time increment $t_1 - t_2$.

IP and resistivity data can be acquired essentially simultaneously, and for different locations/depths by simply shifting the array laterally and varying the electrode spacing.

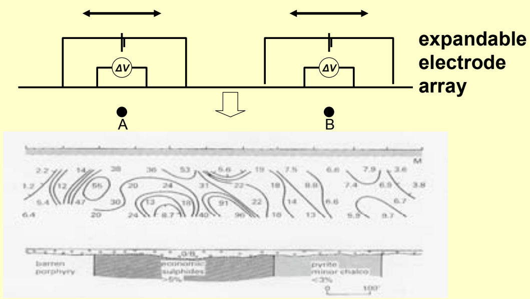

The **electrical capacitance** of the subsurface at different locations and at different depths can be measured by simply shifting the array laterally and varying the electrode spacing.

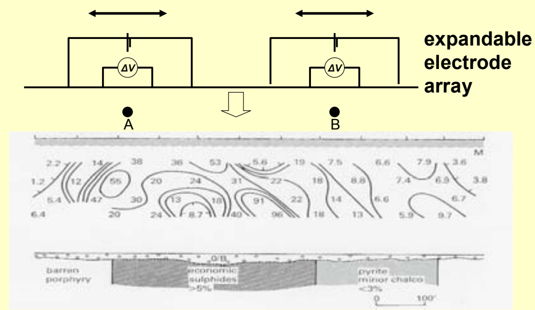

Variations in electrical capacitance can be used to estimate variations in clay and/or metallic mineral concentration in the subsurface.

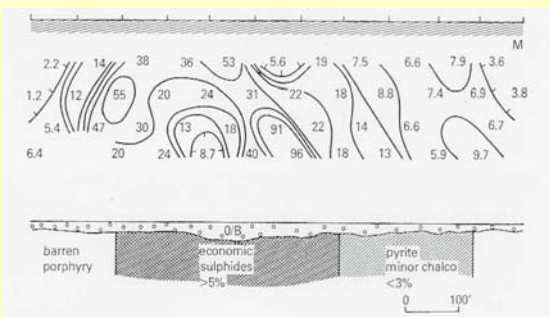

Strengths

- IP method measures variations in the electrical capacitance of the subsurface
- Can be used to estimate spatial variation in clay and/or metallic mineral concentration
- Can be acquired simultaneously with resistivity data
- IP data can be acquired in time and/or frequency domain
- Processing is automated
- Interpretations are generally relatively straightforward (if constrained)
- Interpretations complement and constrain resistivity data

Significant Limitations

- Data acquisition relatively slow, as electrodes must be coupled to ground surface
- Coupling of electrodes can be a problem (rock or dry sand)
- Limited depth penetration (typically 100 ft)
- Resolution diminishes with depth
- All you ever end up with is an interpretation
- Interpretations are non-unique
- Ground truth is needed to constrain interpretations

Significant Applications

- estimating clay content
- estimating metallic mineral content
- complements/constrains resistivity control (re: nature of conductive sources)

Note

IP data can also be acquired in the frequency domain.

TWELVE COMMONLY EMPLOYED GEOPHYSICAL METHODS

gravity	**magnetics**
resistivity	**induced polarization (IP)**
self potential (SP)	**electromagnetics**
refraction seismic	**seismic tomography**
reflection seismic	**cross-hole seismic**
ground-penetrating radar (GPR)	**multichannel analysis of surface waves (MASW)**

Self (Spontaneous) Potential (SP)

↓

Measures spatial variations in naturally occurring potential differences (ΔV)

↓

Maps spatial variations in subsurface current flow due to percolating water and/or oxidization/reduction

↓

Groundwater flow paths or location of metallic mineral body

SP

Current flow in the subsurface is electrolytic (via the movement of cations and anions) rather than electronic (via the movement of electrons).

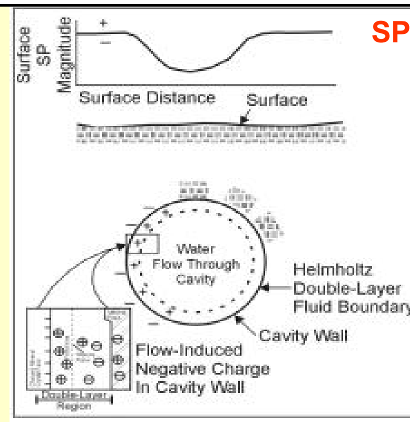

SP

So it should come as no surprise that, when cations and anions move at dissimilar speeds as water flows through the sub-surface, natural current are created. Electrokinetic, or streaming, potential is due to the flow of a fluid with certain electrical properties passing through a pipe or porous medium with different electrical properties.

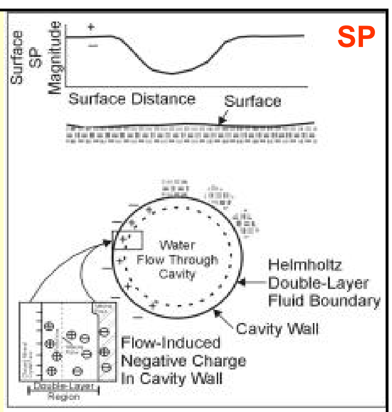

SELF POTENTIAL

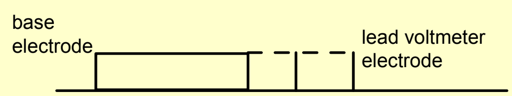

Such natural currents generate natural potentials (referred to as **Self** or **Spontaneous Potentials**) which can be measured using a precise voltmeter. (The voltmeter is actually used to measure natural potential differences between a inert base location and all other test sites.)

SELF POTENTIAL

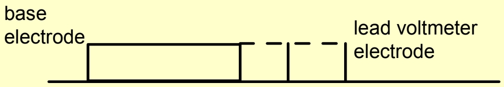

Springs, underground streams, seepage through earth fill dams, etc., typically generate measurable and interpretable SP anomalies.
Typically, recharge areas are characterized by negative potential differences, whereas discharge areas are characterized by positive potential differences.

SP

SP anomalies are also generated by natural oxidization/ reduction processes. These are most typically caused by mineralized bodies that straddle the water table. In short summary, the ions in the pore fluid below the water table are oxidized and release electrons. These electrons flow vertically through the conductor to a point above the water table where they cause the reduction of electrolytes.

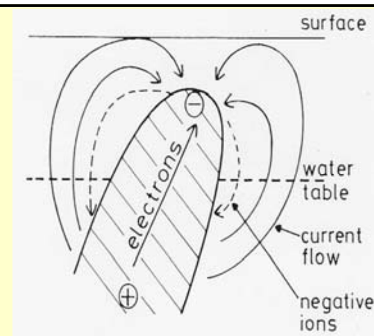

SELF POTENTIAL

A circuit thus exists in which the current is carried electrolytically in the pore fluids and electronically in the body so that the top of the body acts as a negative terminal.

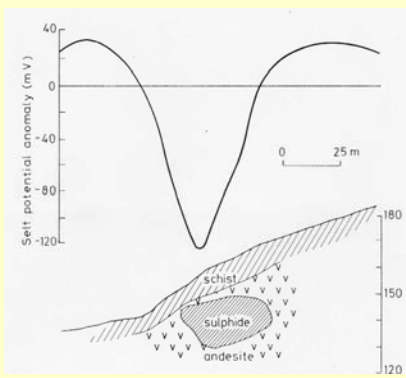

SELF POTENTIAL

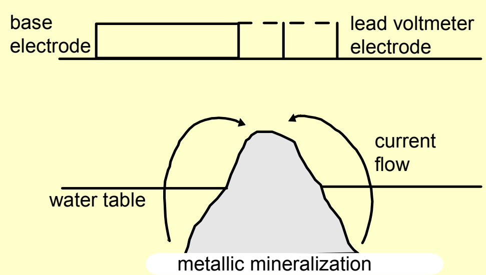

Resultant spontaneous potential differences can be measured at the earth's surface (using a voltmeter), and can alert us to the presence of metallic mineralization.

Strengths

- SP tool measures natural potential differences
- One or two person crew
- Relatively rapid and inexpensive
- Great reconnaissance tool
- Only geophysical tool that responds to flowing water!!
- Also responds to natural oxidization/ reduction

Limitations

- Qualitative interpretations
- Interpretations are non-unique
- Anomalies (undesired signal or noise) can be due corroding metal
- Shallow depth of investigation
- Ore body must straddle water table

Significant Applications

- Locating shallow mineralized ore bodies
- Only geophysical technique that responds directly to flowing water
- Locating zones of seepage through earth fill dam, flow through fractures, springs, etc.

Method	Measured Parameter	Physical Property
Gravity	spatial variations in the strength of the gravitational field of earth	bulk density
Magnetic	spatial variations in the strength of the earth's geomagnetic field	magnetic susceptibility & remnant magnetization
Electrical Resistivity	earth resistance	electrical conductivity
Induced Polarization	polarization voltages or frequency dependent ground resistance	electrical capacitance
Self Potential	electrical potentials	electrical conductivity
EM	response to EM radiation	electrical conductivity and inductance

TWELVE COMMONLY EMPLOYED GEOPHYSICAL METHODS

gravity	**magnetics**
resistivity	**induced polarization (IP)**
self potential (SP)	**electromagnetics**
refraction seismic	**seismic tomography**
reflection seismic	**cross-hole seismic**
ground-penetrating radar (GPR)	**multichannel analysis of surface waves (MASW)**

Electromagnetic methods (EM)

↓

Measure the earth's response to EM radiation

↓

Map spatial variations in the conductivity of the subsurface

↓

Geologic model based on external constraints and mapped conductivity variations

ELECTROMAGNETIC METHODS

When alternating electric current is passed through a coiled wire conductor, electromagnetic radiation (primary field) of the same frequency is emitted from the coil.

When this electromagnetic energy passes through a subsurface conductor, a secondary AC current is induced in the conductor.

This secondary current flow causes the conductor to emit secondary electromagnetic radiation.

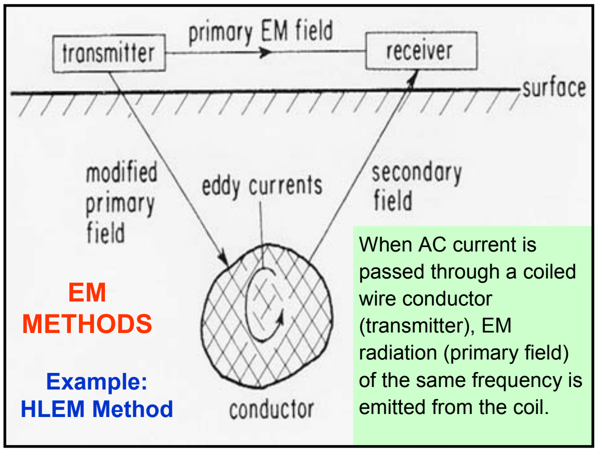

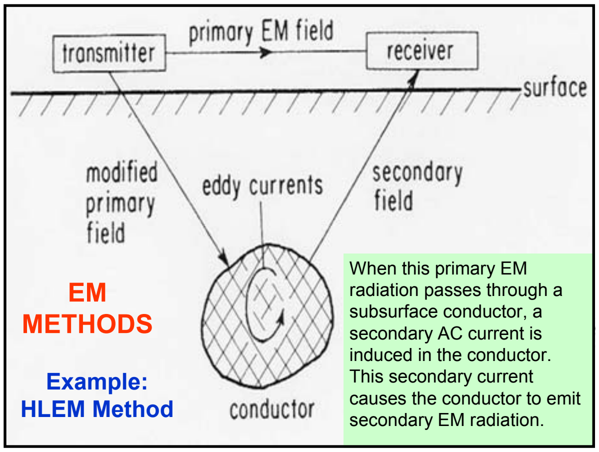
transmitter
primary EM field
receiver
surface
modified primary field
eddy currents
secondary field
conductor
EM METHODS
Example: HLEM Method
When this primary EM radiation passes through a subsurface conductor, a secondary AC current is induced in the conductor. This secondary current causes the conductor to emit secondary EM radiation.

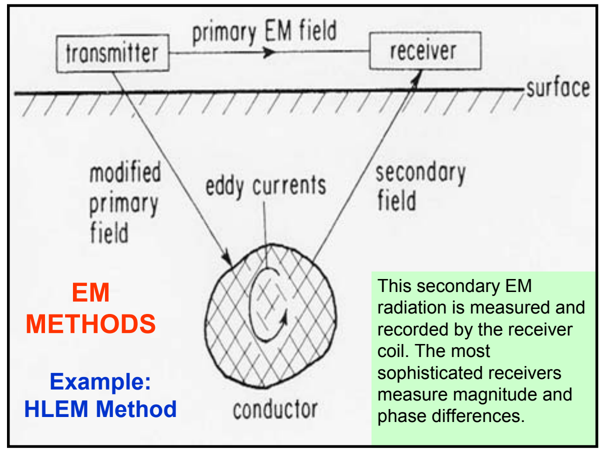
transmitter
primary EM field
receiver
surface
modified primary field
eddy currents
secondary field
conductor
EM METHODS
Example: HLEM Method
This secondary EM radiation is measured and recorded by the receiver coil. The most sophisticated receivers measure magnitude and phase differences.

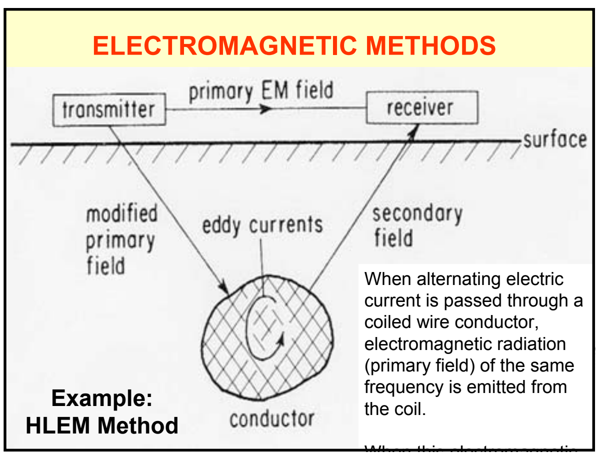
ELECTROMAGNETIC METHODS
transmitter
primary EM field
receiver
surface
modified primary field
eddy currents
secondary field
conductor
Example: HLEM Method
When alternating electric current is passed through a coiled wire conductor, electromagnetic radiation (primary field) of the same frequency is emitted from the coil.

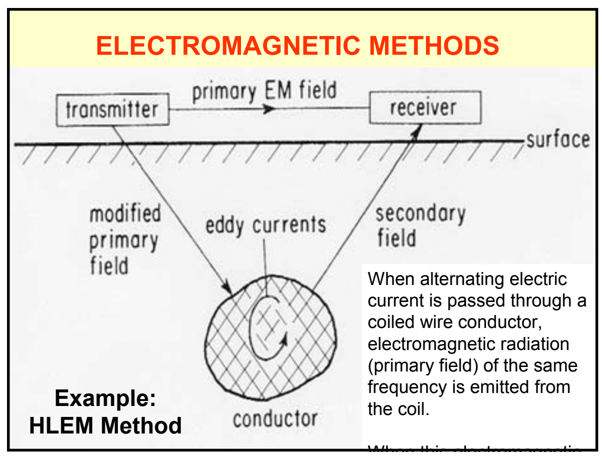
ELECTROMAGNETIC METHODS
transmitter
primary EM field
receiver
surface
modified primary field
eddy currents
secondary field
conductor
Example: HLEM Method
When alternating electric current is passed through a coiled wire conductor, electromagnetic radiation (primary field) of the same frequency is emitted from the coil.

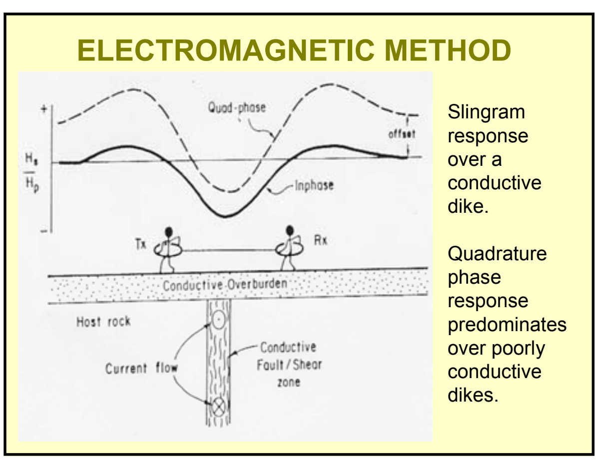
ELECTROMAGNETIC METHOD
Quad-phase
offset
Inphase
Tx
Rx
Conductive Overburden
Host rock
Current flow
Conductive Fault / Shear zone
Slingram response over a conductive dike.
Quadrature phase response predominates over poorly conductive dikes.

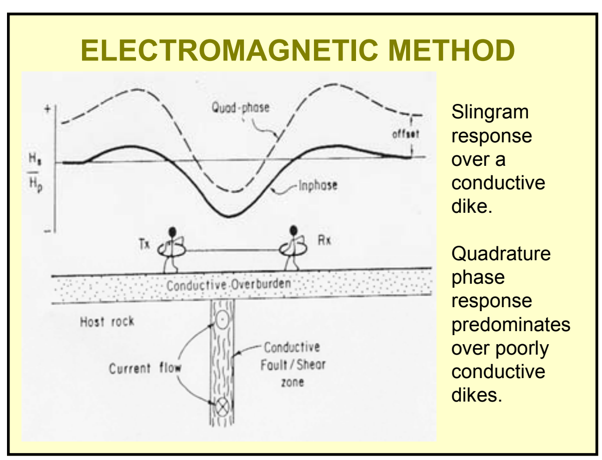
ELECTROMAGNETIC METHOD
Quad-phase
offset
Inphase
Tx
Rx
Conductive Overburden
Host rock
Current flow
Conductive Fault / Shear zone
Slingram response over a conductive dike.
Quadrature phase response predominates over poorly conductive dikes.

ELECTROMAGNETIC METHOD

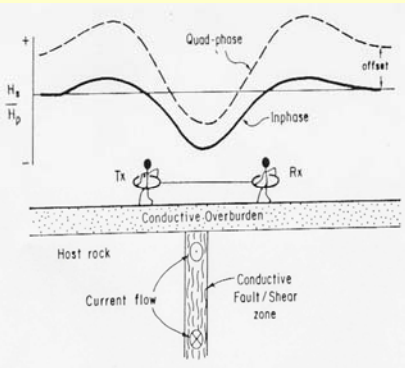

The magnitude and phase of the secondary EM field (relative to primary EM field) is a function of the nature of the subsurface conductor (size, depth, areal extent and conductivity, etc.).

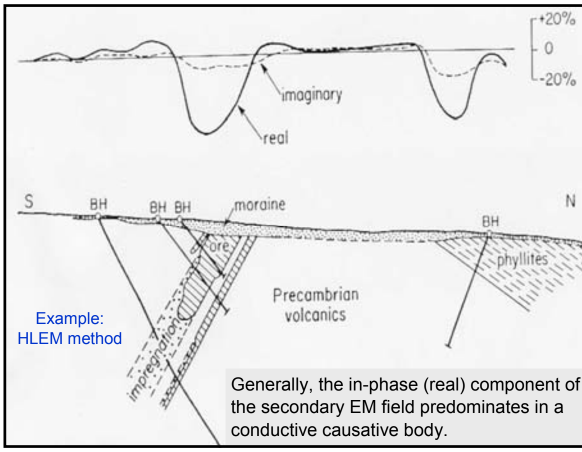

Example: HLEM method

Generally, the in-phase (real) component of the secondary EM field predominates in a conductive causative body.

Strengths

- EM tools measure “conductivity”
- Tool does not need to be coupled to earth
- Data can be acquired simply, rapidly and inexpensively (compared to resistivity)
- Multiple tools available (simple to sophisticated)
- 1-D, 2-D or 3-D conductivity images of subsurface
- Geologic/hydrologic models can be generated
- interpretations, if constrained, can be remarkably accurate
- reconaissance tool, used to optimally locate exploratory boreholes
- cost-effective means of establishing control between boreholes

Limitations

- resolution diminishes with depth
- cultural features can create problems (metal fences, buried pipelines, electric power lines, etc.)
- all you ever end up with is an interpretation
- interpretations are non-unique
- ground truth is needed to constrain interpretations

Significant Applications

- variable depth to bedrock
- variable depth to water table
- variations in porosity and water saturation
- variations in salinity
- mapping clay layers and lenses
- differentiate/map rock units
- mapping faults, fractures, weathered zones
- mapping lithologic contacts
- Estimating porosity clay content
- Locating buried utilities
- Mineral exploration
- Mapping contaminant plumes

Note

EM data can also be acquired in the time domain.

TWELVE COMMONLY EMPLOYED GEOPHYSICAL METHODS

gravity	**magnetics**
resistivity	**induced polarization (IP)**
self potential (SP)	**electromagnetics**
refraction seismic	**seismic tomography**
reflection seismic	**cross-hole seismic**
ground-penetrating radar (GPR)	**multichannel analysis of surface waves (MASW)**

Ground penetrating radar (GPR)

↓

Measures travel times and magnitudes of reflected pulses of EM radiation

↓

2-D image of subsurface (reflection magnitude plotted on 2-D profile with time and distance axis)

↓

2-D or 3-D geologic models constrained by ground truth

GROUND PENETRATING RADAR

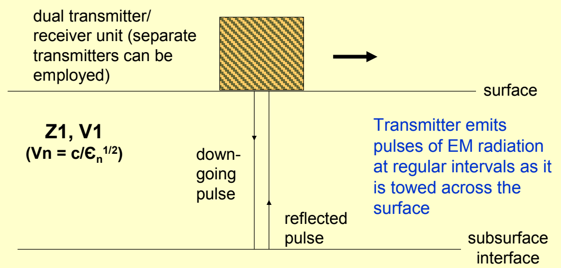

Rc = $(\epsilon_{n+1}^{1/2} - \epsilon_n^{1/2})/(\epsilon_{n+1}^{1/2} + \epsilon_n^{1/2})$

TWTT = **2 Z1/V1**

GROUND PENETRATING RADAR

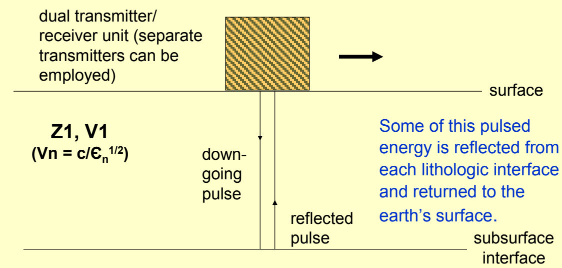

Rc = $(\epsilon_{n+1}^{1/2} - \epsilon_n^{1/2})/(\epsilon_{n+1}^{1/2} + \epsilon_n^{1/2})$

TWTT = **2 Z1/V1**

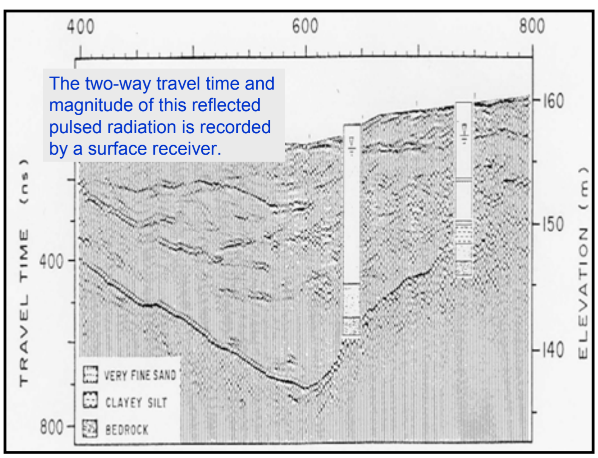

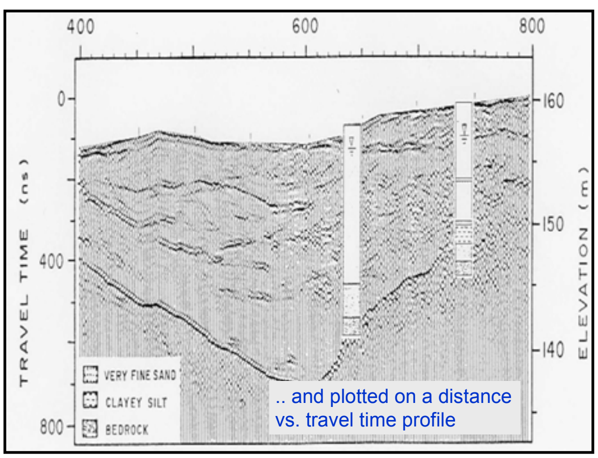

GROUND PENETRATING RADAR

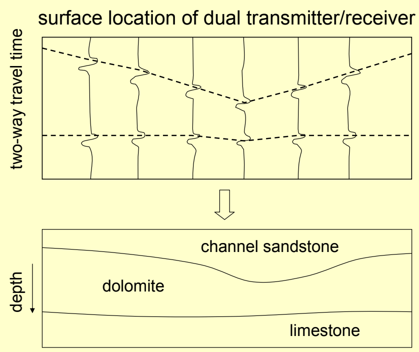

If the velocity with which the EM radiation travels can be determined, and if ground truth is available (as a constraint), a GPR profile can be transformed into a geologic model.

Strengths

- Tool measures travel times and magnitudes of reflected pulsed EM
- Tool does not need to be coupled to earth
- Relatively rapid data acquisition (compared to resistivity and seismic refraction)
- moderate to very high resolution (relative to other methods; decreases with depth)
- Very reliable 2-D and 3-D geologic models can be generated (if constrained)

Limitations

- Limited depth of investigation (<30 m)
- EM radiation does not penetrate moist clays
- Post-acquisition processing may be required
- Interpretations are non-unique
- External constraints are required

Significant Applications

- Mapping lithology
- Mapping top of groundwater
- Mapping contaminant plumes
- Locating rebar in concrete
- Mapping water depths
- Locating cavities beneath pavement
- Bridge deck integrity studies
- Locating utilities
- Archeological investigations

TWELVE COMMONLY EMPLOYED GEOPHYSICAL METHODS

gravity	**magnetics**
resistivity	**induced polarization (IP)**
self potential (SP)	**electromagnetics**
refraction seismic	**seismic tomography**
reflection seismic	**cross-hole seismic**
ground-penetrating radar (GPR)	**multichannel analysis of surface waves (MASW)**

Reflection seismic

↓

Measures travel times & magnitudes of reflected acoustic energy

↓

2-D image of subsurface (reflection magnitude plotted on 2-D profile with time and distance axis)

↓

2-D or 3-D geologic models constrained by ground truth

REFLECTION SEISMIC

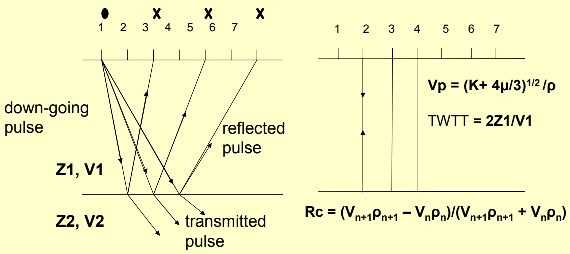

An acoustic pulse is generated by a surface source. Some of this downgoing energy is reflected at each lithologic interface in the subsurface (function of contrast in acoustic impedance).

REFLECTION SEISMIC METHOD

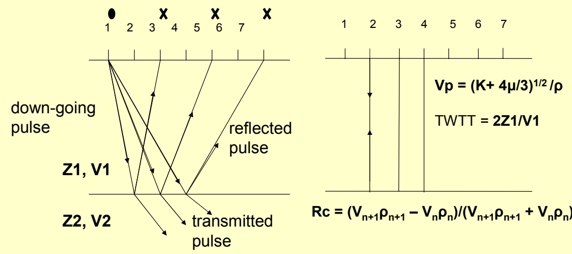

The two-way travel time and magnitude of the reflected pulses are recorded by multiple surface receivers (geophones). It is standard practice to manipulate data (during processing) so that each pulse appears to have had a vertical travel path.

REFLECTION SEISMIC

Magnitudes and average velocities of the reflected pulses are a function of the density and acoustic velocity of the subsurface layers.

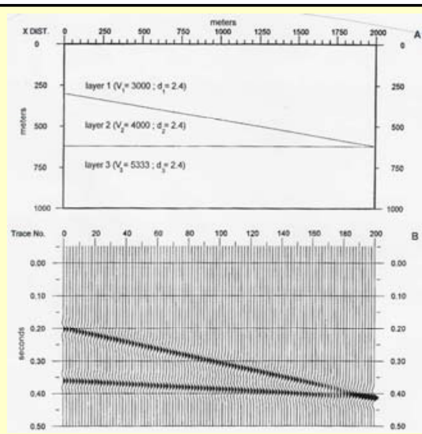

REFLECTION SEISMIC

If acoustic velocities can be determined, 2-D reflection profiles can be converted into 2-D lithology/ structure sections. (3-D data are also acquired.)

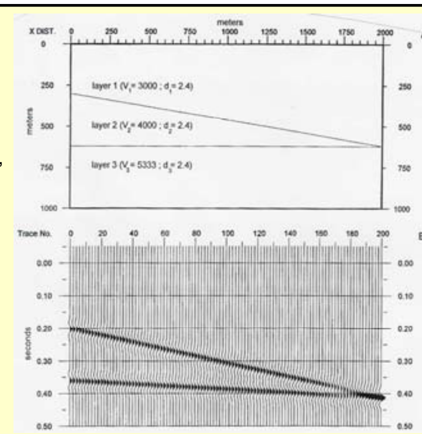

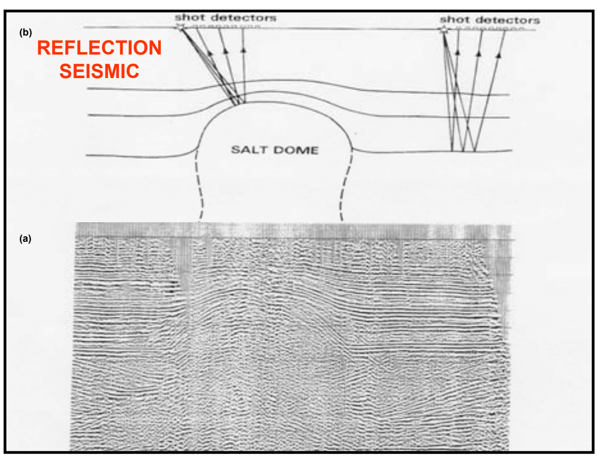

Strengths

- Tool measures travel times and magnitudes of reflected pulsed acoustic pulse
- Shear and/or compressional wave velocities can be measured
- Responds to changes in acoustic impedence
- Depth of investigation (shallow-deep; 50 ft - 20,000 ft)
- Limited resolution (layer thickness >10 ft)
- Very reliable 2-D and 3-D geologic models can be generated (if constrained)

Limitations

- Geophones need to be coupled to the earth
- Depth of investigation (shallow-deep; 50 ft - 20,000 ft)
- Limited resolution (layer thickness >10 ft)
- Interpretations are non-unique
- External constraints are required
- Relatively slow and expensive
- Processing requires considerable expertise
- doesn't work well in "acoustically" noisy areas
- all you ever end up with is an interpretation

Significant Applications

- Mapping lithology and subsurface structures (shallow depths to depths on the order of multiple km)
- Mapping top of groundwater
- Mapping top of bedrock
- Locating low velocity layers
- Mapping abandoned underground mines
- Locating over-pressured shales/sandstones
- Determining in-situ engineering properties
- Shear and/or compressional wave velocities can be measured

Applications (continued)

- Literally billions of dollars are spent each year acquiring/processing/interpreting reflection seismic data in support of oil and gas exploration!

TWELVE COMMONLY EMPLOYED GEOPHYSICAL METHODS

gravity	**magnetics**
resistivity	**induced polarization (IP)**
self potential (SP)	**electromagnetics**
refraction seismic	**seismic tomography**
reflection seismic	**cross-hole seismic**
ground-penetrating radar (GPR)	**multichannel analysis of surface waves (MASW)**

Refraction seismic

↓

Measures travel times & magnitudes of critically refracted acoustic energy

↓

2-D image of subsurface (reflection magnitude plotted on 2-D profile with time and distance axis)

↓

2-D (or 3-D) geologic models constrained by ground truth

Refraction Seismic

Conventional refraction seismic surveying is relatively straightforward. An acoustic source is discharged at the earth's surface.

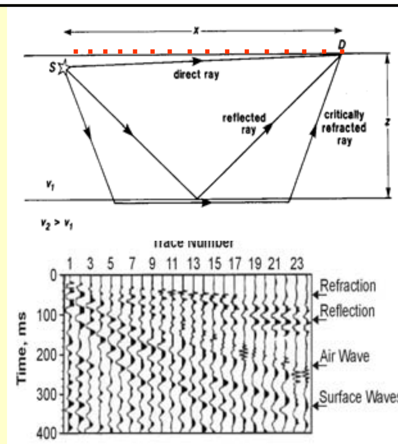

Energy that travels is directly to the sensors or is critically refracted from prominent lithologic interfaces is recorded by sensors placed at multiple locations.

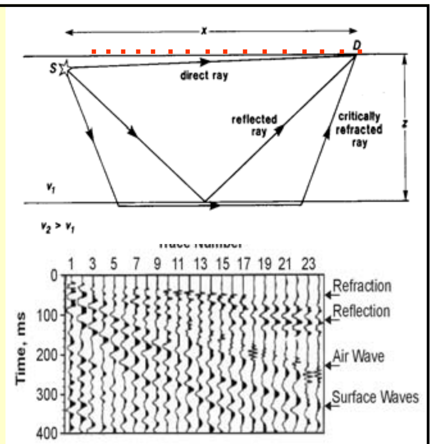

The “travel times” (arrival times) of direct and refracted acoustic energy is plotted as a function of source-sensor separation.

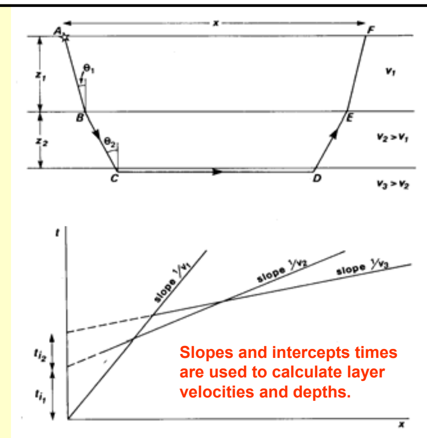

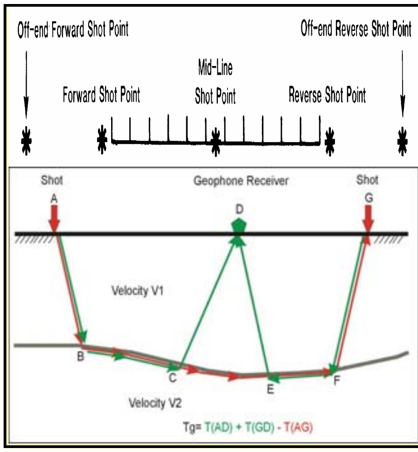

If subsurface is irregular, sources are discharged at multiple locations (typically five). This multiplicity of travel time data allows depths to be estimated with a higher degree of precision.

2-D refraction data can often be transformed into realistic 2-D geologic models. The accuracy of such models will be increased if external constraints (borehole control) is available. Note that low velocity layers are “invisible” and never imaged.

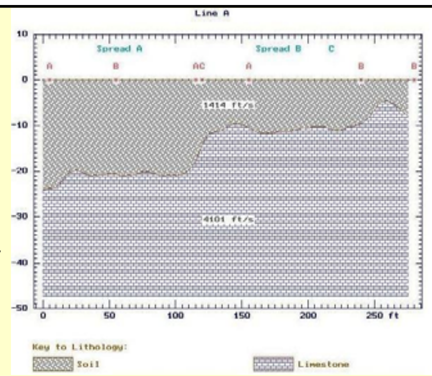

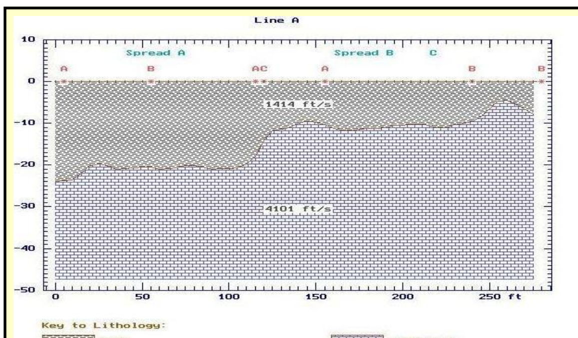

Unless multiple additional sources are employed lateral velocity variations cannot be determined with a high degree of accuracy.

Strengths

- 2-D or 3-D structural images of the subsurface
- Shear and/or compressional wave velocities can be measured
- interpretations, if constrained, can be remarkably accurate
- reconaissance tool, used to optimally locate exploratory boreholes
- cost-effective means of establishing control between boreholes
- acquisition is relatively straightforward
- processing is relatively straightforward if good quality data are acquired
- interpretation is generally relatively straightforward (if constrained)

Limitations

- relatively slow, as sensors (geophones) must be coupled to ground surface
- coupling can be a problem (rock or dry sand)
- limited depth penetration (typically 50 ft)
- only uppermost and most prominent layers can be imaged (typically <4)
- low velocity layers and thin layers are "invisible"
- lateral and vertical velocity variations within a layer are difficult to image using conventional processing techniques

Significant Limitations

- relatively slow, as sensors (geophones) must be coupled to ground surface
- doesn't work well in "acoustically" noisy areas
- all you ever end up with is an interpretation
- interpretations are non-unique
- ground truth is needed to constrain interpretations

Significant Applications

- variable depth to water table
- variable depth to bedrock
- depth to some sub-bedrock interfaces
- estimating rippability
- estimating shear-wave and compressional wave velocities, and Poisson's ratio

Note

Refraction tomography data can be acquired in a very similar manner (but employing many more source locations). Refraction tomography software provides a much more detailed image of the subsurface (including low velocity zones).

TWELVE COMMONLY EMPLOYED GEOPHYSICAL METHODS

gravity	**magnetics**
resistivity	**induced polarization (IP)**
self potential (SP)	**electromagnetics**
refraction seismic	**seismic tomography**
reflection seismic	**cross-hole seismic**
ground-penetrating radar (GPR)	**multichannel analysis of surface waves (MASW)**

MASW

↓

Measures travel times & magnitudes of surface wave (Rayleigh wave) energy

↓

1-D or 2-D image of subsurface (shear wave velocity plotted on 2-D profile)

↓

1-D, 2-D (or even 3-D) geologic models constrained by ground truth

MASW

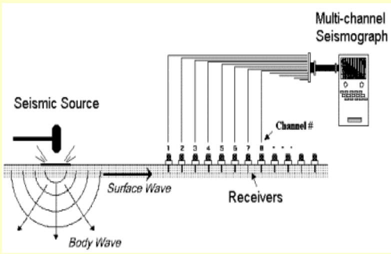

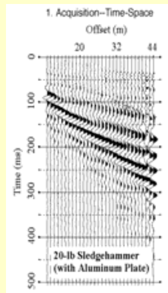

Shot gather

MASW surveying is relatively straight-forward. An acoustic source is discharged at the earth's surface, and the resultant Rayleigh wave energy is recorded by sensors placed at multiple locations.

MASW

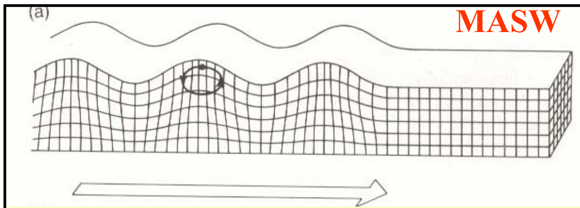

Rayleigh wave particle motion:

- dispersive
- different frequencies travel with different velocities
- highest frequencies involve particle motion at shallow depth and travel with velocities that are a function of the shear wave velocity of the shallow subsurface

MASW

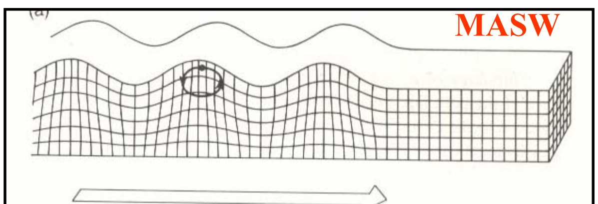

- intermediate frequencies involve particle motions at intermediate depths
- lowest frequencies involve particle motions at greatest depths
- field data can be analyzed and a frequency vs. velocity curve can be generated
- these velocity vs. frequency data can be transformed into depth vs. shear wave velocity data

PROCESSING OF 1-D MASW DATA

1) extraction of fundamental-mode dispersion curves, and
2) inversion of curves to obtain 1-D shear-wave depth profiles.

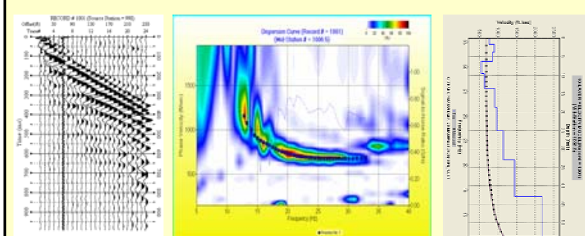

1. Shot Gather **2. Dispersion curves** **3. Velocity Inversion**

2-D Presentation

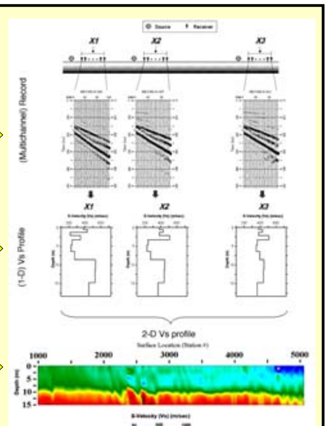

1. Acquire multiple MASW records by moving source-receiver array along traverse.

2. Prepare multiple 1-D Vs profiles (one per array).

3. Construct 2-D shear-wave velocity profile.

Interpreted MASW Profile

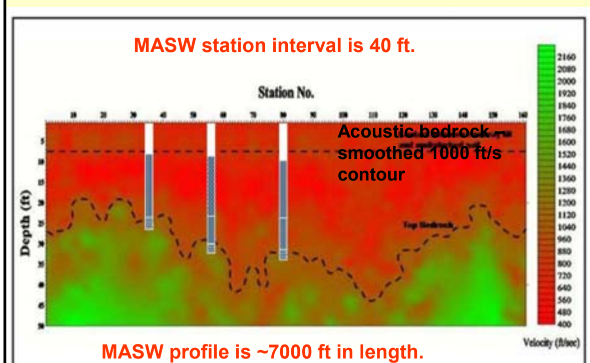

2-D MASW S-Wave Velocity Profiles

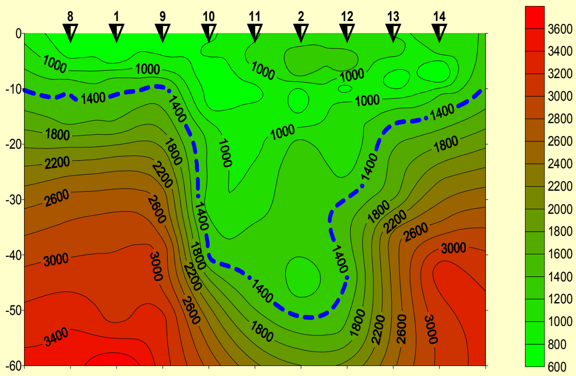

Strengths

- sensors (geophones) do not need to be coupled to the ground
- data can be acquired relatively quickly
- tool can be used in areas inaccessible to drill rigs (paved roadways, beneath bridges, on steep slopes, etc.)
- works well in acoustically noisy areas
- output is 1-D or 2-D shear wave velocity profile of subsurface

Strengths

- output can be transformed into geologic model which includes low velocity layers
- interpretations, if constrained, can be remarkably accurate
- depths of investigation typically 120 ft
- reconaissance tool, used to optimally locate exploratory boreholes
- cost-effective means of establishing control between boreholes

Limitations

- depth penetration typically < 120 ft
- thin layers may be “transparent”
- lateral and vertical averaging occurs as data is acquired using sensor arrays spread over distances on the order of 100+ ft
- hence, tool may not work well in areas where depth-to-bedrock and/or physical properties of soil vary significantly over relatively short distances

Significant Limitations

- all you ever end up with is an interpretation
- interpretations are non-unique
- ground truth is needed to constrain interpretations

Significant Applications

- variable depth to water table
- variable depth to bedrock
- depth to some sub-bedrock interfaces
- estimating rippability
- estimating shear-wave velocities with far greater precision than either reflection or refraction surveying
- results are consistent with SCPT and cross-borehole data

Note

Passive surface wave data can also be acquired. Referred to as ReMi Method (refraction microtremor). The main advantage is that lower frequency natural acoustic energy is used as a source, so greater depths of investigation are possible. However, suitable sources may not always be present.

TWELVE COMMONLY EMPLOYED GEOPHYSICAL METHODS

gravity	**magnetics**
resistivity	**induced polarization (IP)**
self potential (SP)	**electromagnetics**
refraction seismic	**seismic tomography**
reflection seismic	**cross-hole seismic**
ground-penetrating radar (GPR)	**multichannel analysis of surface waves (MASW)**

Cross-hole seismic

↓

Measures travel times & magnitudes of pulsed acoustic energy between paired boreholes

↓

1-D image of subsurface (shear and/or compressional wave velocity)

↓

1-D geologic models constrained by ground truth

CROSS-HOLE SEISMIC METHOD

Acoustic sources (P-wave or S-wave) are generated at different depths in a borehole and are recorded by detectors at the same depth in an adjacent borehole. The direct travel time of the acoustic energy is recorded at each depth tested.

CROSS-HOLE SEISMIC

Acoustic sources (P-wave and/or S-wave) are generated at different depths in one borehole and are recorded by detectors placed at the same depth in an adjacent borehole(s).

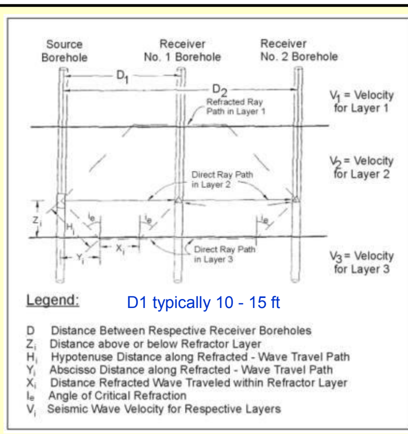

Crosshole Velocity Logging

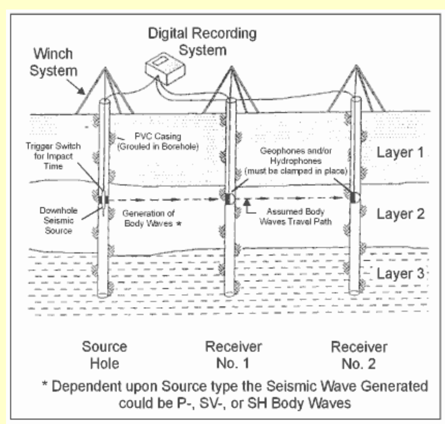

CROSS-HOLE

The inter-borehole velocity (P-wave or S-wave) is therefore determined as a function of borehole depth.
High resolution imaging of the velocity structure can be obtained by using a high frequency source.

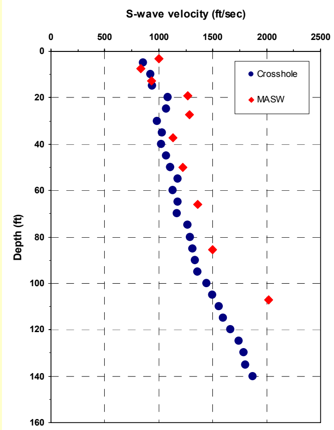

Strengths

- Tool measures inter-borehole P-wave or S-wave velocities
- Average velocities are calculated over relatively short distances (10-15 ft)
- Generates “most accurate” 1-D velocity profiles
- Ground truth is acquired (borehole)

Limitations

- Recorded energy may be refracted as opposed top direct
- Tool is invasive
- Borehole deviation data are required
- Relatively expensive (cost of borehole)

Applications

- Generates a compressional-wave or shear-wave velocity profile (determining in-situ engineering properties)
- Foundation integrity studies
- Slope stability
- Liquefaction potential
- Before and after compaction analysis
- Before and after grouting analysis

TWELVE COMMONLY EMPLOYED GEOPHYSICAL METHODS

gravity	**magnetics**
resistivity	**induced polarization (IP)**
self potential (SP)	**electromagnetics**
refraction seismic	**seismic tomography**
reflection seismic	**cross-hole seismic**
ground-penetrating radar (GPR)	**multichannel analysis of surface waves (MASW)**

Seismic tomography

↓

Measures travel times & magnitudes of pulsed acoustic energy (between paired boreholes)

↓

2-D image of subsurface (shear and/or compressional wave velocity)

↓

2-D geologic models constrained by ground truth

SEISMIC TOMOGRAPHY

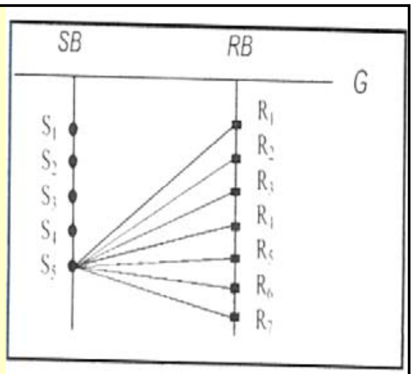

Simply a more sophisticated version of cross-hole seismic! Acoustic sources (P or S wave) are generated at multiple source depths in a borehole. Every time a source is discharged, direct arrivals are recorded by multiple detectors in an adjacent borehole.

SEISMIC TOMOGRAPHY

The travel time of the first arrival is recorded for each source/ detector pair and an average velocity is calculated for each ray path.

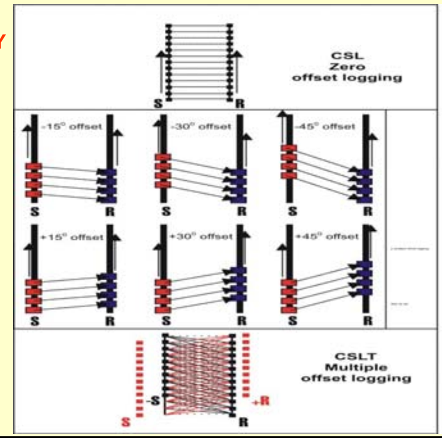

SEISMIC TOMOGRAPHY

The subsurface area between the boreholes is subdivided into pixels of pre-determined size.

On the basis of the statistical analyses of all travel times for all source/receiver pairs, acoustic velocities are assigned to each pixel.

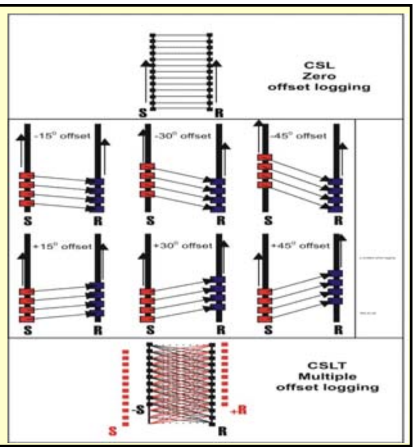

COMPARISON OF CH SEISMIC & TOMOGRAPHIC INTERPRETATIONS

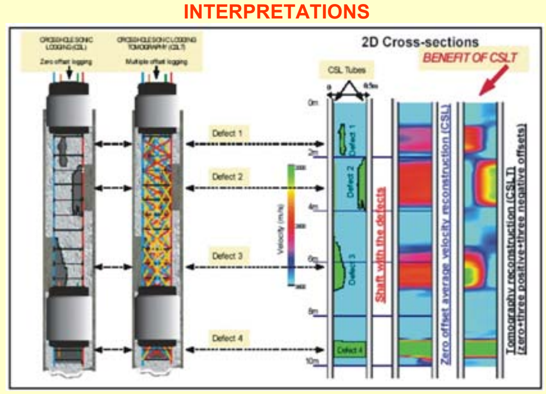

Strengths

- Tool measures inter-borehole P-wave or S-wave velocities
- Assigns acoustic velocities to each pixel (unit area) between boreholes
- More sophisticated programs account for non-linear raypaths
- Tool is invasive
- Relatively expensive (compared to CH seismic)

Limitations

- Tool measures inter-borehole P-wave or S-wave velocities
- Assigns acoustic velocities to each pixel (unit area) between boreholes
- More sophisticated programs account for non-linear raypaths
- Tool is invasive
- Relatively expensive (compared to CH seismic)

Significant Applications

- Depicts how P-wave and/or S-wave velocities vary in inter-borehole area
- Determination of in-situ engineering properties
- Foundation integrity studies
- Slope stability
- Liquefaction potential
- Before and after analysis of compaction
- Before and after grouting analysis

TWELVE COMMONLY EMPLOYED GEOPHYSICAL METHODS

- gravity
- resistivity
- self potential
- refraction seismic
- reflection seismic
- ground-penetrating radar
- magnetics
- induced polarization
- electromagnetics
- seismic tomography
- cross-hole seismic
- spectral analysis of surface waves

NON-UNIQUENESS

- The interpretation of geophysical data is inherently ambiguous.
- All you can ever end up with is an interpretation!

NON-UNIQUENESS

- The reliability of your interpretation is a function of external constraints.
- These can be in the form of ground truth, multiple geophysical data sets, understanding of geologic processes & principles, etc.

GROUND TRUTH CONSTRAINT & VERIFICATION

- Generally speaking, ground truth should be acquired prior to geophysical interpretation in order to constrain interpretations.
- Ground truth should also be acquired after interpretations have been completed in order to verify and/or validate interpretations.

Advantages/Disadvantages

- **Geophysical exploration is generally non-invasive whereas drilling and trenching are invasive.**
- **Geophysical data can provide control between drill holes, and is often times more cost-effective/safer than drilling/trenching.**
- **All you ever end up with is an interpretation!**
- **Invasive control is often necessary to constrain the interpretation of geophysical data.**

Questions?

Selecting Geophysical Methods for Void Detection: Conditions, Limitations, and Method Selection

Mark J. Howell, CPG
Earth Exploration, Inc. Indianapolis, Indiana 46214

Abstract

Subsurface voids result from range of processes and occur at many spatial scales and depths. As a consequence of this diversity of process, scale and geometry, every void detection effort becomes a unique problem. Geophysical surveys should be designed for the specific physical and geometric characteristics at a particular site. In this paper, we intend to enforce awareness that the physical conditions of the subsurface, the limitations posed by acquisition parameters, site conditions and budgetary constraints will ultimately identify the appropriate geophysical method. Often, this level of understanding requires project-specific knowledge of the subsurface geology and the characteristics of developments and activities that are planned for the project.

This paper outlines general principles that apply to void detection problems at all scales. Within the context of a review of the design and selection of geophysical survey parameters, we provide sample datasets that demonstrate a range of subsurface settings. Discussions that associate void size, geometry, and setting with various geophysical methods and design parameters are demonstrated in sample datasets.

1 Geological Conditions and Voids

Voids occur in a wide variety of settings, as a result of various processes, and at a wide range of scales. Perhaps the most familiar and widely distributed voids are related to karst conditions. Voids also form from piping along natural or man-made zones of increased permeability, ruptured water lines, and the excavation of tunnels, mines, vaults, and conduits. Voids form in natural conditions, such as karst, or in man-made structures, such as concrete pier. Within a single process, the formation of voids is influenced by natural characteristics of the geologic mass. Lets consider karst development as an example. Carbonate bedrock will contain structural and compositional irregularities that will influence solutioning by ground water and consequent void formation. Common irregularities include fracture systems, bedding planes, reefs, depositional features, varying calcite or mud content, and lithologic boundaries. The dimensions of karst voids can range from a fraction of an inch of solutioning of a fracture to hundreds of miles of cave development. Unfortunately, predicting the occurrence of voids is usually very difficult. Even though features such as systematic fracture systems may exhibit a very regular pattern, predicting solutioning trends along the fracture system is problematic. Predictive approaches often fail, and the best alternative is usually a mapping program. Mapping efforts may include direct methods such as visiting outcrops or drilling test borings, or indirect geophysical methods such as ground penetrating radar (GPR), seismic refraction, etc.

At least three factors govern the success of a subsurface mapping program. The first factor consists of fundamental limitations related to the detection and imaging of a feature from a discrete number of samples (geophysical measurements). These limitations are a function of the size, shape, orientation, and depth of burial of the void, the resolution and sampling density of the geophysical survey, and the contrast between the void and the surrounding material.

Ambient environmental conditions are a second factor that will influence the success of a mapping program. Here we include site access, the presence of physical obstacles, site topography, and noise. In a geophysical sense, noise is the presence of unwanted signals that interfere with the geologic parameter being measured. Because seismic surveys utilize vibrational energy to create an image of the subsurface, sources of unwanted vibrations are seismic noise. Examples include traffic, wind, and the operation of heavy equipment. A desired mode of energy, a signal, in one method can be noise in another method. For example, the MASW method uses Rayleigh waves (a specific type of surface seismic wave) to map subsurface conditions. However, Rayleigh waves obscure reflected energy and are therefore a source of noise in seismic reflection surveys.

Subsurface materials will exhibit significant variation in their acoustic properties, electrical properties, and moisture content.

A third factor that will determine the success of a mapping program is the selection of appropriate exploratory methods; i.e., methods that are capable of detecting the physical target. Core drilling is certainly able to detect a void *if* a void is encountered. In contrast, surface GPR is not capable of detecting karst voids if the bedrock is covered with a mantle of terra rosa, as radar signals are severely attenuated in moist clayey soils.

Most of the factors listed above cannot be controlled. The size, shape and burial depth of a void, and the type of fill material will not likely change. Nor will the ability to use surface GPR through several feet of wet clay. Alternatively, factors such as traffic noise or sampling density can be managed. The manipulation of those factors that can be controlled is usually the greatest driver of both the cost and success of the exploratory mapping program. Additional acquisition and processing costs may be incurred by increasing the sampling density (the number of geophysical sensors). An increase in the signal to noise ratio may require the rerouting of traffic or the halting of equipment operations.

2 Limitations of Resolution, Sampling Density, and Contrast

The success of all exploratory programs, whether by direct or indirect methods, is determined in part by the resolution and sample density of the exploratory program, and the contrasts between the target (void) and the surrounding media. In actuality, the three parameters are interdependent. However, at the level of designing an exploration plan, it is often useful to consider them independently.

2.1 Resolution

Sheriff (2002) defines resolution as “the ability to separate two features that are close together” and “the minimum separation of two bodies before their individual identities are lost on the resultant map or cross section.” This concept is graphically demonstrated in Figure 1, which depicts an air void in ice that was obtained by Paulo Monteiro (2006) using electron emission microscopy (a very small void indeed!) The figure shows an image that was progressively downsampled from 1024 x 1024 pixels to 1 x 1 pixels. While the ability to detect the void itself is not completely lost until the next-to-the-last (the eighth) image, finer detail, such as any two bumps inside of the void, is poorly resolved by the fourth image. One perspective is that the loss of resolution is due to a decreased sample density, as the first panel consists of over 1 million pixels and the last panel consists of only one. However, that perspective can obscure another.

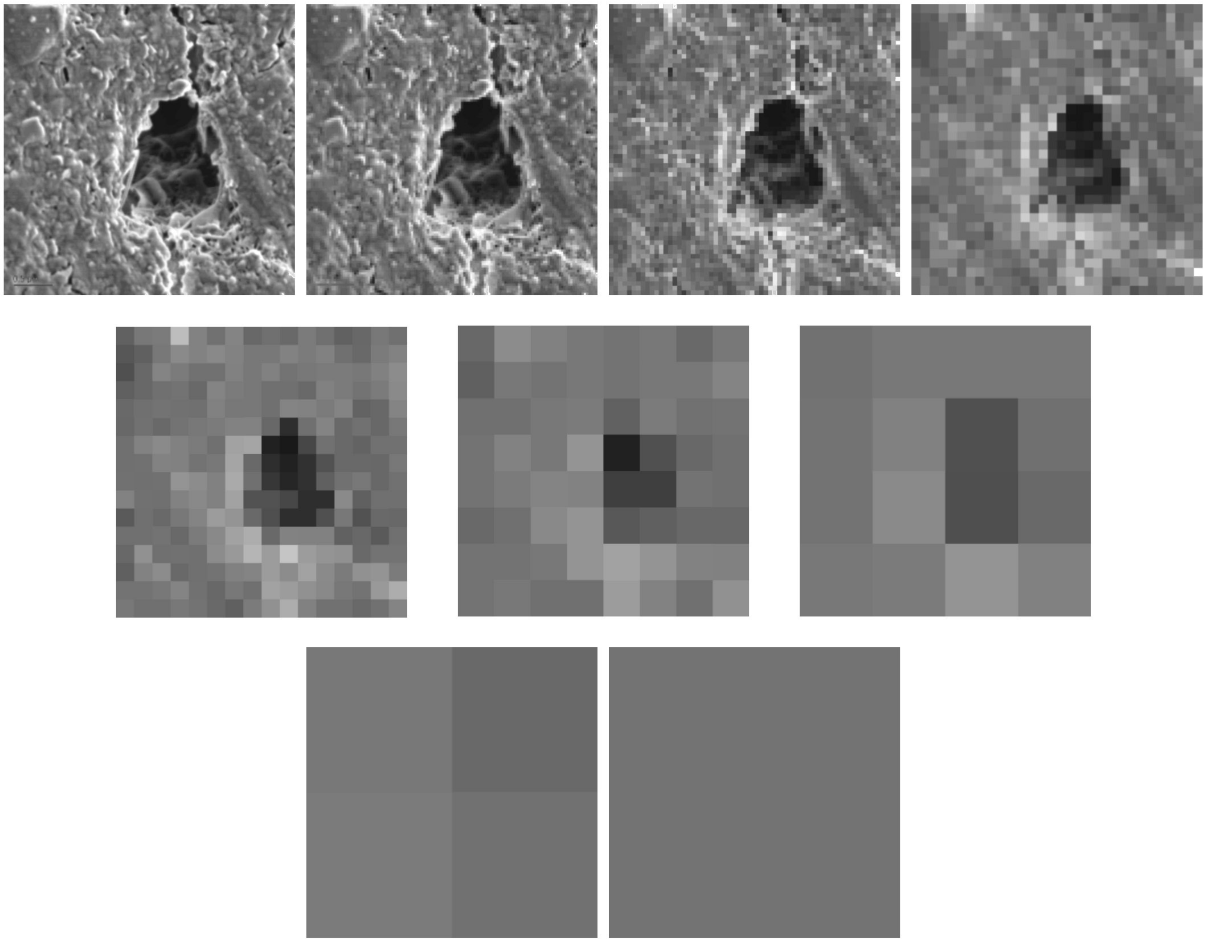

Figure 1: Image of a void with varying resolution.

Each panel contains the exact same number of pixels because each panel was resampled back to a 1024 x 1024 size. Otherwise the 1 x 1 pixel image would be about the size of the period at the end of this sentence. The important point here is that the sample density of each panel is the same: approximately 1 million samples per panel. Each image can be understood as depicting a different sampling resolution. Progressively larger areas are assigned only one of sixty-four available shades of gray.

In subsurface work, it is often useful to distinguish between vertical and horizontal resolution. Although a continuous rock core has very high vertical resolution, the horizontal resolution of subsurface conditions is dependent on the spacing between borings. Horizontal resolution can be increased by collecting more measurements per unit distance, whether it be by decreasing the spacing between sensors or geophysical traverses, decreasing grid intervals, or increasing the number of borings per acre. However, increasing the vertical resolution is often a more difficult problem. In reflection methods like GPR or seismic reflection, an increase in the frequency of the source energy will result in an increase in the vertical resolution (Figure 2). Unfortunately, the tendency of the earth is to absorb high frequency energy, so that high frequency signals will exhibit a lower depth of penetration than high frequency signals. Note that

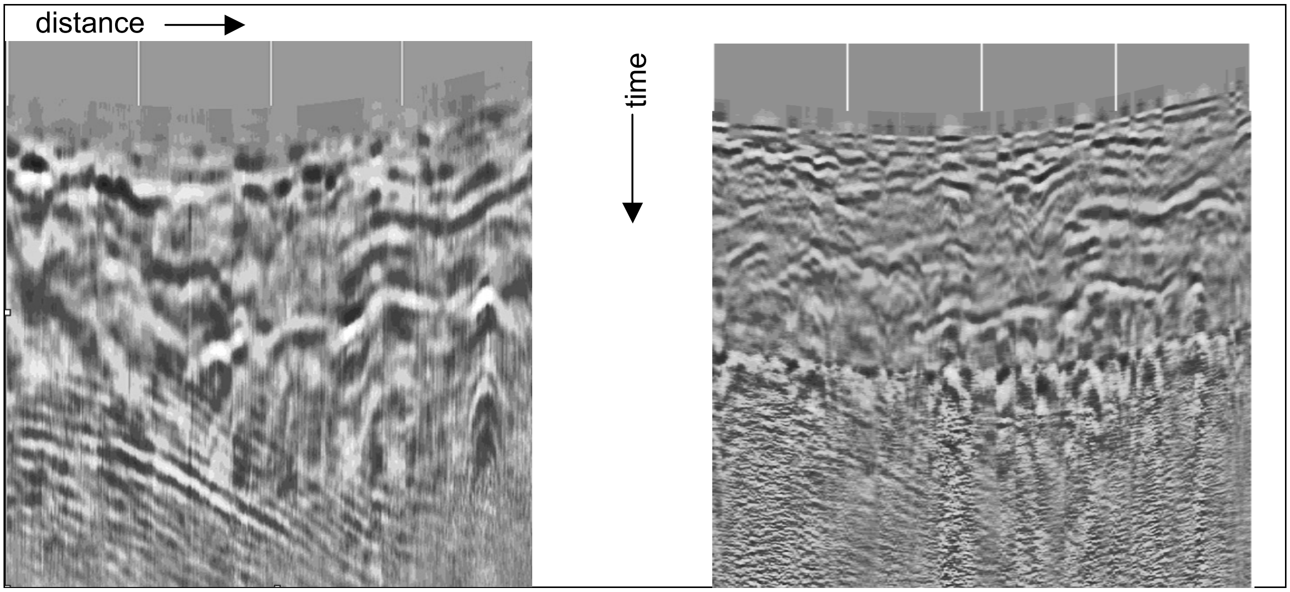

Figure 2: GPR image showing changes in vertical resolution and depth of penetration with antenna frequency (80 MHz on left, 300 MHz on right). Both images show geophysical cross sections through the same area and are scaled similarly. The increase in resolution is a result of increased antenna frequency (i.e., increased sampling density in time).

the sample density and the horizontal resolution are the same for both images; the source frequency, hence the vertical resolution, is the only difference between the two panels.

2.2 Sample Density

Sample density is intimately related to resolution, in that an increase in sample density can increase the resolution. Returning to Figure 1 as an example, each of the nine panels could have been constructed by sampling the original image with increasing number of data points. In other words, the ninth panel could have been constructed from a single sample (1 sample/panel) and the first panel could have been constructed from a million samples (1024^2 samples/panel). In this example, a minimum sample density of 16 samples/panel was required to resolve the void (the eighth panel).

Figure 3 demonstrates the effect of increasing sampling density could have on the interpreted location, size and shape of Monteiro's original void. The top panels represent an increased spacing between geophysical traverses, as might be gathered during a seismic, GPR, or electromagnetic survey. In contrast, the bottom represents point measurements as sampled in a gravity survey or a test boring program. Note that the detail of the shape and size of the void are increased with increasing sampling density, indicating greater spatial resolution. Figure 4 shows actual GPR images that demonstrate the effect of sample density. The vertical resolution does not change between images; only the horizontal resolution diminishes with increased sampling intervals. Also note the difference between *detection* and *imaging* that are achieved with the three different sampling densities.

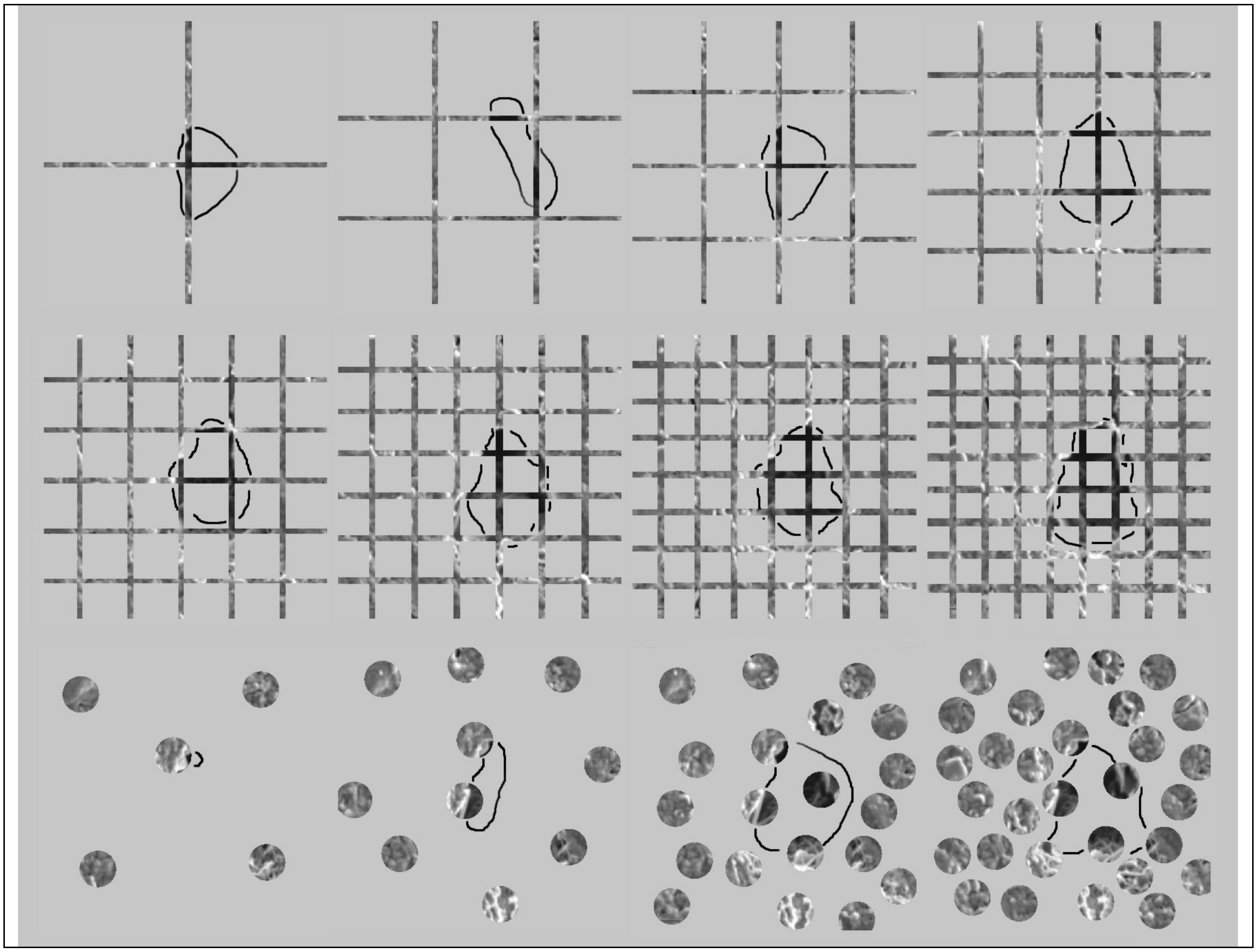

Figure 3: The effect of sample density on interpreted void location, size, and shape. The void is detected in each case, but is poorly imaged where coverage is sparse.

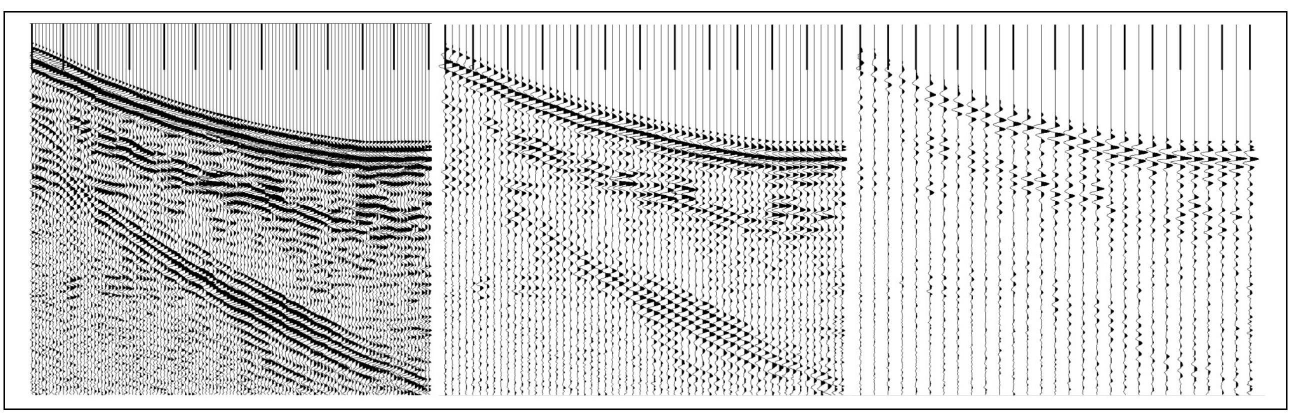

Figure 4: GPR images showing changes in resolution with sample density. Each image shows geophysical cross sections through the same area and is scaled similarly. Various features are well imaged in the leftmost panel, but barely detected in the rightmost panel.

Figure 5 demonstrates that the optimum traverse spacing for the detection of a given target is less than one half of the targets minimum dimension. If the minimum dimension is equal to (L), the grid spacing needs to be less than or equal to (L/2), as shown in the bottom center panel. Unfortunately, the minimum dimension of L is not usually known. Also note that drilling test borings at the grid corners of the bottom center panel would result in the detection of only 50% of the targets. Increasing the sampling density is often expensive, though it is preferable to conducting an exploratory program that has little chance of detecting the targets of interest.

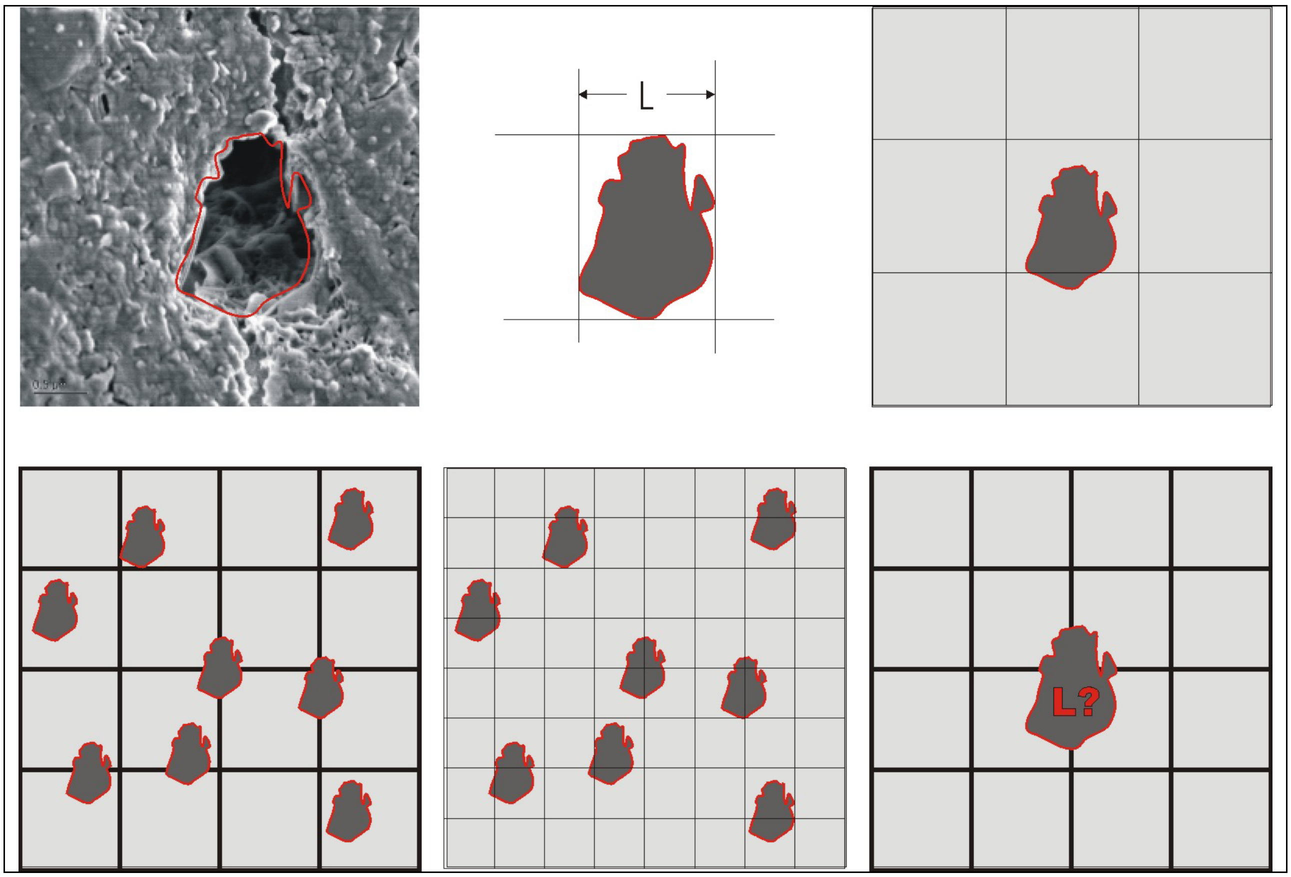

Figure 5: Determination of minimum traverse spacing for the detection of a target of dimension (L). The likelihood of detecting an object increases with grid spacing, and is optimized at L/2 (bottom center panel). Unfortunately, the value of L is not usually known.

2.3 Contrast

Every geophysical method relies on a contrast in some physical property between the target and the host material. The type of contrast dictates the geophysical methods that are candidates for detecting and mapping the target. Seismic and gravimetric methods are sensitive to density contrasts. Similarly, GPR, electromagnetic, terrain conductivity and earth resistivity methods are sensitive to contrasting electromagnetic properties, such as dielectric permittivity, magnetic susceptibility, or bulk resistivity. A cursory review of a few basic equations will illustrate this concept. Geophysical methods will only detect conditions where contrasts exist between physical parameters, and specific geophysical methods rely on differing physical parameters.

Gravity anomaly due to a void in bedrock (G) goes to zero as the density of the void (ρ_v) approaches the density of the rock (ρ_r). Other equation variables describe the void geometry. (Telford et al., 1976)

$$G = (\rho_v - \rho_r) \cdot \frac{4\pi a^3 z}{3(x^2 + z^2)^{\frac{3}{2}}}$$

Seismic reflection coefficients (R) at a void boundary are a function of the acoustic impedance (velocity·density) of the void ($V_2\rho_2$) and the rock ($V_1\rho_1$). As the difference in impedances approach zero, the reflected energy also approaches zero. (Sheriff, 2002)

$$R_{seismic} = \frac{V_v\rho_v - V_r\rho_r}{V_v\rho_v + V_r\rho_{r1}}$$

GPR reflection coefficients are also related to differences in the intrinsic impedances (Z_v-Z_r) of the void and bedrock, where Z is related to the magnetic susceptibility (μ), electric permittivity (ε), conductivity, (σ) of the materials, and the antenna frequency (ω). (Ulriksen, 1982)

$$R_{GPR} = \frac{Z_v - Z_r}{Z_v + Z_r} \quad where$$

$$|Z| = \sqrt{\frac{\mu}{\varepsilon}} \Big/ \sqrt[4]{1 + \left(\frac{\sigma}{\omega\varepsilon}\right)^2}$$

Often, the detected contrasts are not between the target and the surrounding material per se, but are due to the properties of the material that occupies the pore space. For example, gravel layers can be detected by earth resistivity largely because of the relatively large volume of low-resistivity ground water that occupies the pores within the gravel. For voids, the contrast will be between the host material and the material that fills the void, be it air, water, clay, or something else. Figure 6 demonstrates the effect of diminishing contrast between the void (dark) and the surrounding material. The deleterious effect of spurious noise, which is always present in real world geophysical datasets, is shown in the bottom series of panels.

Figure 7 presents a longitudinal GPR profile along an earthen dam. Lateral drains were evidenced by the presence of poorly- to well-defined diffraction hyperbolas. The locations of the laterals were independently determined by a video inspection of the toe drain. A comparison of the drain locations mapped in the toe drain and the drains detected by GPR show that not all of the drains could be detected using this dataset. We interpreted these results as evidence that the drains were plugged with sediment, an interpretation in general agreement with observed flow amounts. Flowing drains or empty drains would contain water or air, both of which have a high contrast in dielectric permittivity with the surrounding soil. Once the drain is plugged with sediment, the contrast is reduced, and the lateral drains can no longer be detected.

3 Geophysical Methods: Physical Limitations and Constraints

There are numerous site-specific conditions that must be understood before a geophysical survey can be properly designed and conducted. An evaluation of these conditions in light of the types of limitations described above may determine which geophysical methods are appropriate

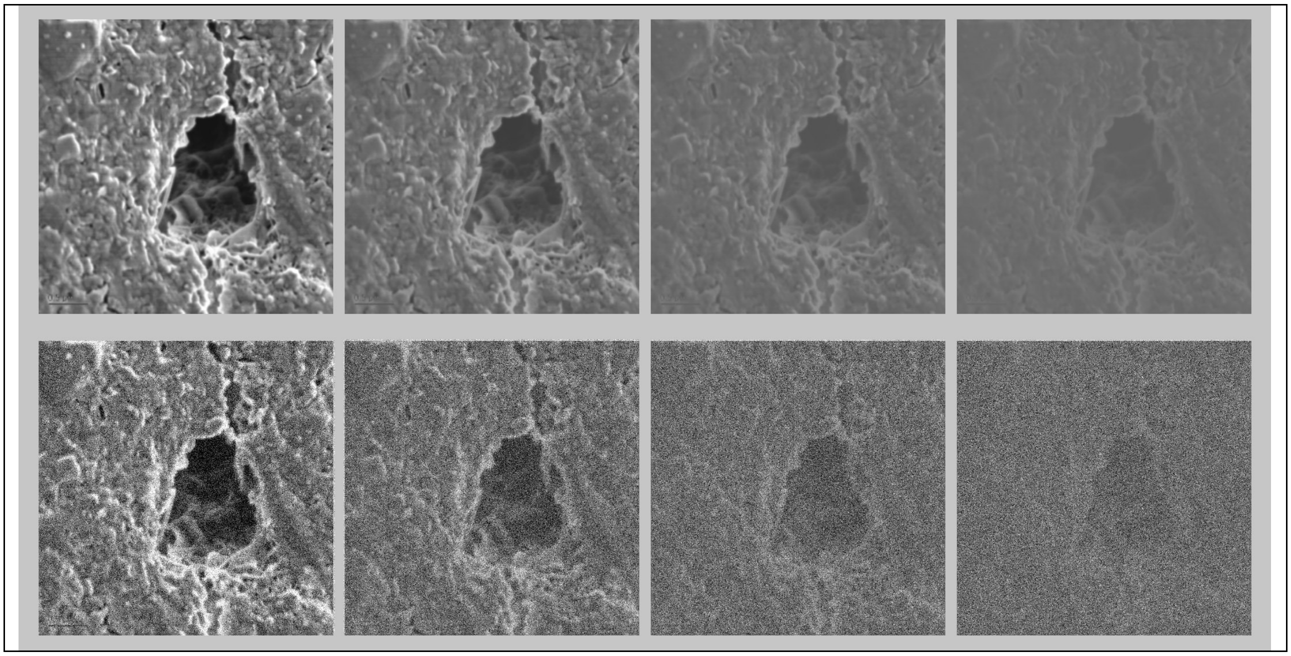

Figure 6: Effects of decreasing physical contrast. The bottom series of panels demonstrate the effect of noise on the detection of weak anomalies.

or may find that there is no method that is likely to detect the target of interest. It is not possible to provide a reliable evaluation of the success of any geophysical method (let alone provide a meaningful cost proposal!) unless these conditions are known. This list is not exhaustive, but will give an idea of types of parameters that change with each project.

3.1 Target Parameters

Target parameters include the size, shape, orientation and depth of burial of the target. Its vertical and horizontal extents are critical variables. The nature of the surrounding bedrock; the overlying bedrock and the near-surface conditions are important. Materials surrounding and infilling the void must be evaluated. Additionally, one must consider the possibility of false positives, that is, the presence of an anomaly that is created by something other than the target of the survey.

3.2 Site Access

Site access conditions often limit the degree of coverage that can be achieved. Obvious restrictions include heavily vegetated areas, physical obstacles (buildings, debris, uneven terrain), or ground conditions (swamps, rivers, pavements, mud, etc.) The measurement geometries of some methods, seismic reflection, refraction and earth resistivity are examples, have diminishing geographic coverage with depth (Figure 8). In these cases, the geophysical profile at the surface is longer than the area covered in the subsurface. In practical terms, this may require access to adjoining property or reduction in anticipated subsurface coverage. Less obvious restrictions include prohibitions against noise from seismic blasting sources, electrical currents from resistivity surveys, or radio signal interference from unshielded GPR antennas. While some equipment can tolerate decontamination procedures at environmental sites, others are more sensitive and may not be a good choice for the project.

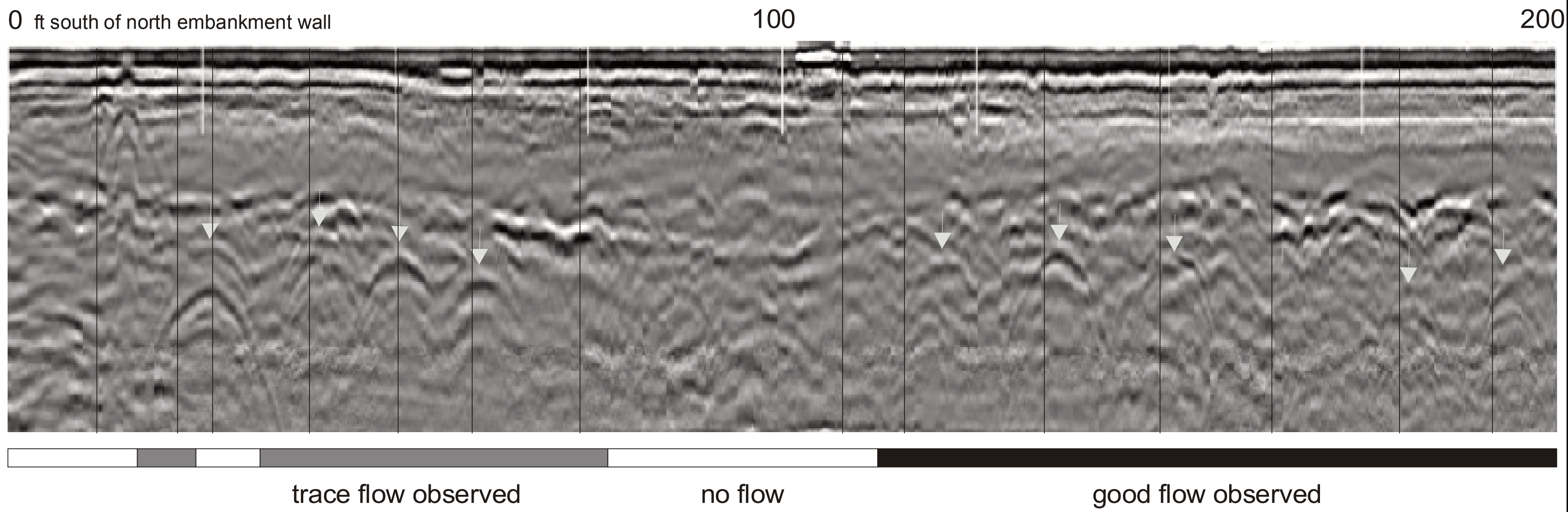

Figure 7: GPR profile showing the effect of varying contrasts between the target and surrounding materials. In this image, lateral drains within an earthen dam are evidenced by broad diffraction hyperbolas. The tops of the hyperbolas are marked with light gray arrows. The locations of the lateral drains (as mapped by video camera survey of the toe drain) are represented by black vertical lines. Undetected drains are interpreted to be plugged with sediment, resulting in a low contrast between the target and surrounding material. The scale bar at bottom indicates the reported flow through the drains at the time of a video inspection with good flow shown in black, trace flow in gray and no flow conditions in white.

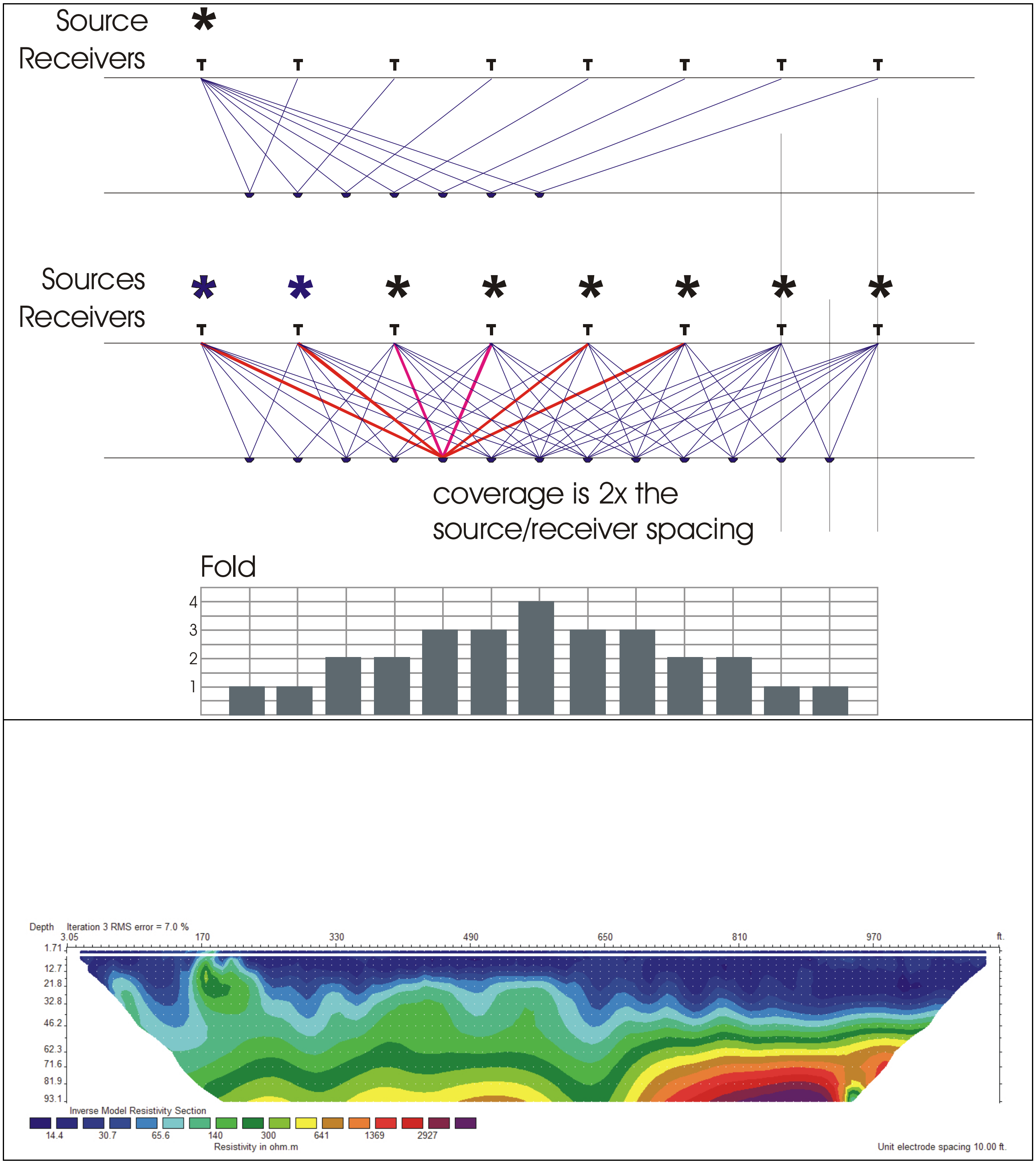

Figure 8: Seismic reflection (top) and earth resistivity (bottom) coverage lessens with depth. The fold diagram indicates the level of redundant measurements at common midpoints along a bedrock surface. Redundant sampling points increase the signal to noise ratio of bedrock reflections. Fold values of 1 will provide relatively poor image results. [Note that the purple portion of the bottom image, with resistivities > 2,900 Ω·m represents an underground mine void.]

3.3 Topography

Significant topographic relief can be problematic for many geophysical methods. Gravity surveys are particularly sensitive to topography. Not only do many microgravity surveys require topographic surveys of 0.1 ft or better, but the topographic conditions must also be modeled. For example, a site that is at the top of a cliff may require modeling to account for the absence of earth at the cliff! Rough topography, such as in corn stubble, may be problematic for a sensor mounted on a wheeled cart (an E/M survey), but is generally not a problem for methods that use cables and sensors (seismic or earth resistivity).

3.4 Noise

Sources of noise are specific to the geophysical method under consideration. Alternatively, the types of ambient noise often determine the geophysical methods of choice. While there are sources that can be controlled or mitigated, there are others that cannot be mitigated or even anticipated until field operations are underway (such as guided waves caused by the subsurface acoustical structure of a site). Some examples are tabulated below.

Seismic methods (vibrational noise)	Traffic, wind, and the operation of heavy equipment or pumps. Site-specific acoustical structure of the subsurface.
Earth resistivity, terrain conductivity (electrical conductivity)	Fences, buried utilities, metal buildings, grounding grids, reinforced pavements. Overhead metallic objects such as poles, buildings or automobiles.
Ground penetrating radar (electrical conductivity)	Wet clayey soils, conductive pore fluids. Fences, buried utilities, metal buildings, grounding grids, reinforced pavements. Overhead power lines. Radio signals.
Magnetic surveys (ferrous iron)	Steel objects including buried cast iron pipes, steel fences, dumpsters, and reinforcement steel. Magnetic storms.

3.5 Weather

Weather conditions are unpredictable by nature but must be considered for all work except indoor surveys. Many geophysical systems are weather resistant but few systems function correctly after exposure to a downpour. Standing water is an issue for methods that use cables and sensors and can be hazardous in earth resistivity surveys. Lightening is particularly dangerous with cable and sensor spreads. GPR methods are not particularly sensitive to pure snow, but may encounter difficulties following winter salt applications. Sunspot activity will affect magnetic surveys, but magnetic storms predictions are available from the Internet.

3.6 Required Accuracy

The accuracy that is required in a project is a primary factor in evaluating the feasibility of geophysical methods for target detection and mapping. Two types come into play; geophysical accuracy and geographical accuracy. By geophysical accuracy, we mean the accuracy in determining the depth, position or size of a target. A rule of thumb that is often quoted for depths determined by geophysical work is ± 10%, but this can vary significantly. Positional accuracy may increase with increasing vertical resolution (Figure 2) and sample density (Figure 3). Also note that it is usually difficult or impossible to constrain the dimensions of a specific anomaly. Images produced through inversion modeling are common but the limiting assumptions that are built into the inversion algorithms must also considered.

The accuracy of measurement locations is also an issue. Many small sites are favorable to the use of a grid established with measuring tapes. Large areas may require the use of GPS while small targets may preclude it. Small targets in large areas raise the issue of being able to locate the position of the target at some future date following its detection.

4 Considerations for Contracting Geophysical Services

Often, little consideration is given to the development of a scope of work for a geophysical survey. A purchaser of geophysical services often requests something like “a seismic refraction survey for bedrock mapping” or “costs per acre for a GPR survey.” Proposals that are received in response to vague requests should be reviewed with due caution, not because of malicious intent of the respondent but because they were provided too little information to properly design the geophysical exploration parameters. Meaningful scopes and fees can only be reached by a proper evaluation of site characteristics and survey goals followed by a determination of the required survey resolution, sample density, and geophysical method.

Geophysical methods are indirect methods. Consequently, they are best employed with subsurface control. This is usually realized from test borings but can include excavations, outcrops, cross sections or other sources of geological information. Because geophysical solutions are characteristically non-unique, greater reliability can be achieved by employing two or more geophysical methods in tandem, particularly when the two methods are based on differing physical parameters (such as resistivity and seismic). For projects that are large enough to have a test-boring program, we strongly recommend a phased approach with a sequence of exploratory borings, geophysical survey, and confirmation borings. This provides control for the geophysical interpretations and allows confirmation drilling of anomalies.

Consider a survey conducted by the National Cooperative Highway Research Program. Seventy transportation agency representatives, mostly within the geotechnical engineering branches and sections (NCHRP, 2006) were queried about their experiences with the application of geophysical methods. Responses to the survey were received from each of the fifty state departments of transportation (DOTs), the District of Columbia, a port authority, eight Canadian and three federal agencies. In their conclusions, the authors state the following:

“The implementation of geophysical investigation techniques is increasing among transportation agencies, with project specific applications continuing to diversify. However there remains some skepticism among those engineers and geoscientists who are attempting to implement the technology on their projects or within their agencies…It appears that in some instances implementation of geophysics is being undertaken

- Without proper selection of the technique for the specific application(s),
- With an inadequately defined scope of work,
- With an inadequate means to acquire and objectively interpret data, and
- By individuals with inadequate education or experience in the field.”

We suggest that the incidences of project failures of the first three categories would be reduced by the thoughtful consideration of the limitations of sampling and site-specific conditions prior to scoping the project.

5 Summary

This paper presented some basic geophysical concepts regarding the design of subsurface geophysical programs. Examples of acquisition parameters are included that strongly influence the success of any exploratory program for the detection of voids or any other geophysical target. Our goal is to elevate the awareness of basic limitations that are rarely considered before scoping geophysical survey requirements. This awareness becomes increasingly important as the community of consumers of geophysical information continues to increase. Ignoring any of these limitations can result in a failed project, regardless of its cost or effort. As stated by Shunryu Suzuki, “The most important thing is to find out what is the most important thing.”

References

Monteiro, P.J.M., http://www.ce.berkeley.edu/~paulmont/Images/ice/field%20emission/AV8-void-at-wall1-2kv.jpg

NCHRP, 2006, Use of Geophysics for Transportation Programs: NCHRP Synthesis 357, Transportation Research Board, Washington, D.C., 109 p.

Sheriff, R.E., 2002, Encyclopedic dictionary of applied geophysics: Fourth Edition, Society of Exploration Geophysicists, 429 p.

Telford, W.M., L.P. Geldart, R.E. Sheriff, and D.A. Keys, Applied Geophysics: Cambridge University Press, 860 p.

Ulriksen, 1982, Application of Impulse Radar to Civil Engineering: Doctoral Thesis, Lund University of Technology, Lund, Sweden, distributed by Geophysical Survey Systems, Inc., Salem, New Hampshire, 179 p.

Land Development over Karst Terrain
Beaumont Farm Unit 14-C, The Sanctuary
Lexington Kentucky

Hugo Aparicio, PE[1]
Kip Anderson, PE, PG[2]
Associate[1]*, Senior Project Engineer*[2]
Fuller, Mossbarger, Scott and May Engineers, Inc.

Abstract

When exploring subsurface conditions in the Lexington Bluegrass Region, one can expect to encounter fat residual clay soils less than twenty feet in thickness followed by bedrock belonging to the Lexington Limestone Formation. The limestone within this formation often produces vugs or voids that over time may develop into sinkholes, springs, fissures or sometimes interconnecting caverns. The latter of the three is uncommon within this formation but does exist in some areas within Fayette, County. The most common karst feature produced and observed within this formation are sinkholes which range in size from a few feet to as much as twenty feet in diameter. They may also contain open throats (holes) at the ground surface which extend down into the underlying bedrock units.

As a result of the continued growth and prosperity of the local residents, karst terrain within Fayette and the surrounding counties is routinely being developed. As more of the land is developed, geotechnical investigations need to be performed such that proper treatment and protection of these features can be maintained. The typical treatment sequence of a sinkhole consists of exploring/cleaning the feature, placement/lining of Type II geotextile fabric over the opening, backfilling with No. 2 or No. 57 stone over the fabric, and finally wrapping or enclosing the fabric around the crush stone filter. This treatment allows water to drain into the feature while reducing the likely hood of soils or debris blocking the drainage path. The treatment area can then be backfilled with engineer approved fill and a buffer zone constructed around the feature.

The development of The Sanctuary at Beaumont Farm, occurred around a known system of interconnecting fissures within the Lexington Limestone Formation. The main feature contained a large opening/room that extended under the site splitting the proposed track of land into two individual halves to develop. An extensive geotechnical exploration of the feature was conducted by FMSM Engineers, Inc. from 2002 to 2005 and consisted of past research/documentation of the feature, traverse/survey of the fissures (those accessible to humans), and an exhaustive drilling program to locate the main system of fissures and select a non-buildable area around the karst feature. A down hole camera was also used during the field exploration to review/determine potential voids or clay seams within the bedrock. This paper discusses the scope of the geotechnical work performed to evaluate the atypical karst feature and formulate recommendations to explore, treat and protect, and ultimately develop residential land over karst terrain.


LAND DEVELOPMENT
OVER KARST TERRAIN
BEAUMONT FARM
LEXINGTON, KENTUCKY
ORVSS XXXVII
Innovations in Exploration
Of Subsurface Voids
EMSM
ENGINEERS

Beaumont Farm

ORVSS XXXVII
Innovations in Exploration
Of Subsurface Voids

MSM ENGINEERS

Presentation Outline

- Project Location & Site Geology
- Historical Data of Crystal Cave
- 2002 FMSM Cave Survey
- 2003 FMSM Exploration
- Initial Street Layout & Non-Buildable Limits
- 2004 FMSM Exploration
- TV Exploration
- Revised Non-Buildable Limits
- Revised Street Layout
- 2005 Construction Monitoring & Karst Treatment
- Cave Access/Entry
- Current Development
- Summary

Project Location Map

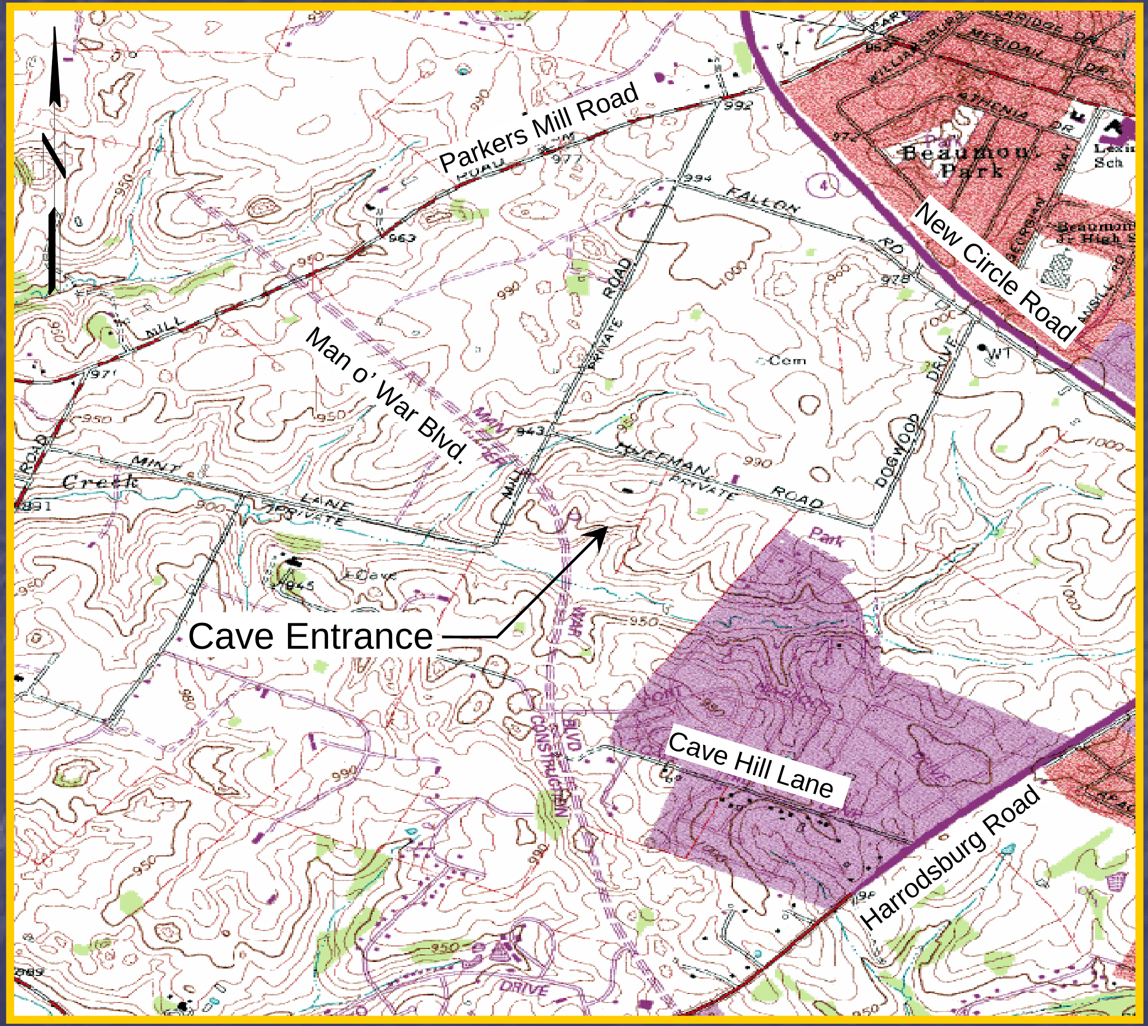

Lexington East Topographic Quadrangle
1965 (Revised 1993)

ORVSS XXXVII
Innovations in Exploration
Of Subsurface Voids

Aerial Photo Pre-Construction

ORVSS XXXVII
Innovations in Exploration
Of Subsurface Voids

MSM ENGINEERS

Site Geology

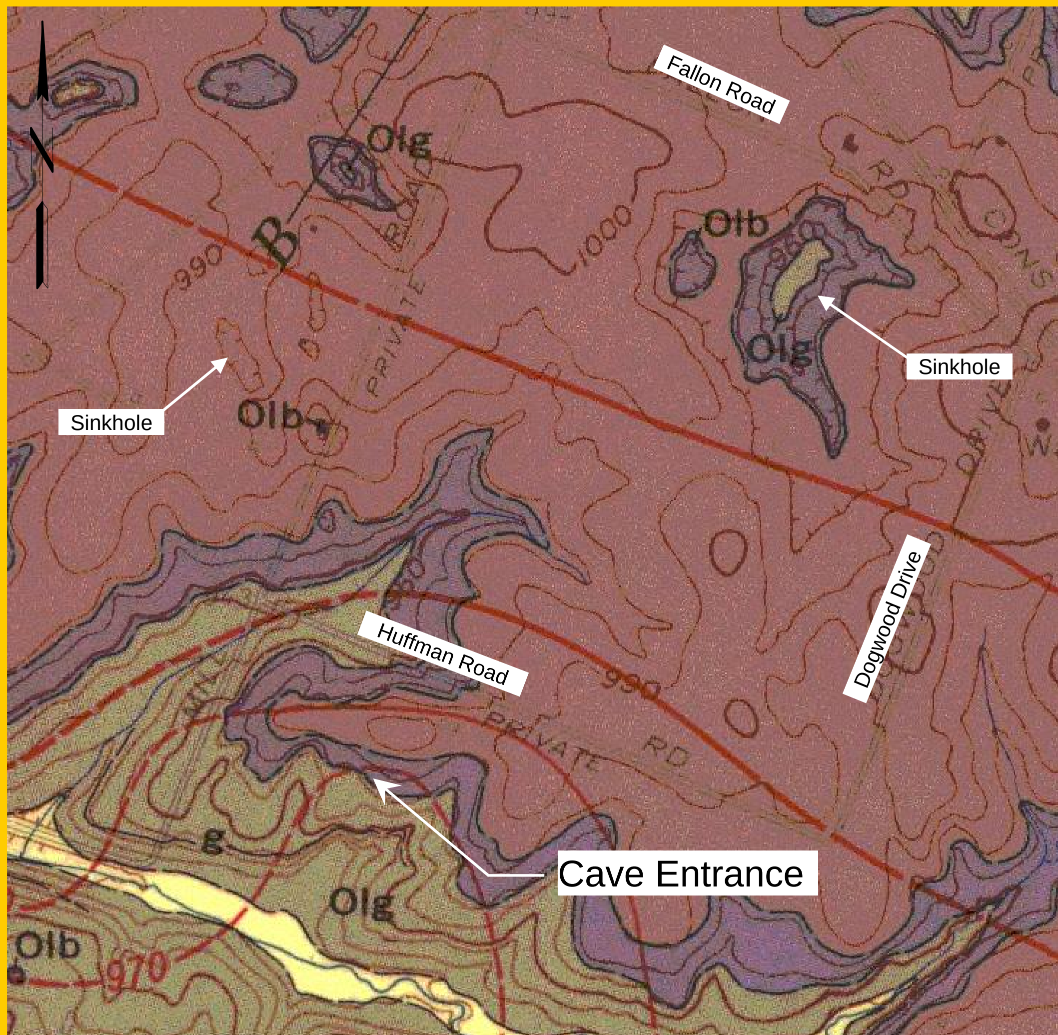

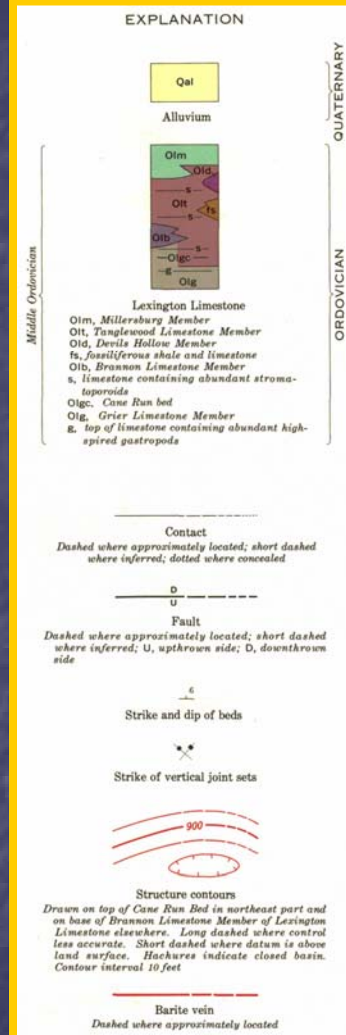

Lexington East Geologic Quadrangle
1967

FMSM ENGINEERS

1964 C & T Survey

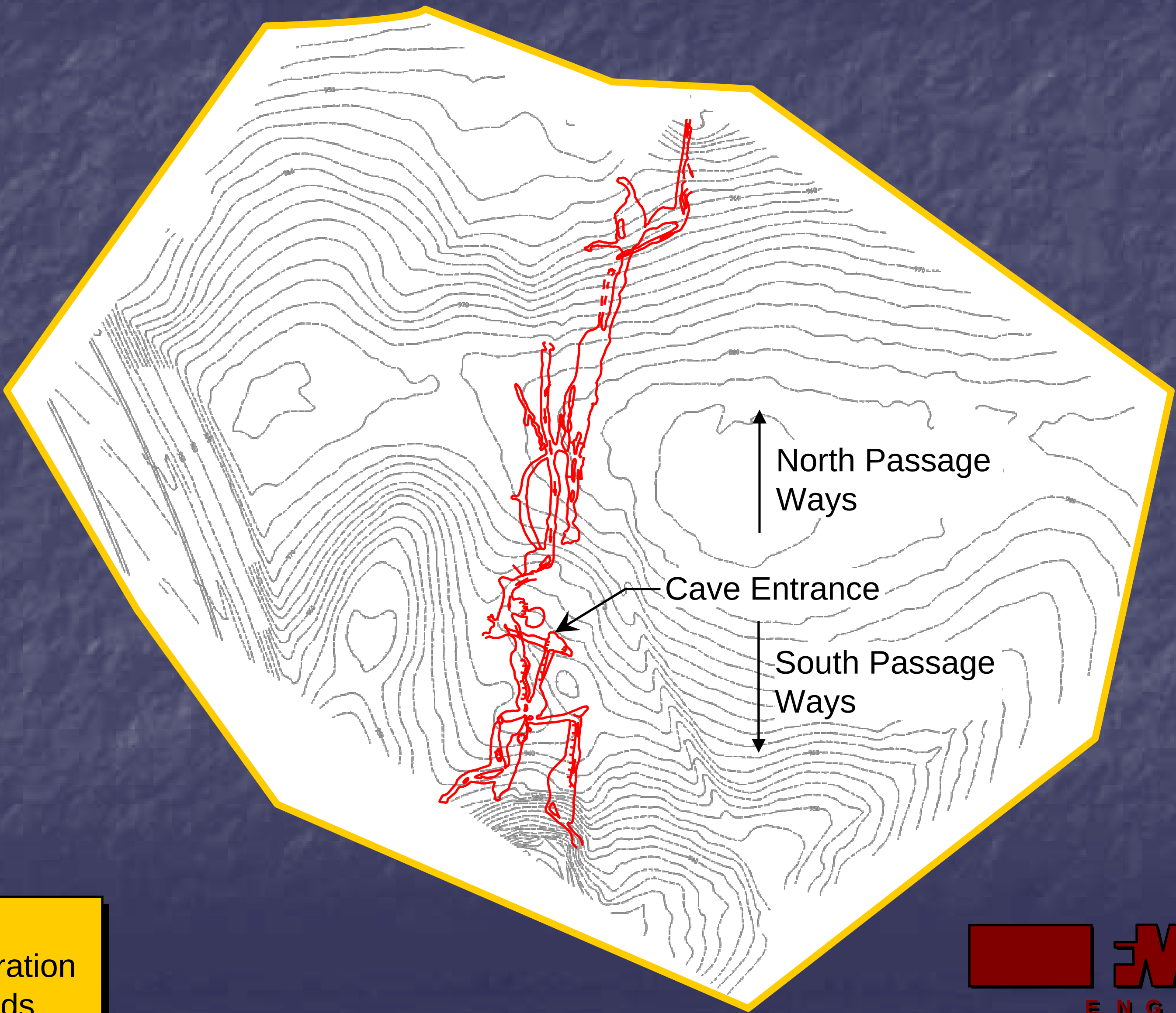

ORVSS XXXVII
Innovations in Exploration
Of Subsurface Voids

MSM ENGINEERS

Historical Cave Description (Pre 1970)

- **Sinkhole Entrance Located On Valley Slope**
- **Rock Outcrop Southeast of Entrance – Discharge of Water in Wet Weather**
- **Sinkhole Served as a Convenient Trash Site with Trash Spilling Into Cave**
- **Cave Contains Multiple Passage Ways with Occasional Passages Containing Water**

  <u>South Passage Ways</u>
  - Walking Passages with occasional crawlways
  - Thick slippery mud banks
  - Humid Atmosphere
  - Heavily vandalized formations

  <u>North Passage Ways</u>
  - More extensive crawlway passages
  - Passages are joint-controlled and numerous
  - Passages contain occasional muddy pits which are extremely difficult to traverse
  - Many passages become non-negotiable

- **In 1970 Owner Bulldozed the Entrance Shut – Only a Shallow Depression Under a Tree Marked the Entrance**

1988 Microgravity and Resistivity Survey

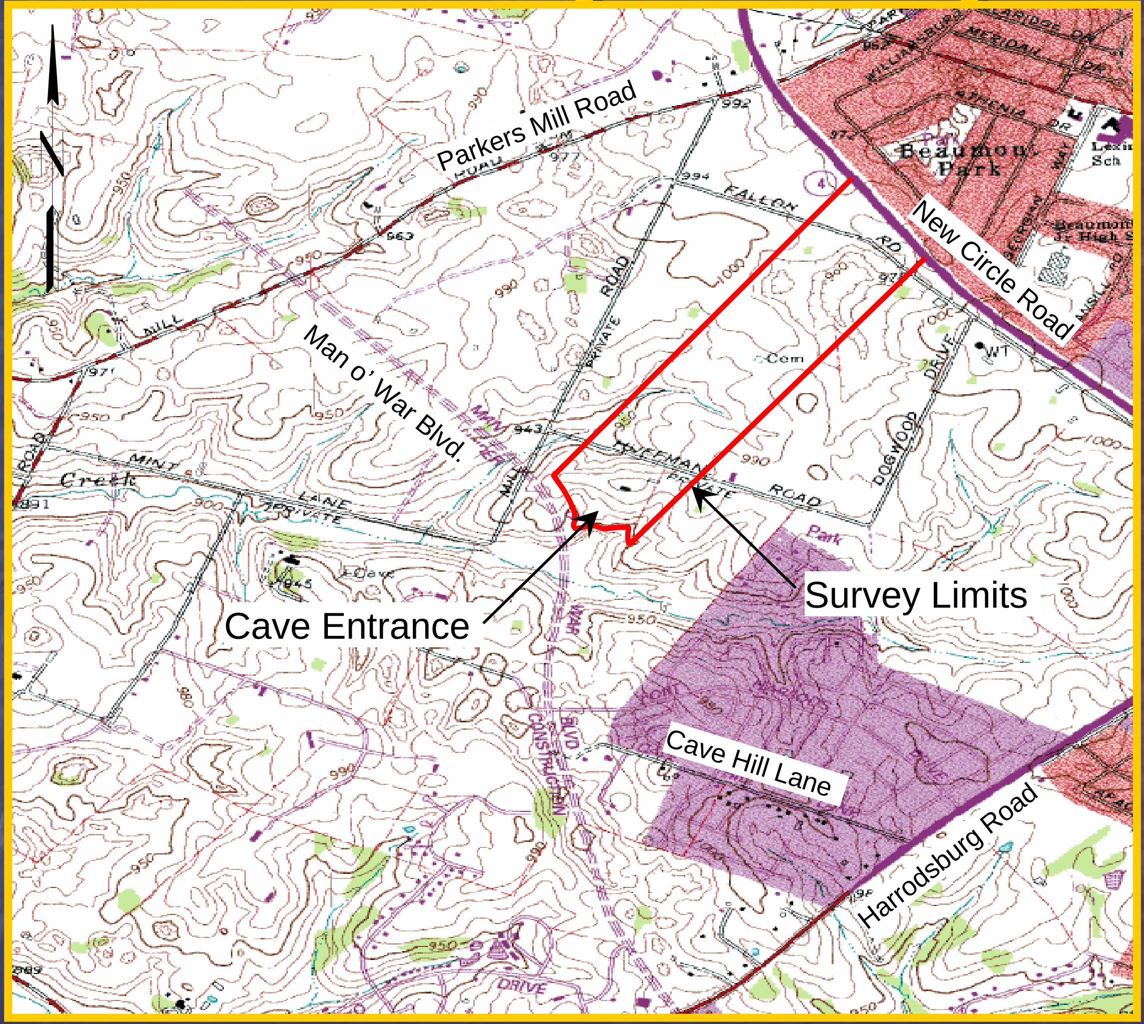

ORVSS XXXVII
Innovations in Exploration
Of Subsurface Voids

MSM ENGINEERS

Results of Microgravity Survey

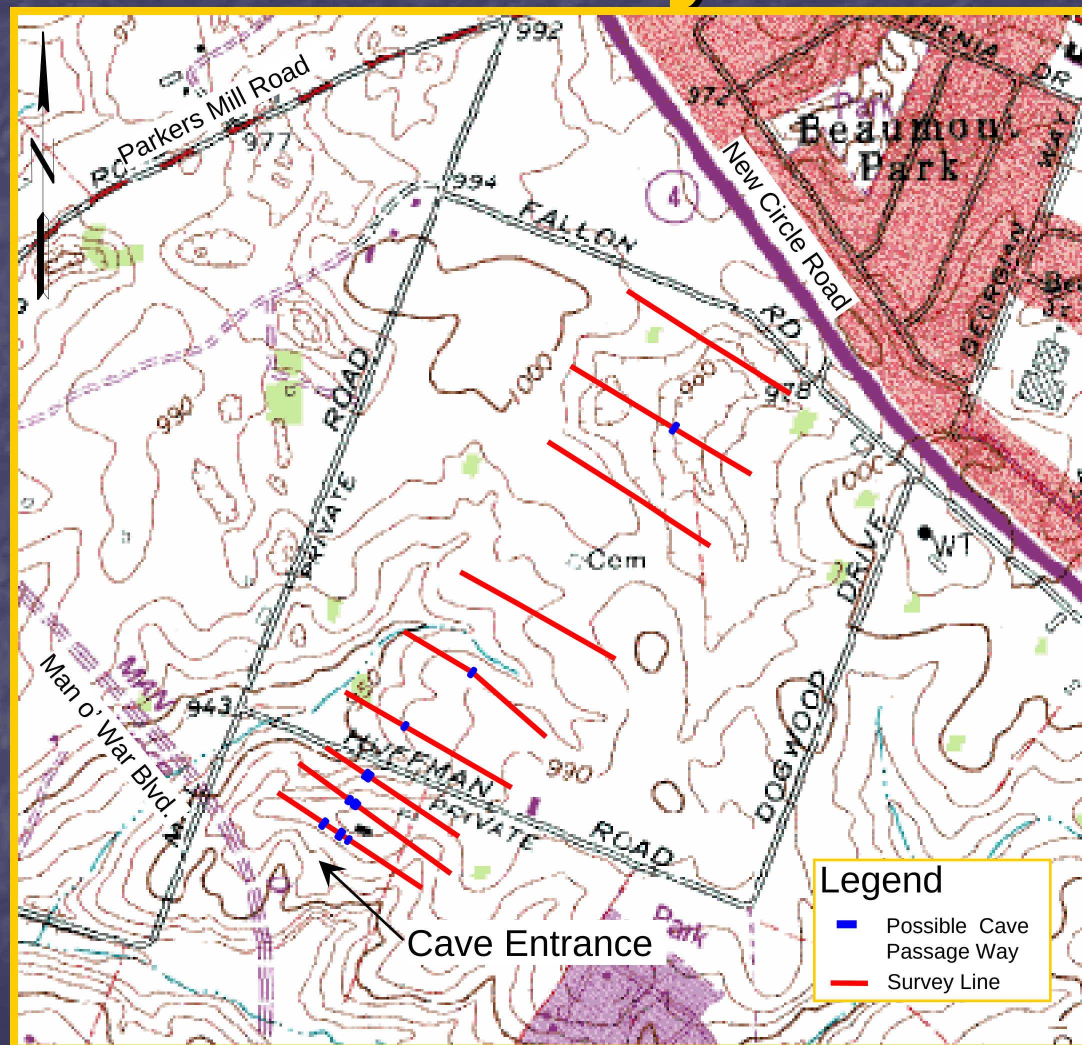

ORVSS XXXVII
Innovations in Exploration
Of Subsurface Voids

E N G I N E E R S

1990 Parrot, Ely & Hurt Engineers Cave Survey

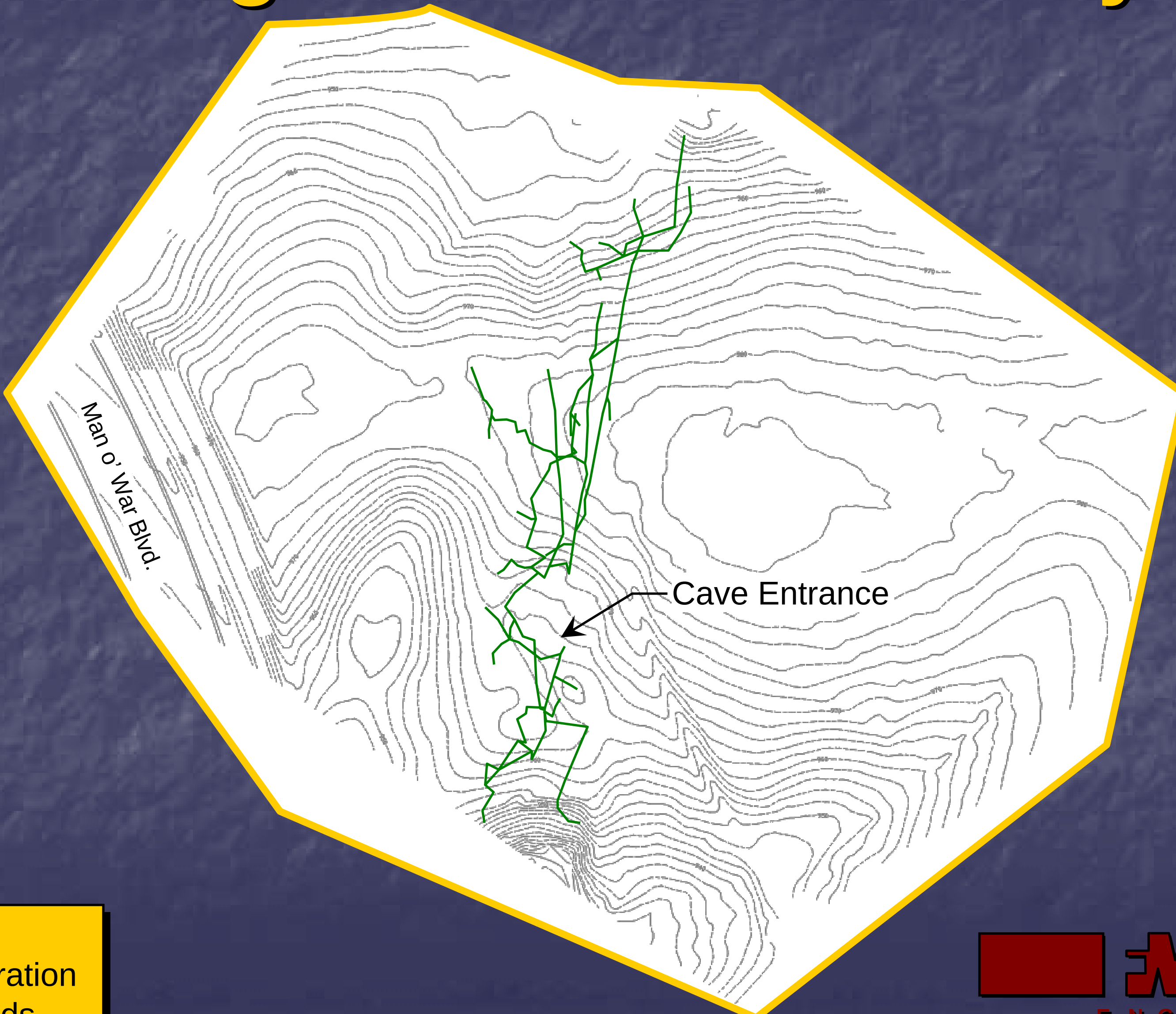

ORVSS XXXVII
Innovations in Exploration
Of Subsurface Voids

FMSM ENGINEERS

2002 FMSM CAVE SURVEY

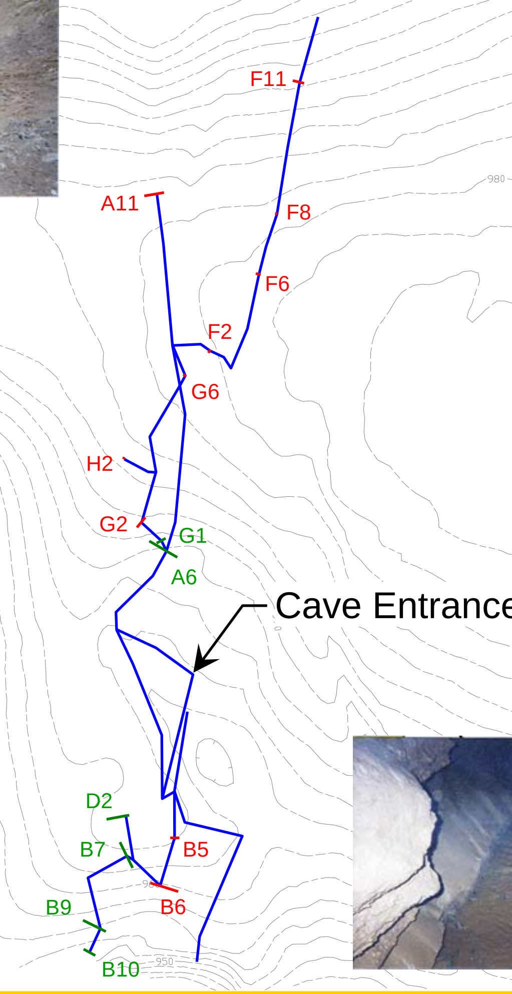

TRAVERSE POINT LOCATION TABLE

Traverse Point Number	Ceiling Elevation (Feet)	Floor Elevation (Feet)	Passage Height (Feet)	Passage Width (Feet)
A6	945.6	926.6	19.0	25.0
A11	921.5	920.3	1.5	16.0
B5	939.4	938.9	0.5	6.0
B6	942.5	942.1	0.4	23.0
B7	945.4	937.8	7.6	22.0
B9	945.8	939.8	6.0	20.0
B10	946.1	943.1	3.0	10.0
D2	945.2	941.2	4.0	18.0
F2	924.7	921.7	3.0	2.5
F6	933.4	931.4	2.0	4.0
F8	938.8	937.3	1.5	2.5
F11	938.5	937.0	1.5	9.0
G1	945.8	935.8	10.0	8.0
G2	936.9	935.4	1.5	10.0
G6	937.1	932.6	4.5	2.5
H2	932.5	926.5	6.0	2.0

Legend

- 2002 FMSM Cave Survey
- Ceiling Elev. Above 945.0 Feet
- Passage Height Less Than 2.0 Feet or Passage Width Less Than 2.5 Feet

ORVSS XXXVII
Innovations in Exploration
Of Subsurface Voids

FMSM ENGINEERS

Cave Survey Overlays

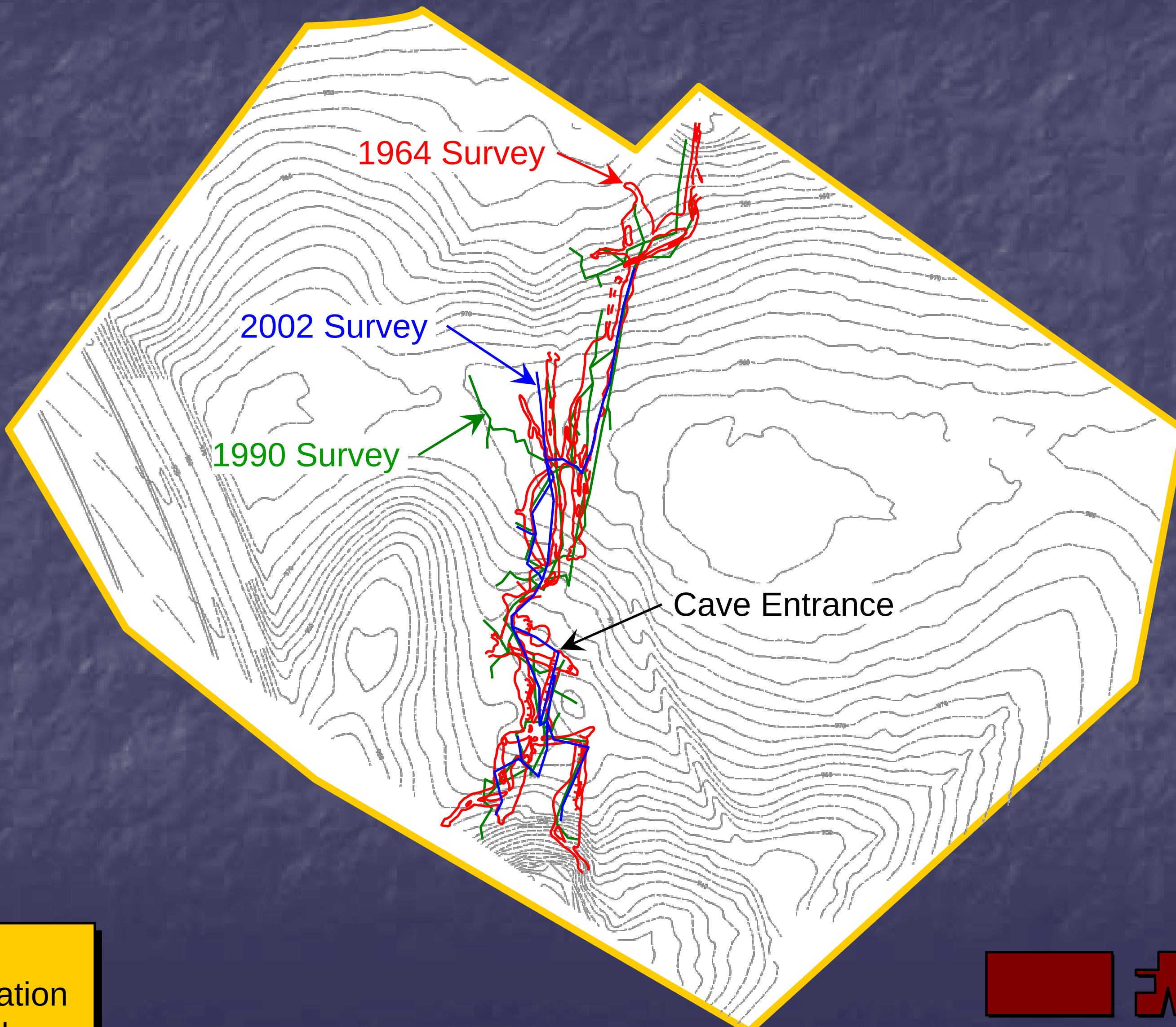

ORVSS XXXVII
Innovations in Exploration
Of Subsurface Voids

FMSM ENGINEERS

2003 FMSM Exploration

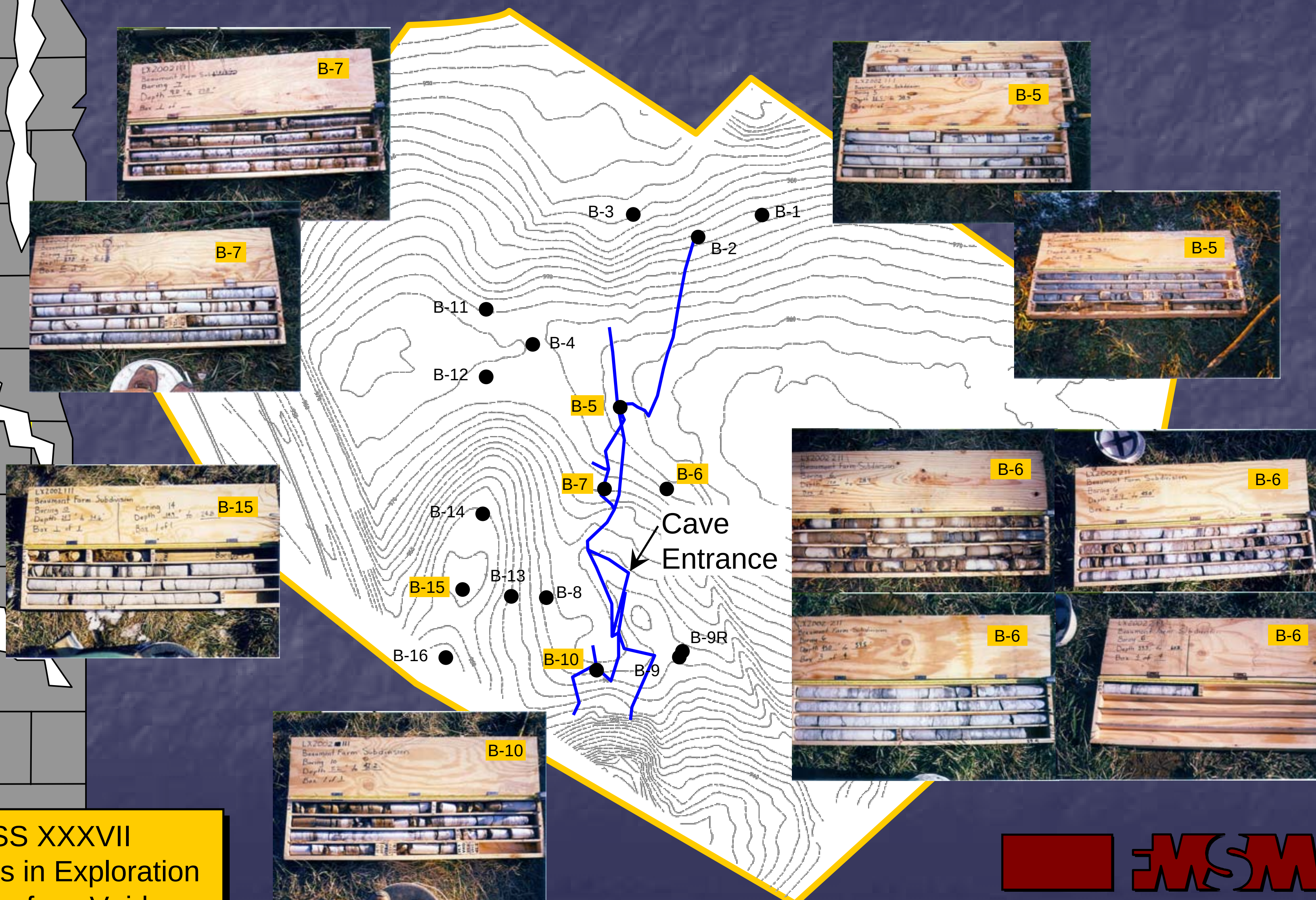

ORVSS XXXVII
Innovations in Exploration
Of Subsurface Voids

FMSM ENGINEERS

Limit of Recommended Non-Buildable Areas

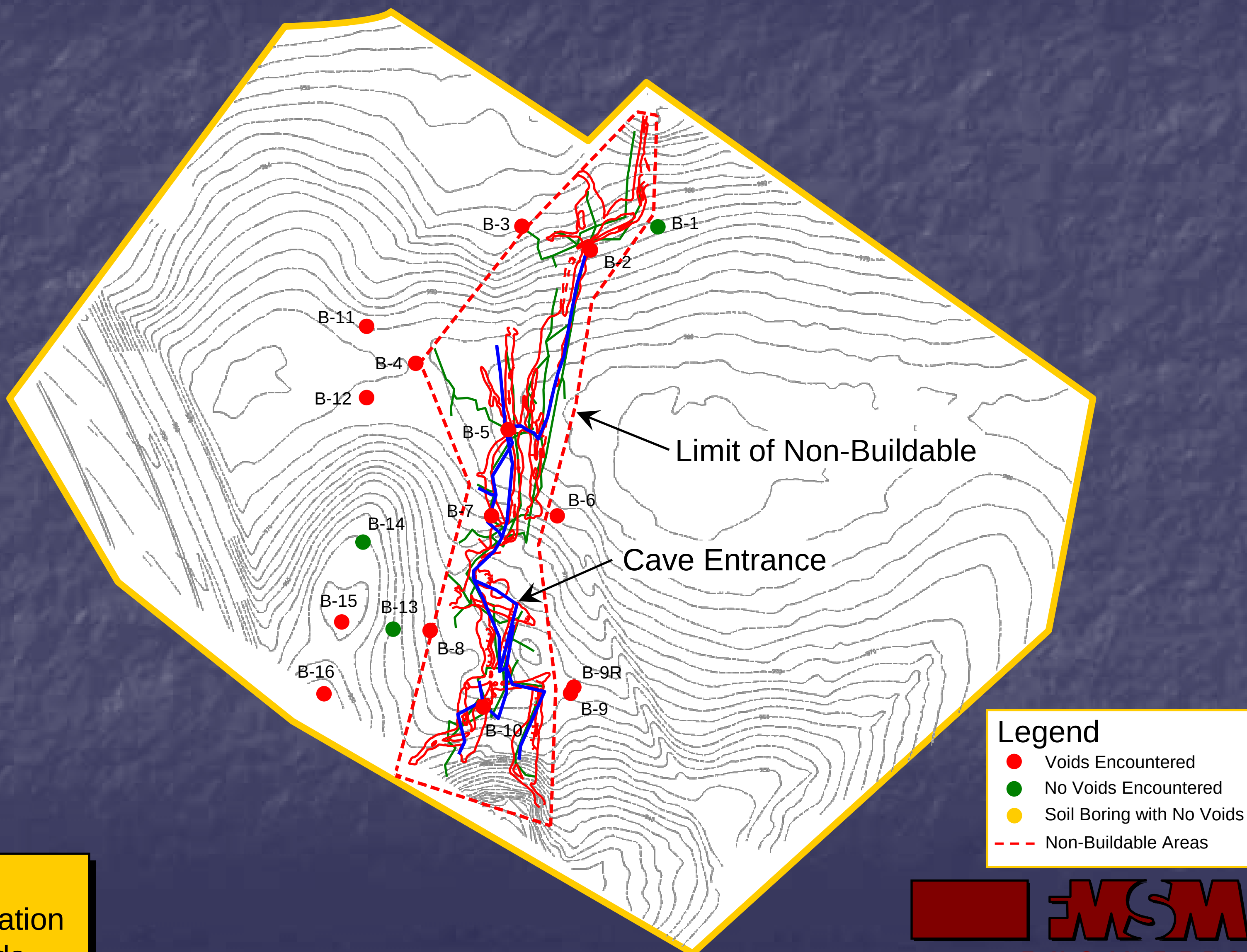

ORVSS XXXVII
Innovations in Exploration
Of Subsurface Voids

FMSM ENGINEERS

Initial Street Layout

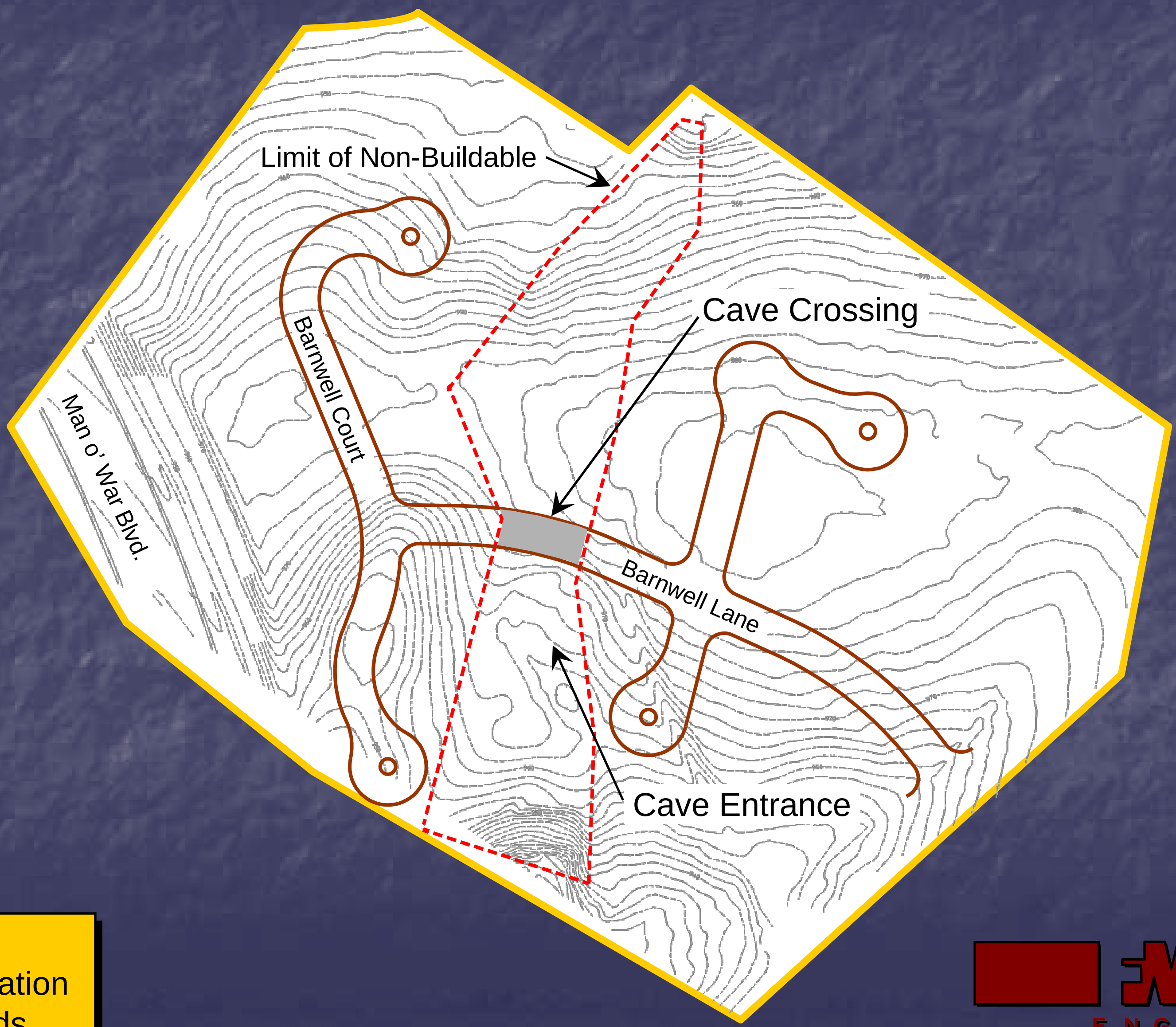

ORVSS XXXVII
Innovations in Exploration
Of Subsurface Voids

MSM ENGINEERS

2004 FMSM Exploration

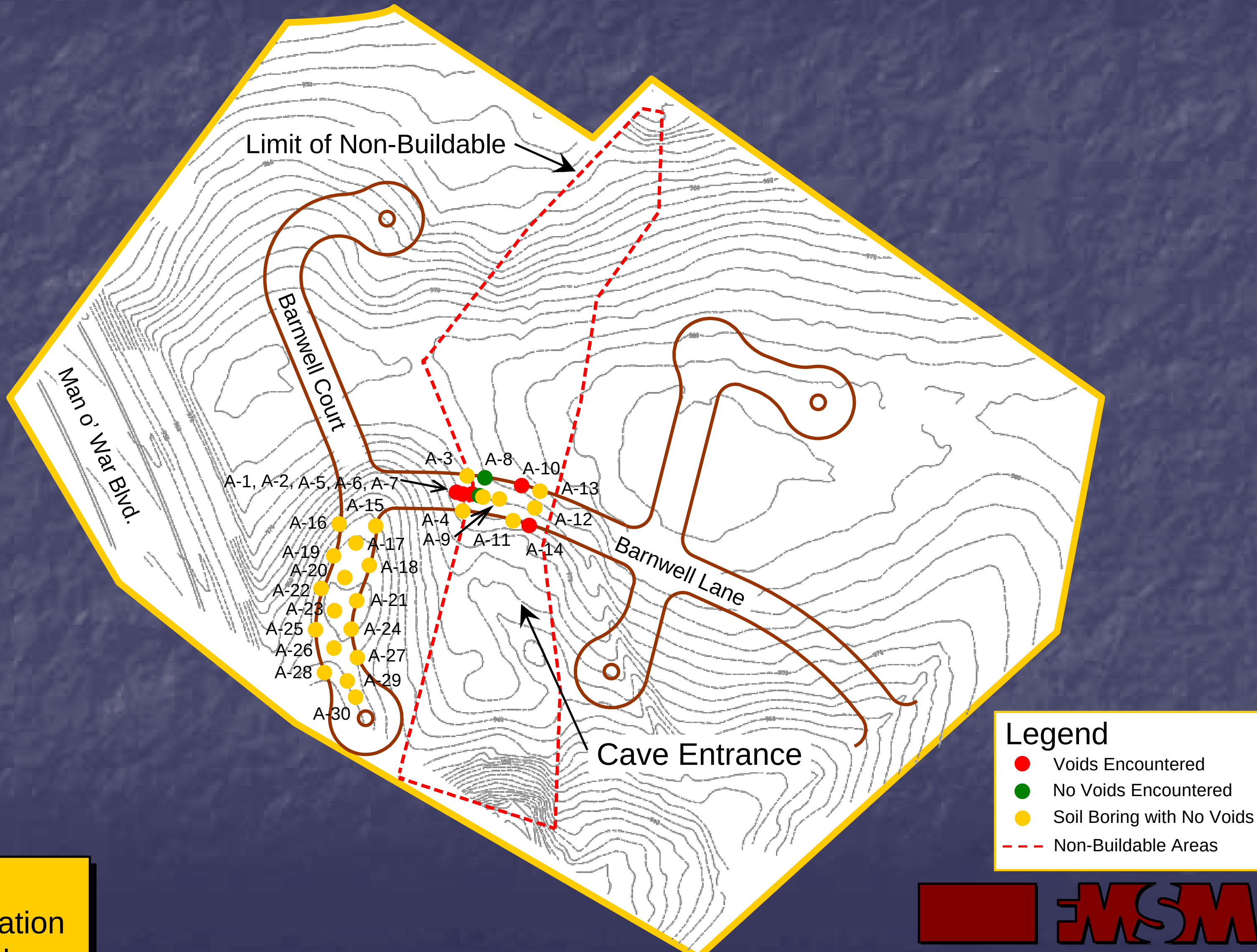

ORVSS XXXVII
Innovations in Exploration
Of Subsurface Voids

FMSM ENGINEERS

TV Exploration

Results of 2004 Exploration

Barnwell Lane

- Roof Rock consisted of hard limestone
- The Top of Rock surface was relatively flat
- Small voids and soil filled openings were encountered
- At Borings A-2 and A-5 only 7-Feet of roof rock available
- Largest void was 5-Foot thick and located in Boring A-5
- A 58-Foot soil filled zone was encountered in Boring A-5
- Non-Buildable limits should be extended

Barnwell Court

- Depth of rock varied
- No open throats observed
- No voids encountered within the soil

Extended Limit of Non-Buildable Area

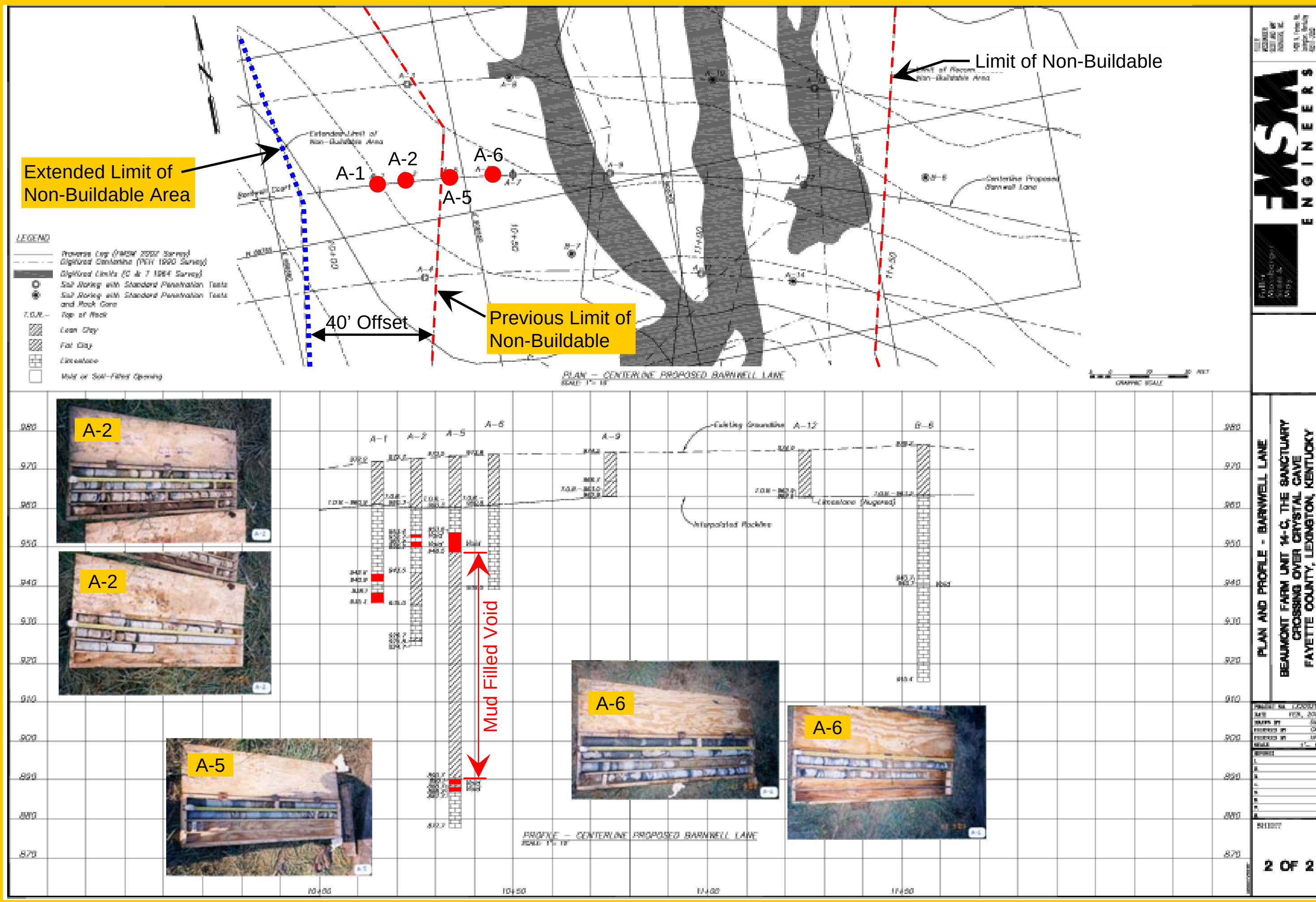

ORVSS XXXVII
Innovations in Exploration
Of Subsurface Voids

Revised Non-Buildable Area

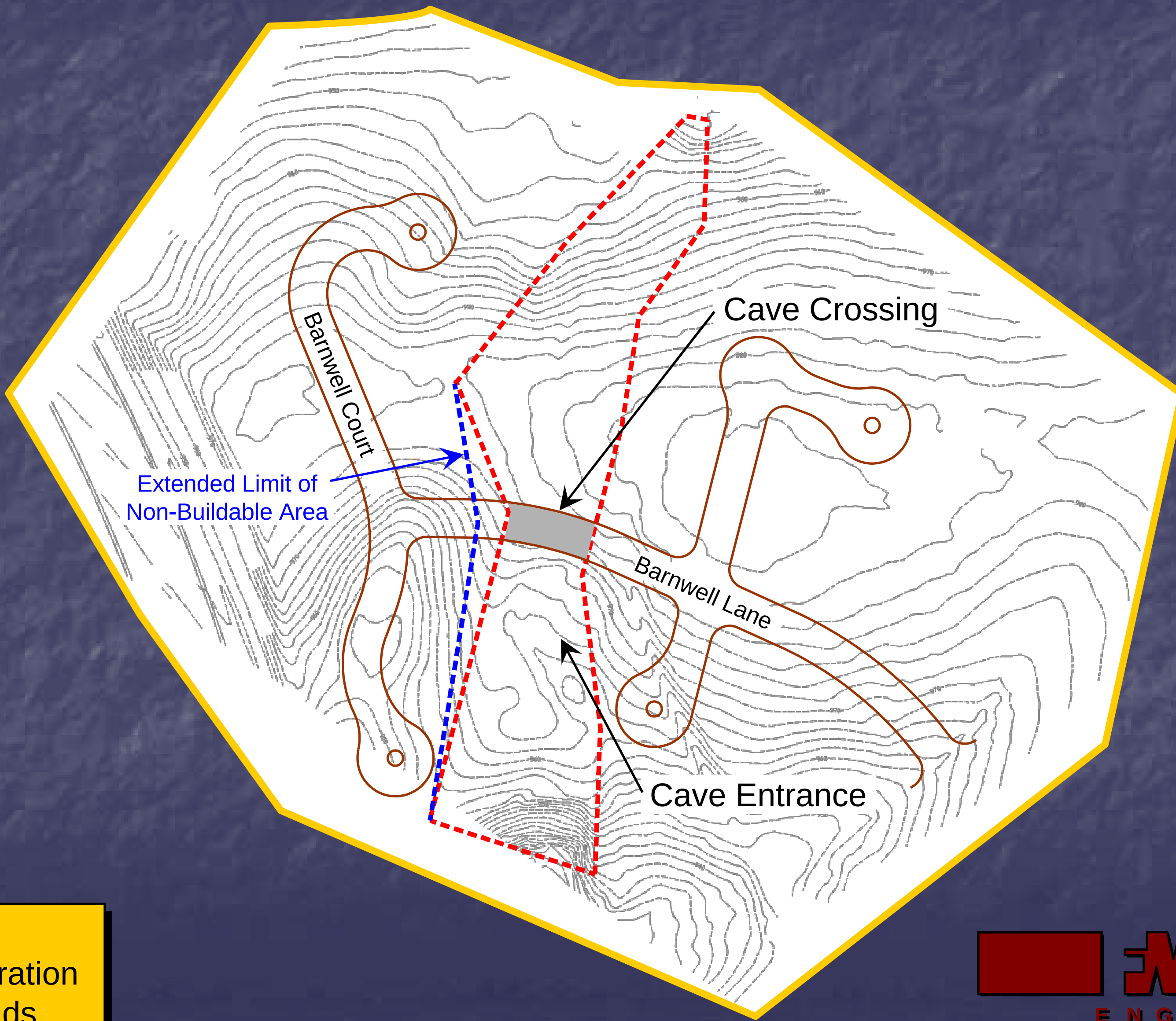

ORVSS XXXVII
Innovations in Exploration
Of Subsurface Voids

MSM ENGINEERS

Revised Street Layout

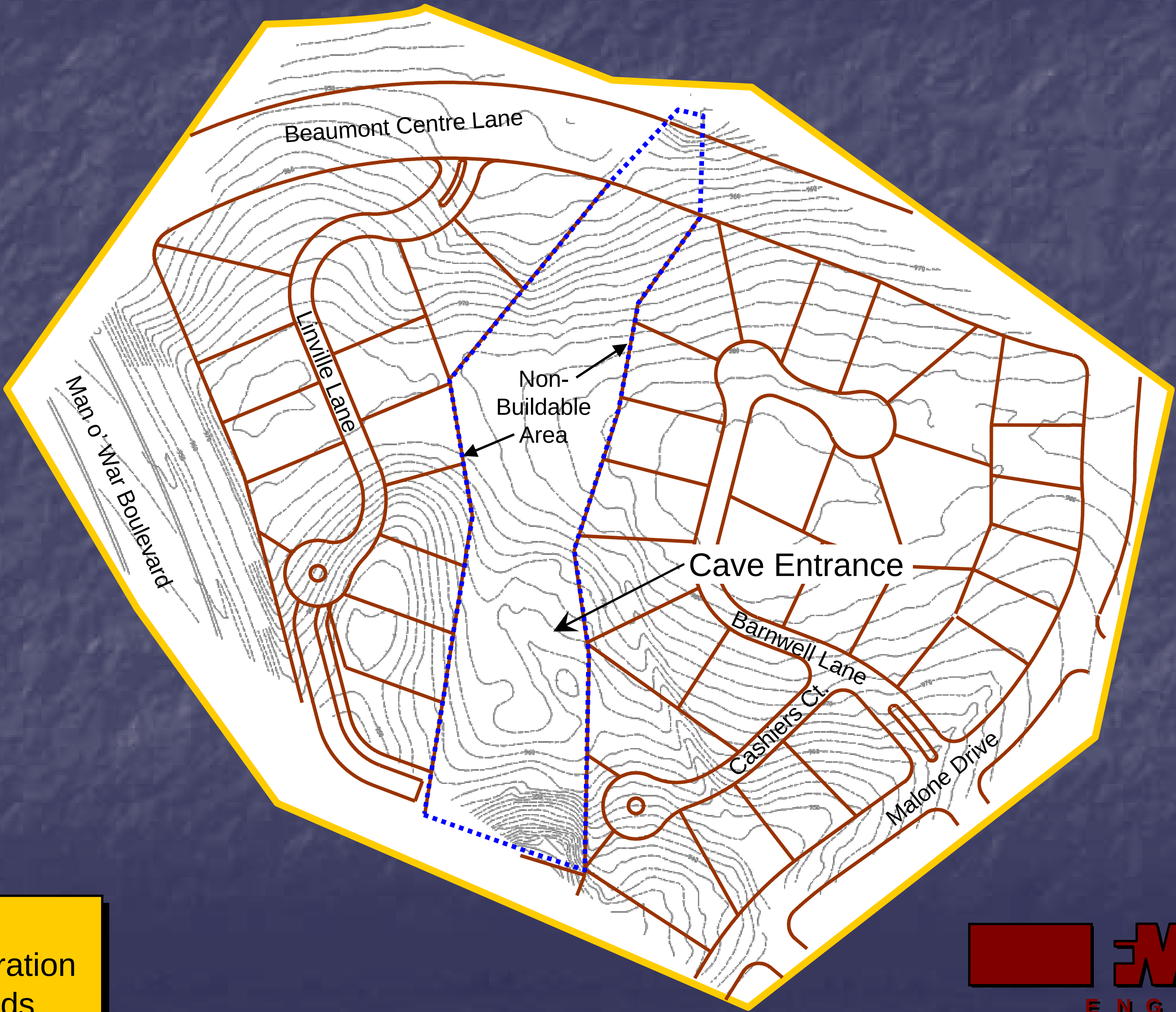

ORVSS XXXVII
Innovations in Exploration
Of Subsurface Voids

MSM ENGINEERS

2005 Construction Monitoring

ORVSS XXXVII
Innovations in Exploration
Of Subsurface Voids

FMSM ENGINEERS

Karst Treatment (Typical)

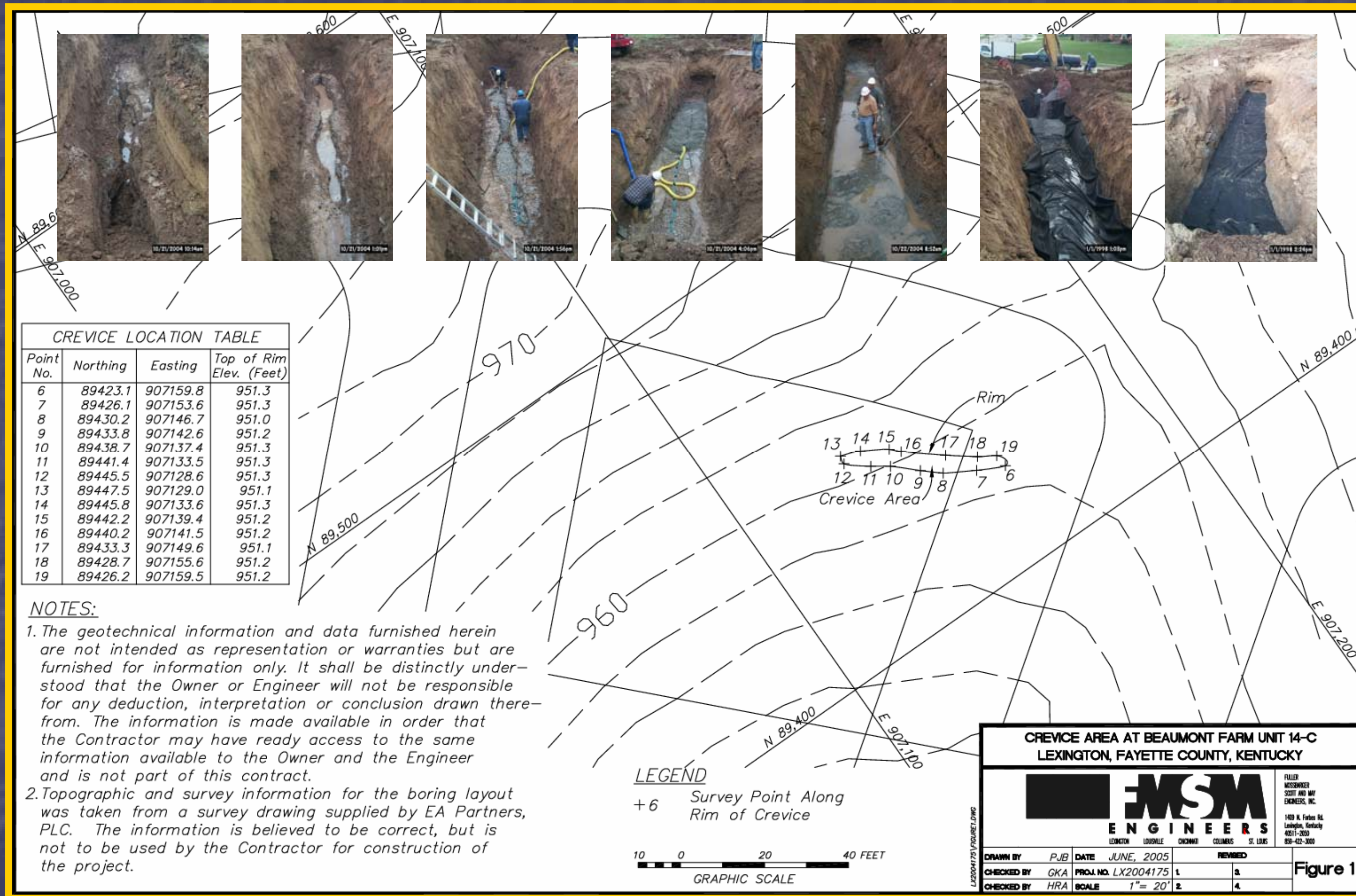

CREVICE LOCATION TABLE

Point No.	Northing	Easting	Top of Rim Elev. (Feet)
6	89423.1	907159.8	951.3
7	89426.1	907153.6	951.3
8	89430.2	907146.7	951.0
9	89433.8	907142.6	951.2
10	89438.7	907137.4	951.3
11	89441.4	907133.5	951.3
12	89445.5	907128.6	951.3
13	89447.5	907129.0	951.1
14	89445.8	907133.6	951.3
15	89442.2	907139.4	951.2
16	89440.2	907141.5	951.2
17	89433.3	907149.6	951.1
18	89428.7	907155.6	951.2
19	89426.2	907159.5	951.2

NOTES:

1. The geotechnical information and data furnished herein are not intended as representation or warranties but are furnished for information only. It shall be distinctly understood that the Owner or Engineer will not be responsible for any deduction, interpretation or conclusion drawn therefrom. The information is made available in order that the Contractor may have ready access to the same information available to the Owner and the Engineer and is not part of this contract.
2. Topographic and survey information for the boring layout was taken from a survey drawing supplied by EA Partners, PLC. The information is believed to be correct, but is not to be used by the Contractor for construction of the project.

FMSM ENGINEERS

Karst Treatment (Typical Section)

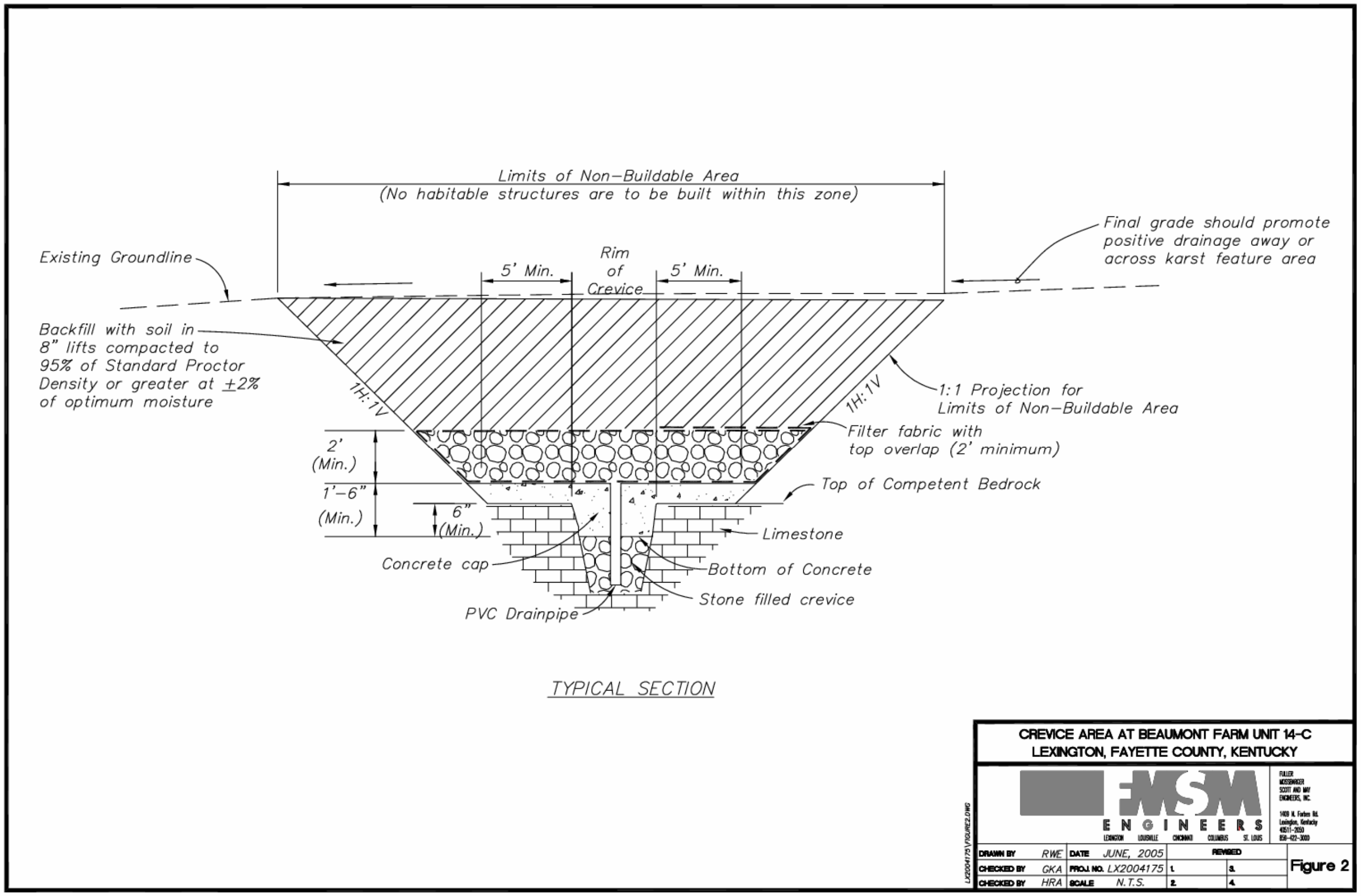

ORVSS XXXVII
Innovations in Exploration
Of Subsurface Voids

Cave Access/Entry

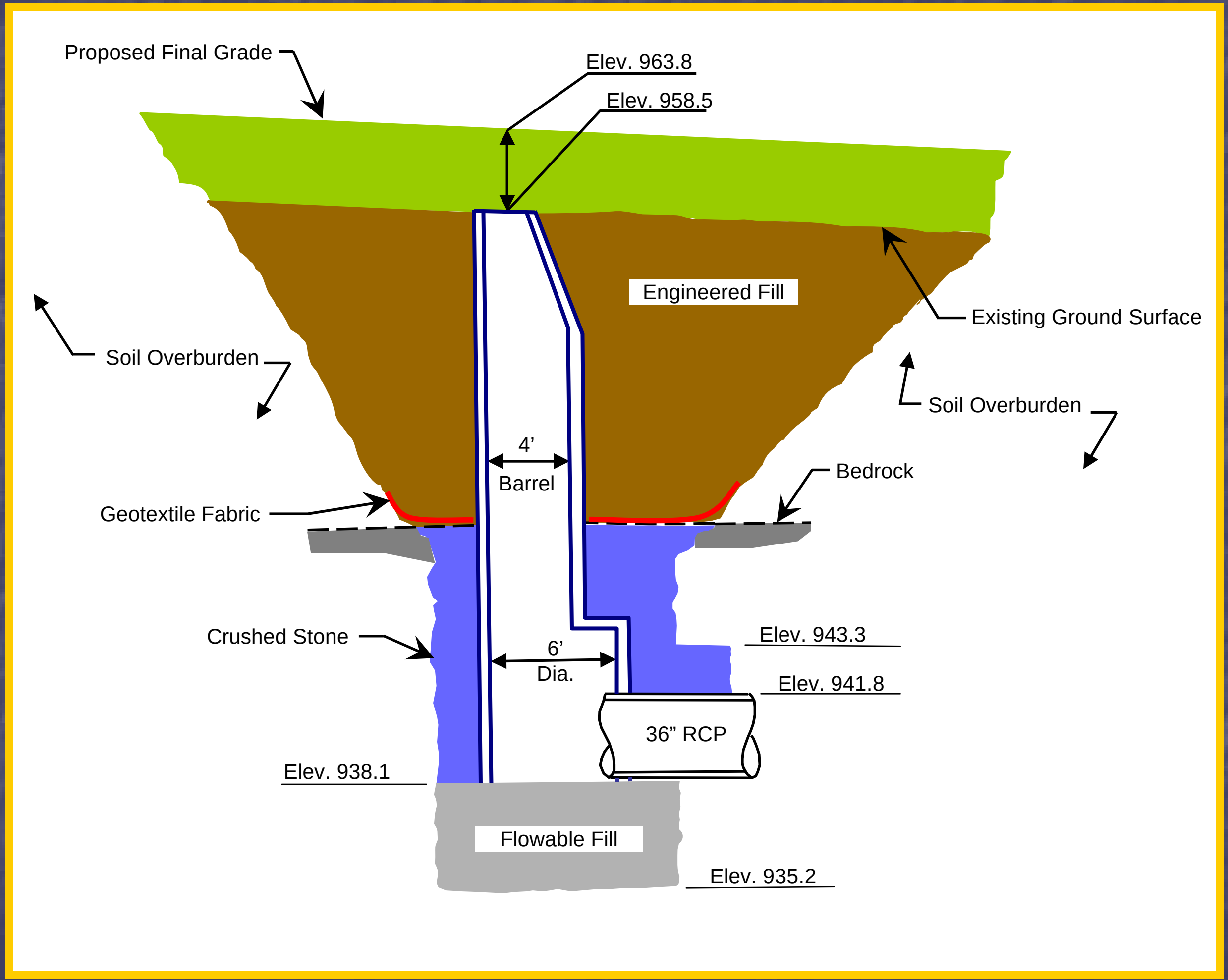

FMSM
ENGINEERS

Current Lot Development

ORVSS XXXVII
Innovations in Exploration
Of Subsurface Voids

MSM ENGINEERS

Project Summary

- **Land Development Over Karst Terrain Requires an Extensive Geotechnical Exploration**
- **Karst Features In Central Kentucky are Typically Sinkholes Which Can Be Explored & Treated**
- **A Combination of Exploratory Methods (Field/Cave Survey, Drilling, Microgravity & Resistivity Surveys) Should be Utilized**
- **Non-Buildable Areas Should be Constructed Around Karst Features**
- **FMSM Developed & Implemented the Following Procedures For Developing Beaumont Farm Around Cave Area**
    - Research/Document Review & Integration
    - Microgravity Survey
    - Cave/Field Survey
    - Subsurface Explorations
    - Construction Monitoring
    - Lot Specific Explorations
    - Site Specific Recommendations/Treatments

FMSM ENGINEERS

Any Questions ?

ORVSS XXXVII
Innovations in Exploration
Of Subsurface Voids

Special Thanks to:
Haymaker Development Company, LLC
EA Partners, PLC
and Mrs. Renee Flynn (FMSM) in the
development of this project / presentation.

NICHOLSON

Nicholson Construction Company
Midwest District Office

5945 West Main Street
Suite 102
Kalamazoo, MI 49009
Telephone: 269-353-8421
Facsimile: 269-353-8435
Web Site: www.nicholsonconstruction.com

Low Mobility Grouting Applications in Karstic Gypsum

by

Dan Thome, P.E., Member, ASCE and
Steve Elliott, P.E., Member ASCE

Published at:

Ohio River Valley Soils Seminar XXXVII
Lexington, KY
October 27, 2006

Low Mobility Grouting Applications in Karstic Gypsum

Dan A. Thome[1] P.E., Member ASCE and Steve Elliott[2] P.E., Member ASCE

ABSTRACT

Underneath the alluvial outwash deposits in much of Western Michigan lies sedimentary rock consisting of layers of limestone, sandstone, shale and gypsum. Karstic features have been found within the gypsum formations near the surface of the bedrock in Kent County and the surrounding areas. Excessive settlements from the voided gypsum have been observed on existing structures located along the Grand River in downtown Grand Rapids and some of the outer lying suburbs. A ground improvement method for remedying this type of karstic geology for both new and existing structures is to perform low mobility grouting (LMG) within the gypsum rock formation by installing vertical grout points over the questionable area. Micropiles can also be installed as deep foundation elements where there are higher structural design loads, utilizing the same drill hole as the LMG operation.

One of the advantages that LMG and micropiles have over other available foundation systems is their ability to be installed through difficult ground conditions not suitable for other techniques. Using specialized drilling methods, the drill casing can be advanced through man-made obstructions, cobbles, boulders, and deep into rock formations, which is typical of Western Michigan. Having this capability makes this technique an excellent choice for drilling in karstic formations where the casing can be advanced until conditions are encountered that confirms adequate bedrock. Where some projects may require the use of LMG to fill these voids, micropiles can serve a dual purpose by providing a structural deep foundation element as well as a mechanism for delivering ground treatment.

This paper will look at several case histories where LMG, with and without micropiles, was used in Western Michigan to treat the voided gypsum rock. The construction projects will cover both new and existing structures to include parking garages, buildings, schools, restaurants and bridges.

GEOLOGICAL SETTING

Overburden soils for Western Lower Michigan were predominantly deposited in glacial environments during the Pleistocene, the initial epoch of the Quaternary period. The upper soil strata consist mostly of stratified sand and gravel deposited from melt waters while the glaciers were retreating northward. Increased concentrations of gravel, cobbles and boulders are found within the outwash deposits near river valleys from the high water velocities. Occasionally, silt or clay layers will be found within the outwash deposits caused by periods of low flow from glacier melt waters.

[1] Project Manager, Nicholson Construction Company, 5945 W. Main St., Suite 102, Kalamazoo, MI 49015, dthome@nicholsonconstruction.com
[2] President, Materials Testing Consultants, 693 Plymouth NE, Grand Rapids, MI 49505

Glacial till is present beneath the majority of the glacial outwash deposits along the west side of the lower peninsula. The till was deposited by the glaciers as they advanced and retreated within the state. The majority of the till matrix is comprised of clay with varying amounts of sand, silt and gravel. Cobbles and boulders are also present within the till with random concentrations.

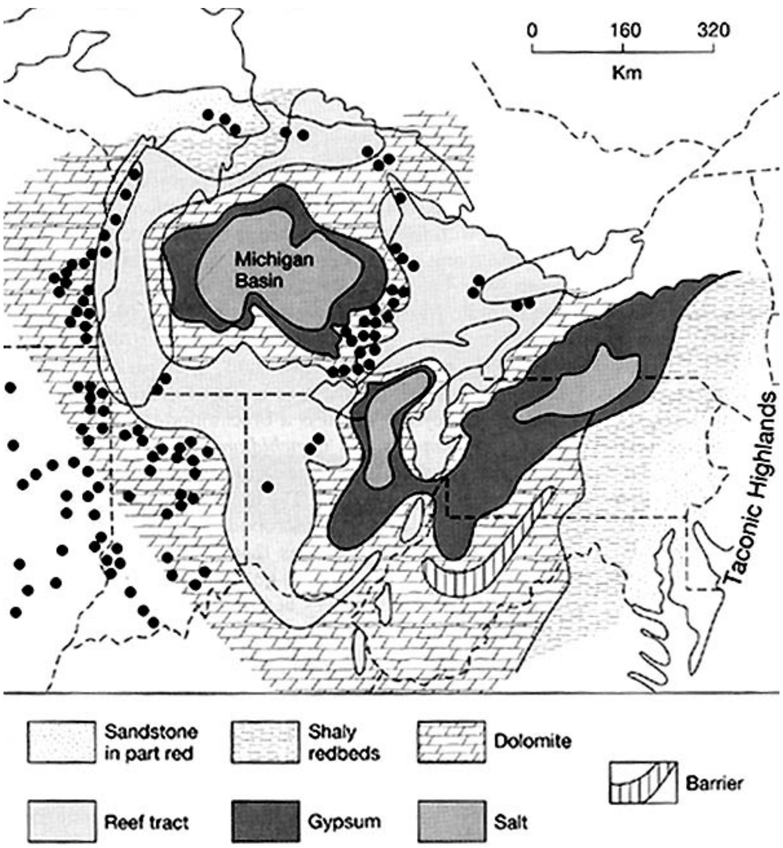

Figure 1: Sedimentary Rock Deposits - Michigan Basin

The upper bedrock layers were formed during the Paleozoic Era. These sedimentary rock strata consist primarily of limestone, sandstone, shale and gypsum. During the formation of these sedimentary rock deposits, the majority of the earth was flooded by sea water. Subsidence of the ground surface in the lower peninsula of Michigan formed an inland salt water lake known as the Michigan Basin. Over time the water evaporated causing the salt to precipitate into the underlying minerals and organic material. The varying degrees of minerals and organic matter created the stratified formations of limestone, sandstone, shale and gypsum, known as the Michigan Formation. Refer to Figure 1, which shows the Michigan Basin in relation to the surrounding states.

Gypsum deposits range in thickness from 4 to 20 feet throughout the Michigan Basin. Due to the concave geometry of the basin, the sedimentary rock of the Michigan Formation is closest to the ground surface near the perimeter of the basin and can be over 1,200 feet near the center. Figure 2 shows the approximate depth to the top of the Michigan Formation from existing ground surface. A high concentration of gypsum can be found near the bedrock surface in Kent County where gypsum mining operations have occurred since 1841. These deposits are susceptible to karstic solution cavities that could cause excessive settlements near the ground surface.

Figure 2: Depth to Michigan Formation

The solubility rate of gypsum in water is ten to twenty times more than limestone. The accelerated karstic features in gypsum require foundation solutions that quickly remedy the problem in existing structures or alleviate problems for new developments.

LOW MOBILITY GROUTING

Low mobility grouting (LMG) is defined as pumping low slump grout, generally with a slump of 0 to 5 inches, to enhance the overburden soils (compaction grouting) or to fill voids (karstic bedrock). The rate of pumping and slump will define what type of low mobility grouting will be performed. Compaction grouting uses grout with a slump of 2 inches or less and is pumped at a rate of less than 2 cubic feet per minute. Void filling applications use a grout with a slump of up to 5 inches, pumped at a rate of greater than 2 cubic feet per minute. LMG for void filling prevents excessive grout volumes associated with filling cracks and fissures within the rock by using a low slump sand cement mix rather than a low viscosity neat cement grout. This paper describes LMG applications that were performed for void filling in karstic gypsum rock located in Western Michigan.

Figure 3: Rotary Percussive Eccentric Drill Tooling

Void filling LMG applications are usually determined by excessive settlements at the ground surface or by previous experience within the known regional geology. Soil borings are performed for the new construction or near the existing subsidence to confirm the presence of gypsum near the bedrock surface. It is important to note that the voids causing the subsidence of the existing structures or those that would be problematic after new construction are not always found prior to starting the LMG program.

LMG consists of drilling steel casing to either a known tip elevation within the bedrock based on previous geotechnical exploration or using the grout point itself to intersect the voided layer and find sound rock. Steel drill casing is advanced to the tip elevation using a rotary percussive eccentric duplex drilling system, a drilling technique that has come from the oil industry and reconfigured for specialty geotechnical construction. Low slump grout is then pumped through the steel casing to the tip until a cutoff pressure is reached or excessive ground heave is noted near the grout point. The steel casing is withdrawn in 2 foot intervals satisfying the refusal criteria at each stage. Refer to Figure 3, which is a picture of the rotary percussive eccentric duplex drilling system.

MICROPILES

Micropiles are drilled in deep foundation elements typically ranging in diameter from 5 to 12 inches. Traditionally in the United States, micropiles consist of a permanent steel casing, a central steel reinforcement bar and cement based grout. The drill casing is typically left in place through the unsuitable overburden material shedding the axial load in friction to a competent soil or rock stratum below the casing. With the load shed in friction, micropiles can resist both axial compression and tension loads. Permanent steel casing left in the upper portion of the micropile can also be designed to resist lateral loads with limited lateral deflection.

Micropiles tend to be more economical than other deep foundation systems when there are one or more installation challenges on a project. These challenges can be separated into two major descriptions: physical and geotechnical. The following is a list of potential physical challenges encountered for deep foundation installation:

- Limited overhead clearance
- Vibration, settlement or noise sensitivity
- Limited plan access or the desire to work multiple operations
- Installation of foundation elements close to or through existing footings, walls or other structures

Geotechnical challenges that warrant micropile technology are:

- Variable weathered rock or karstic rock (voided or soil filled solution cavities)
- Cobbles, boulders or glacial till
- Uncontrolled fill containing natural or man-made obstructions
- Granular soils below the water table

In addition to the site challenges, potential downdrag forces on the micropiles can be eliminated when low mobility grouting has filled voided rock strata that could have collapsed within the cased length of the pile.

Codes and manuals for designing micropiles are beginning to be published from federal, state and international organizations. The following are a list of current publications with specific design guidelines for micropiles:

- FHWA-SA-97-070 - 2000
- Massachusetts Building Code 1998 – Section 1820.6 - Small Diameter Grouted Piles
- International Building Code - 2006

CASE HISTORIES

Several case histories are available to describe the various low mobility grouting applications that have occurred in Western Michigan. These projects will be separated into new construction and existing structures.

NEW CONSTRUCTION

Grand Rapids Convention Center

The Convention Center is located along the east bank of the Grand River in downtown Grand Rapids. Construction of the original structure occurred in the early 1980s on a site that previously contained industrial facilities and the Welsh Auditorium. Excessive settlements of portions of the original structure were discovered in 1992. Geotechnical exploration near the subsidence area revealed voided gypsum approximately 40 feet below the ground surface. 1,700 cubic yards of low mobility grouting was used to fill the voided gypsum prohibiting further movement.

Expansion and renovations to the existing convention center in 2002 prompted the need for a deep foundation system due to the loose alluvial deposits within the overburden soils. Regardless of the deep foundation element selected, LMG was specified to a predetermined tip elevation in order to fill any potential voids within the karstic gypsum rock formation based on the previous settlements found on the site.

Construction for the expansion was separated into three phases. The first two phases were performed by other contractors consisting of a combination of drilled caissons and micropiles. The micropiles were installed in limited access situations while the caissons were installed in areas of unrestricted access and headroom. LMG was performed within each micropile and caisson.

The third phase of construction, performed by Nicholson, consisted of low mobility grouting and micropiles. The total number of LMG micropiles for this phase was 344, 100 ton piles at an average depth of 52 feet from ground surface. In addition sixteen LMG points were placed at the addition close to where the subsidence in 1992 occurred. LMG with micropiles was chosen for the third phase of construction over caissons due to the following factors:

Grand Rapids Convention Center

- Ability to penetrate man-made or natural obstructions without additional associated costs
- Drilling technique allowing for the installation of the micropile while simultaneously performing LMG
- Smaller installation equipment allowed for more operations onsite condensing the overall construction schedule
- Reduced spoils due to smaller hole sizes associated with contaminated soils

State Road M-78

The Michigan Department of Transportation replaced the bridge over the Battle Creek River on state road M-78 just west of the city of Bellevue. The previous bridge was originally constructed in the 1970s and founded on shallow foundations. Geology at the project consisted of primarily sand and gravel glacial outwash deposits within the overburden and stratifications of limestone and karstic gypsum. Deep foundations were required for the bridge because it was a scour critical structure due to recent flood events on the Battle Creek River. A total of 77, 60 ton micropiles were installed in the three cofferdam structures after demolition of the existing bridge and foundations due to the karstic gypsum rock.

State Road M-78

Alticor Project & Grand Valley State University Parking Garage

LMG and Micropiles were specified for both the Alticor Project and the Grand Valley State Parking Garage due to their geographical proximity to the Grand Rapids Convention Center. Geotechnical explorations for both projects verified the presence of gypsum rock near the bedrock surface, but were not as voided to the degree as the gypsum underneath the convention center. Due to the high solubility of the gypsum, micropiles were installed to protect the structures from future settlement if the rock were to become more severe.

The Alticor Project was located approximately 500 feet south of the Grand Rapids Convention Center on the same side of the Grand River. Construction for the Alticor Project was separated into three major structures: the main hotel, parking garage and plaza. A total of 729 LMG micropiles, with design loads ranging from 100 to 200 tons to depths up to 65 feet were installed for the Alticor Project.

Grand Valley State University decided to construct a parking garage at their downtown Grand Rapids location. The site was located near the convention center on the opposite side of the Grand River adjacent to railroad tracks. LMG with micropiles were originally designed for the stairwells, where higher concentrated loads were present over the gypsum rock. A cost analysis concluded that substituting LMG micropiles versus over excavation with shallow foundations on engineered fill would be more economical due to the temporary shoring that would have been required near the railroad tracks. The parking garage required the installation of 133, 100 ton LMG micropiles.

EXISTING STRUCTURES

Calvin Christian High School

Calvin Christian High School

Calvin Christian High School was originally built in the 1960s in Grandville, a southwestern suburb of Grand Rapids. An addition on the southeast side of the building was built in 1998. Approximately five years after the addition was constructed, excessive settlements were noted in the new structure. Further geotechnical investigation confirmed the original geological profile consisting of silty sand within the overburden and sedimentary limestone, shale and gypsum within the exploratory depths of the bedrock. The settlement was thought to be within the granular overburden, but did not rule out the possibility of voided gypsum rock. Helical pier foundations were connected into the existing shallow foundations within the addition to remedy the solution.

Settlement after the helical pier retrofit gradually continued over the next few years. The geotechnical consultant concluded that the settlements must be the result of voids within the gypsum rock underneath the building and preceded to layout a low mobility grouting program for the new addition. It was determined that micropiles would not be required due to low building loads from the addition as long as the voids were filled.

A total of 28 LMG points were installed within the disturbed area on an average rectangular spacing of 8 feet. Each grout point was extended to a depth of 50 feet, gradually removing the drill casing and pressurizing with low mobility grout for the bottom 35 feet of the hole until either the pressure criteria was met or heave was noted at the concrete floor. The upper 15 feet was simply tremied full to minimize the negative impacts that the helical piers may have had on the structure. Continuous survey monitoring was performed throughout the grouting program to verify heave or excessive subsidence.

Voided gypsum was encountered in almost all of the LMG points. The grouting program filled all of the voids within the gypsum rock and consolidated the loosened granular material within the overburden. Settlement of the addition was impeded, with existing cracks in the brick mortar closed due to the slight heave created by the LMG grouting operation. Discussions with the school superintendent and maintenance department described an existing well that was within 50 feet of the building addition that was drawing water from rock formation. Periodic cleaning of the well screen produced rock chips, which may give some validation to the well promoting a higher solubility rate within the gypsum rock.

Arby's Restaurant

Nicholson received a call from a local contractor requesting a price for performing low mobility grouting in the drive through lane at an Arby's Restaurant in Grandville. Geotechnical investigation of the existing structure concluded subsidence due to voided gypsum rock.

A total of five grout holes were drilled approximately 10 feet apart centered at the drive through window and following the drive up lane in either direction. Each grout point was extended to a depth of 40 feet, gradually removing the drill casing and pressurizing with low mobility grout until either the pressure criteria was met or heave was noted at the concrete pavement. All voids within the gypsum were filled during the LMG program and the settlement cracks within the existing structure tended to close due to the grout pressures that were recorded.

ACKNOWLEDGEMENTS

The authors would like to thank the numerous owners and design consultants who provided the forward thinking to allow the use of low mobility grouting technology and micropiles to be used at the projects mentioned above.

REFERENCES

Pearlman, S. L., "Pin Piles for Structural Underpinning", Proceedings of the 25th Annual Deep Foundations Institute Meeting, October 2000.

Tarquinio, F. S. and S. L. Pearlman, "Pin Piles for Building Foundations", Proceedings of the 7th Annual Great Lakes Geotechnical and Geoenvironmental Conference, May 1999.

Tarquinio, F. S. and S. L. Pearlman, "Pin Piles in Karst Topography", Proceedings of the 8th Multidisciplinary Conference on Sinkholes and the Engineering Environmental Impacts on Karst, April 2001.

Fitzgerald, C. and D. Lewis, "Installation of Drilled Cased Micropiles Using Low Mobility Grout", Proceedings of the 12th Annual Great Lakes Geotechnical and Geoenvironmental Conference, May 2004.

Schaetzl, Randall J., Evaporites: Gypsum And Halite (Rock Salt). Retrieved September 25, 2006, from Michigan State University, Department of Geography Website: http://www.geo.msu.edu/geo333/evaporite.html

Schaetzl, Randall J., Gypsum. Retrieved September 25, 2006, from Michigan State University, Department of Geography Website: http://www.geo.msu.edu/geo333/gypsummining.html

Heinrich, E. William, (1976). The Mineralogy Of Michigan, [Electronic version], Bulletin 6.

Tarhule-Lips, Rozemarijn F.A., (2001) Cave Development Rates Of Gypsum Caves In Oklahoma: Preliminary Results, [Electronic version]

Presentation

Three Case Studies:

1. Assessment of karst features at two sites in Missouri, using the resistivity method
2. Investigation of sinkhole, Nixa Missouri, using the resistivity and MASW methods
3. Investigation of karst terrain, Lexington Kentucky, using multiple geophysical methods

Case Study #1:

ASSESSMENT OF KARST ACTIVITY AT HIGHWAY CONSTRUCTION SITES IN GREENE AND JEFFERSON COUNTIES, MISSOURI, USING THE ELECTRICAL RESISTIVITY METHOD

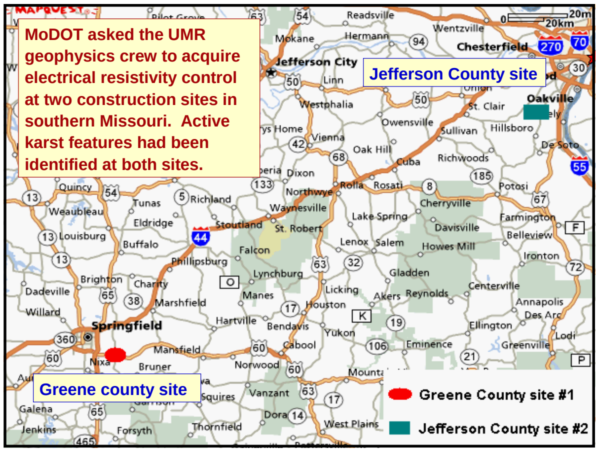

Located at the proposed intersection of Route 125 over Route 60.
The MoDOT district geologist identified several active sinkholes (narrow-throated; ~1.5 ft diameter tubular-shaped voids; undetermined depth.
Maintenance records also indicated that relatively small volumes of fill had been placed into subsidence features within the existing DOT ROW on an irregular and as needed basis.

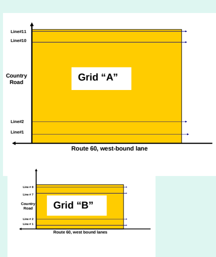

The district geologist was concerned that the small active sinkholes might be connected to larger air-filled voids that could compromise the integrity of the planned highway intersection. He authorized the acquisition of two grids of electrical resistivity profiles.

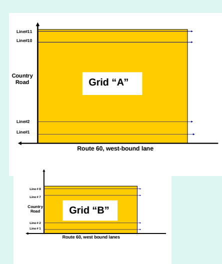

It was anticipated that such cavities would have developed along solution-widened joints, so the resistivity profiles were oriented west-east effectively perpendicular to the NNW-trending dominant joint system.

Greene County

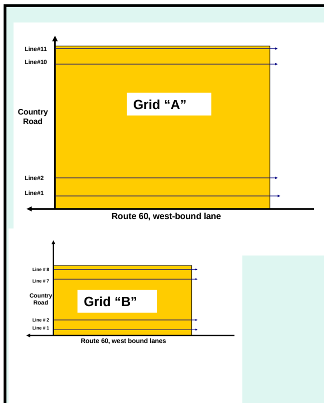

Two grids of electrical resistivity profiles were acquired at the Greene County site. Grid "A data, consisting of 11 profiles spaced at 25 ft intervals, were acquired using an electrode spacing of 5 ft.
Grid "B' data, consisting of 8 profiles spaced at 10 ft intervals, were acquired using an electrode spacing of 3 ft.

Greene County

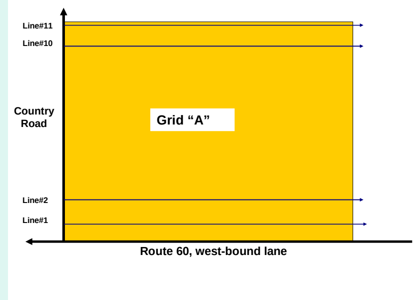

Grid "A" (11 W-E traverses, spaced at 25 ft intervals) encompasses the current Route 60 ROW, the current Route 125 ROW and the area across which a planned westbound Route 60 exit ramp will extend. The 2-D profiles were acquired using a 40-channel SuperSting Resistivity unit, a dipole-dipole array configuration and an electrode spacing of 5 ft.

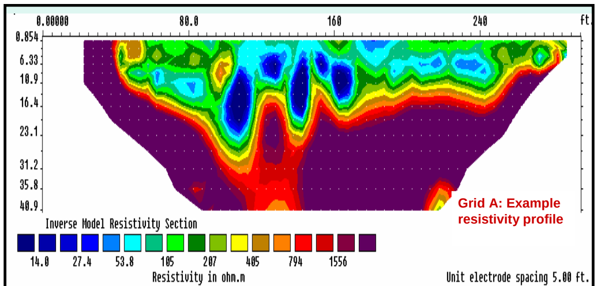

Grid A: Example resistivity profile

Processed resistivity profiles consist of rectangular pixels with widths of 5 ft and heights that vary from 2 ft (min. depth) to 5 ft (max. depth). During processing each pixel was assigned an average "resistivity" value. The pixel size is one estimate of the upper end of spatial resolution.

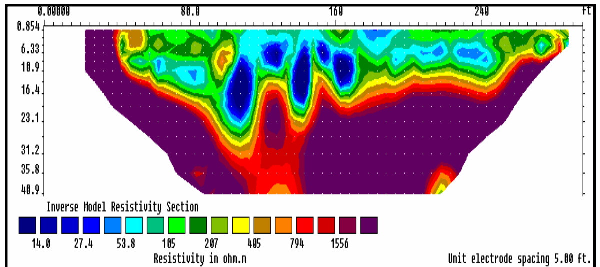

Geologic interpretation was relatively straightforward.

1. Units with resistivities >405 ohm-m were mapped as limestone
2. Units with resistivities <105 ohm-m were mapped as moist soil or clay.
3. Units with resistivities >105 ohm-m and <405 ohm-m were interpreted as transitional zones consisting of moderately to intensely fractured and/or weathered limestone with clay in-fill.

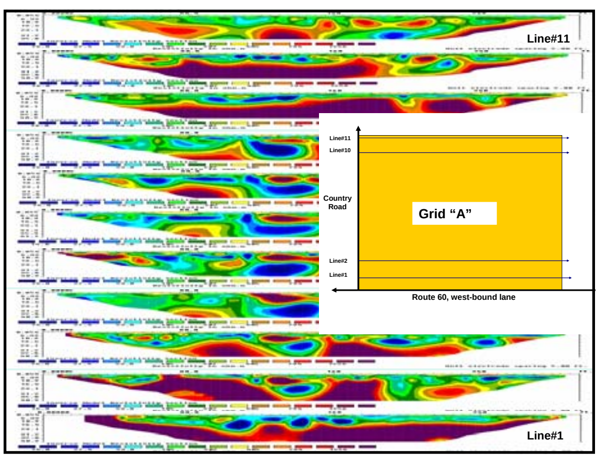

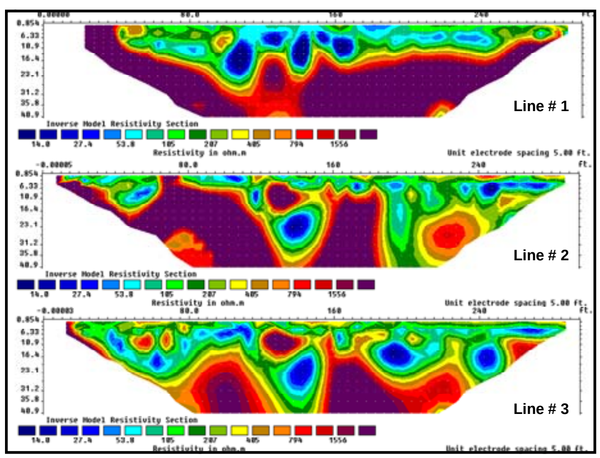

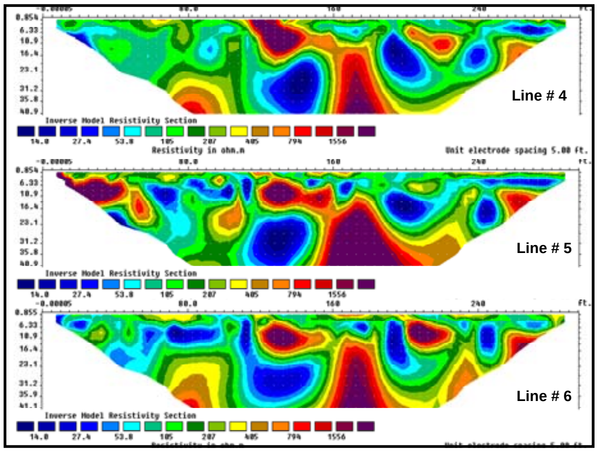

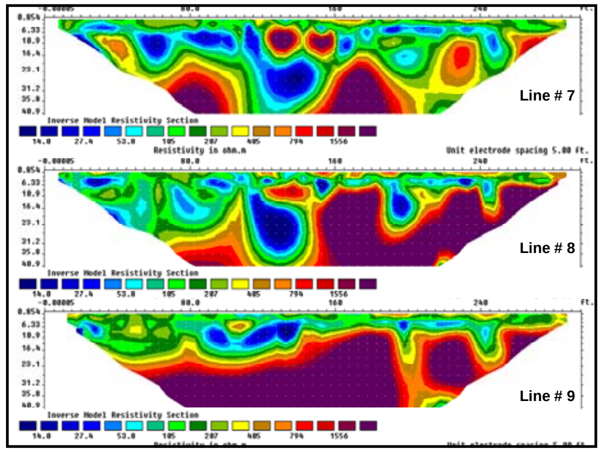

The interpreted resistivity data were used to generate a 3D image of bedrock.

Bedrock is dissected by four prominent solution-widened joints.

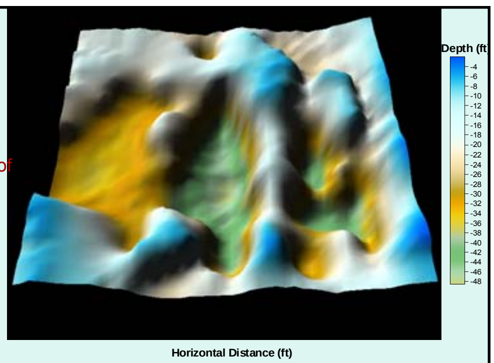

Solution-widened joints of most concern to MoDOT are those that underlie the planned westbound off-ramp. These features are of concern because thick clay in-fill could densify under load.

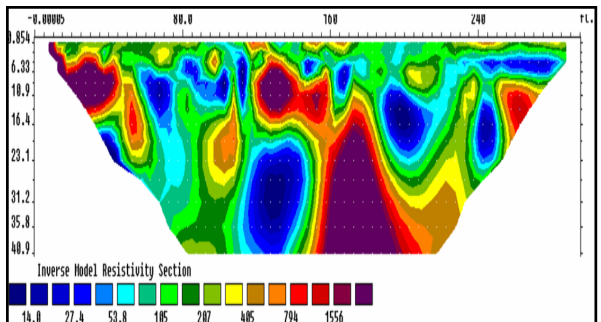

Bedrock is overlain by soil or clay, and in places by relatively continuous limestone lenses and intervening clay.

Bedrock is overlain by soil or clay, and in places by relatively continuous limestone lenses and intervening clay.

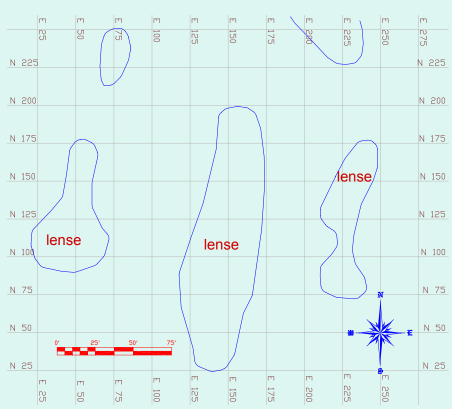

The bedrock model correlated reasonably well to acquired borehole control (20 boreholes).

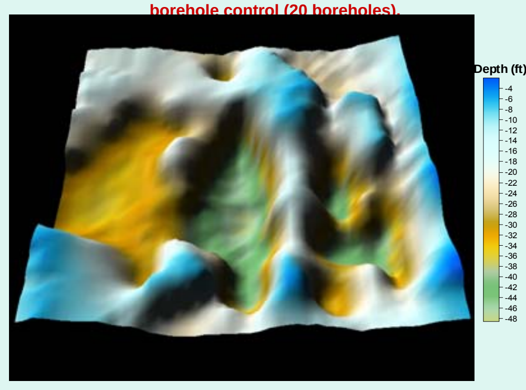

Geologic model correlates well with borehole data (20)

Borehole	Borehole depth (ft) to bedrock or remnant	Resistivity depth (ft) to bedrock or remnant
2	1 (remnant)	1' (remnant)
4	11.7 (remnant)	11 (remnant)
5	10.5	14
8	1 (remnant)	3 (remnant)
14	32.6	32
15	37.9	32
17	25.2 (clay 30.7 - 41.5)	17 to 30
18	12.8	15
19	26.7	>40
20	28.4	26 to 40

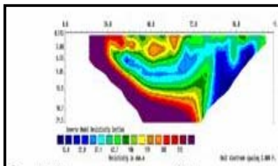

A second grid ("B") of resistivity profiles were also acquired using an electrode spacing of 3 ft, providing for better spatial resolution but shallower maximum depth of investigation.

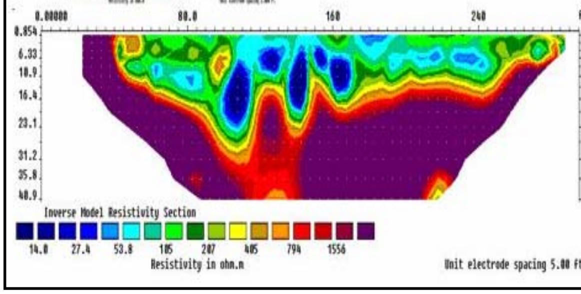

JEFFERSON COUNTY SITE

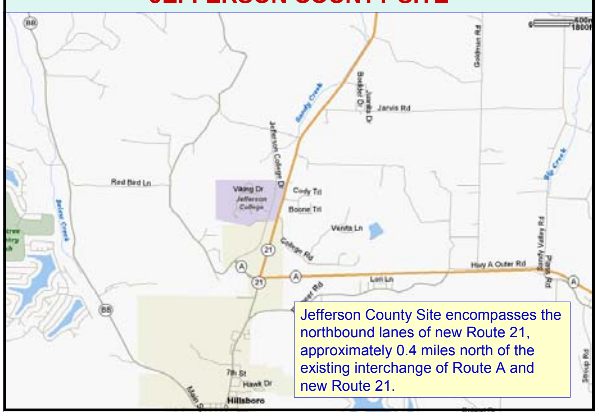

Jefferson County Site encompasses the northbound lanes of new Route 21, approximately 0.4 miles north of the existing interchange of Route A and new Route 21.

JEFFERSON COUNTY SITE

A grid of electrical resistivity data was acquired because a large clay-filled previously-unidentified oval-shaped sinkhole near the centerline of the northbound lanes emptied overnight.

The "emptying" of the sinkhole was preceded by the stripping of topsoil (to bedrock) and heavy rains, the run-off from which was channeled towards the sinkhole by pre-existing topography on the top of recently exposed rock.

Photo of Jefferson County site, prior to the "emptying" of the sinkhole. The approximate location of the sinkhole has been superposed.

The "emptied" sinkhole was oval-shaped, ~50 ft long, ~35 ft wide & ~15 ft deep (top of water to top of sinkhole). The base was covered with ~2 ft of ponded water and up to 2 feet of soft clay which proved to have sufficient strength to support 8 ft long vertically-imbedded copper electrical resistivity electrodes.

The walls were steep and weathered, supporting the thesis that the sinkhole was a pre-existing feature that had been rapidly emptied of clay, rather than a newly-developed catastrophic collapse feature. The upper ~5 ft of exposed rock was dissected by several prominent joints, but was otherwise relatively intact; the lower ~10 ft was much more intensely fractured and weathered.

The upper 5 ft of rock was jointed but not extensively fractured; the lower 10 ft (to water line) was extensively fractured and could be readily dislodged with a shovel.

Visually, the “emptied” sinkhole was similar to a clay-filled sinkhole located several hundred feet to the south-east, near the outer eastern edge of the construction site. This clay-filled sinkhole had been dissected by excavation equipment, and in cross-section appeared to have near-vertical walls and a relatively flat base comprised of intact limestone.

The in-filled sinkhole appeared to have near-vertical walls and a relatively flat base, comprised of intact limestone.

The MoDOT geologist visually inspected the “emptied” sinkhole. His principle concern, because of the speed with which such a significant volume of clay had been “drained”, was that the feature could be underlain by a large air-filled cavity or series of interconnected cavities that could pose a risk to construction crews and/or compromise the integrity of overlying new Route 21.

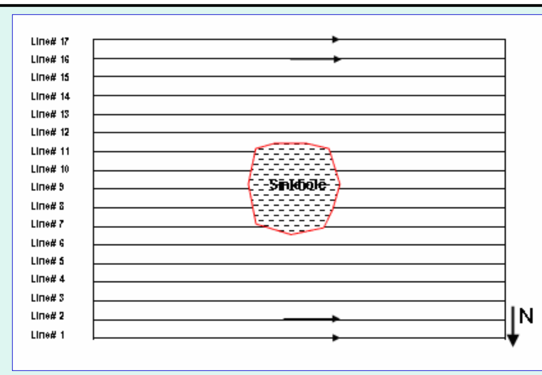

In an effort to image the subsurface below and in proximity to the “emptied” sinkhole to depths on the order of 80 ft, MoDOT acquired a grid of electrical resistivity profiles.

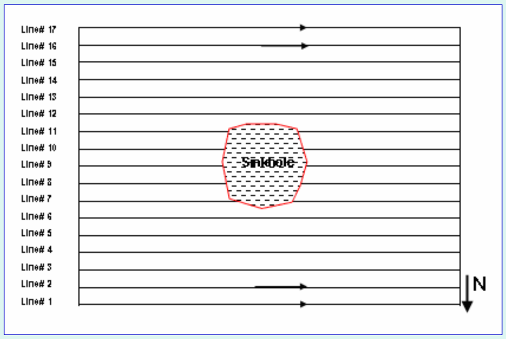

The resistivity profiles were oriented west-east effectively perpendicular to the long axis of the oval-shaped sinkhole and the most prominent joints. Data were acquired using a SuperSting resistivity unit and an electrode spacing of 12 ft

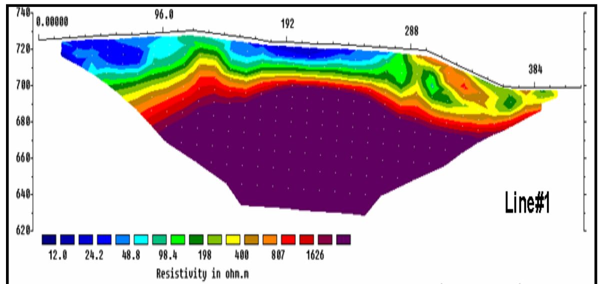

The interpretation of the resistivity data in the absence of borehole control was relatively straightforward. Units with resistivities >400 ohm-m were interpreted as intact limestone; units with resistivities <100 ohm-m were interpreted as clay-infill (or ponded water-clay infill in the base of the sinkhole); units with resistivities >100 ohm-m but <400 ohm-m were interpreted as transitional zones probably consisting of fractured and/or weathered limestone and clay in-fill.

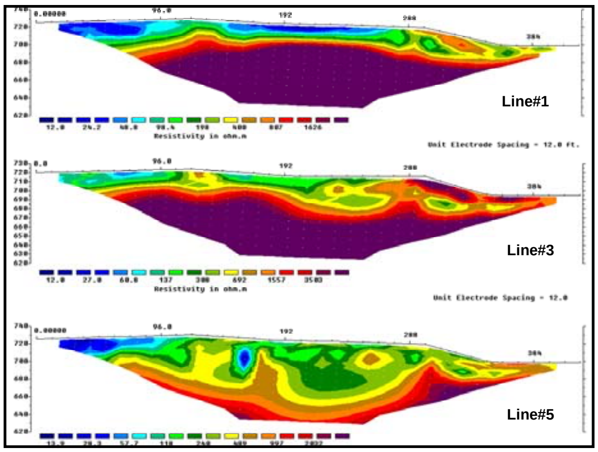

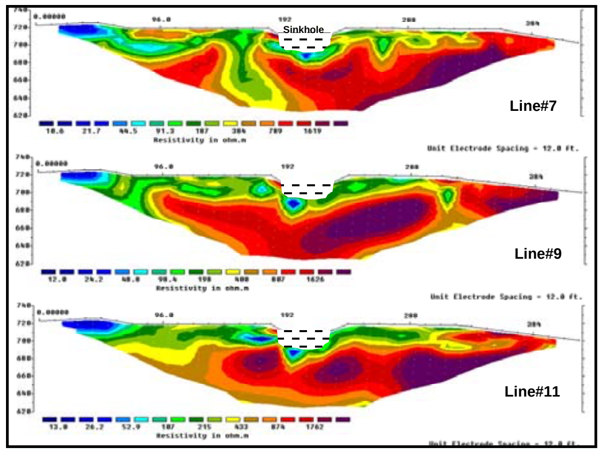

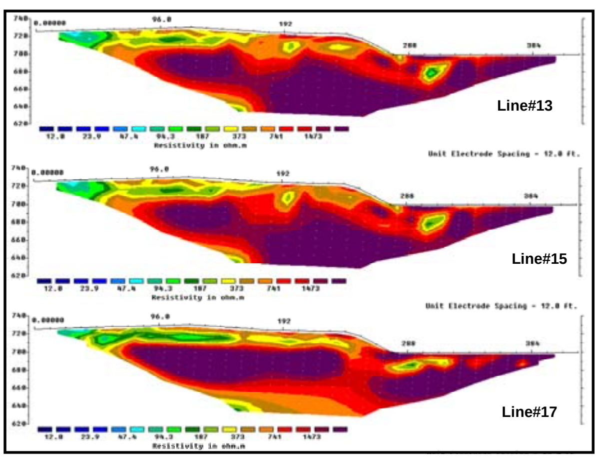

Resistivity data support the interpretation that the "emptied" sinkhole is not underlain by a substantive air- or fluid-filled cavity. Further, the data support the interpretation that the sinkhole was "drained" by runoff that flushed the clay into the subsurface through existing joint/fracture conduits to the northeast of the sinkhole. The fact that the postulated conduit is now characterized by low resistivities and the observation that ponded water remained in the sinkhole months after the feature formed, suggests drainage stopped after the conduit became "choked" with clay.

CASE STUDY #2:

DELAWARE AVENUE SINKHOLE NIXA, MISSOURI

Site is located at 327 Delaware Avenue, in Nixa, Missouri.

se occurred the morning of August 13, 2006. According
esses, the initial sinkhole opening was approximately
in diameter and 75 feet in depth. At its base, a throat of
15 feet in diameter was observed.

Electrical resistivity and MASW data were acquired in an effort to image the subsurface immediately adjacent to the sinkhole.

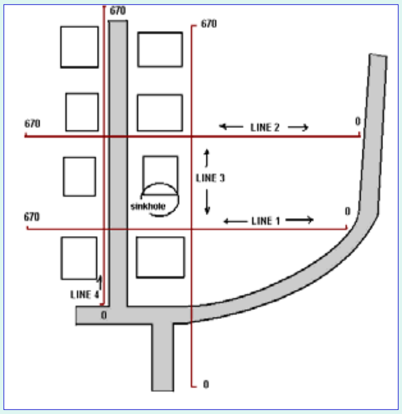

Electrical resistivity data were acquired using a SuperSting R8 unit equipped with 68 electrodes. A Wenner array with an electrode spacing of 10 feet was employed. Field data were processed using the commercially available software package RES2DINV. The output was a suite of 2-D resistivity profiles that image the subsurface to depths in excess of 120 ft.

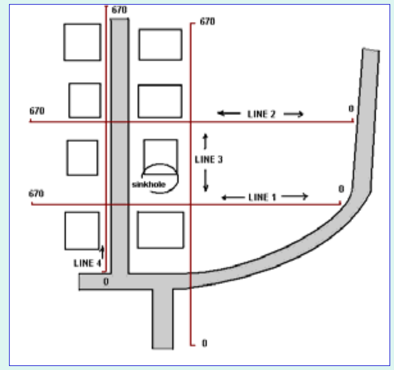

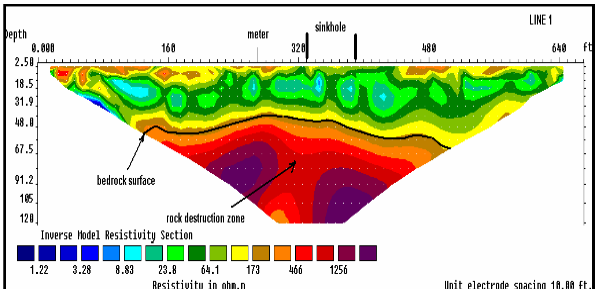

Top of bedrock was correlated across each resistivity profile. Depth to bedrock correlations were based on available borehole control and the contoured resistivity values. Bedrock, as mapped on the profiles, is characterized by resistivity values equal to or in excess of 200 ohm-m, whereas soil is characterized by resistivity values less than 200 ohm-m.

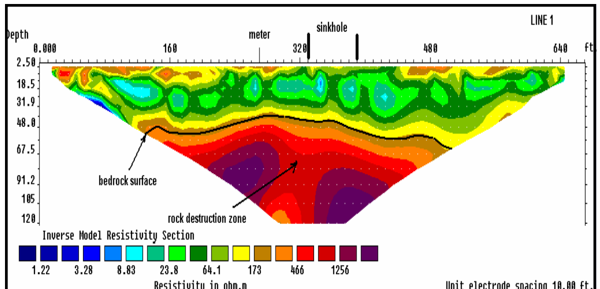

Two prominent linear geologic features are observed on the resistivity profiles. These features are interpreted as near-orthogonal 60 ft wide sets of solution-widened joints characterized by varying degrees of leaching, clay infill and bedrock subsidence. The Nixa sinkhole appears to have developed near the intersection of these interpreted joint sets.

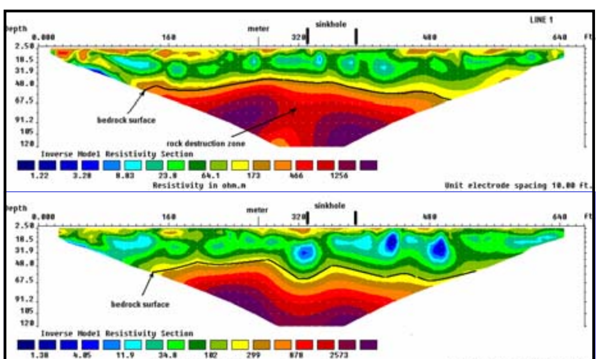

The first set of solution-widened joint trends ~NNW. Imaged on resistivity profile C1 (centered at trace 300) and resistivity profile C2 (centered at trace 320).

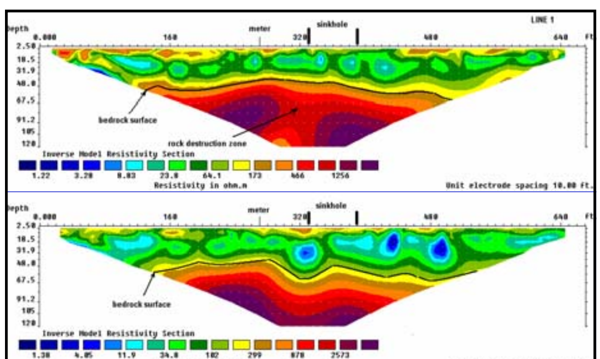

This zone of anomalously low bedrock resistivities is interpreted as an area in which rock has been extensively leached and partially replaced by clay or other fine grained sediment.

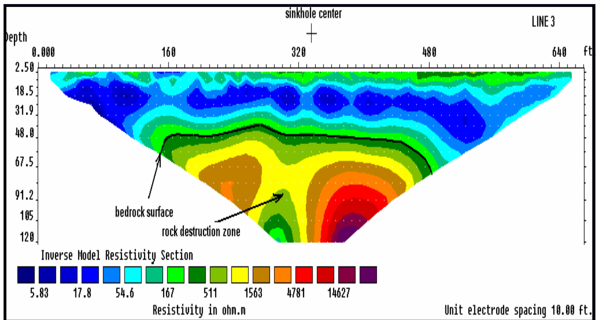

The second prominent set of solution widened joints is observed only on resistivity profile C3 (centered at trace 290). We suspect the feature imaged on profile C3 trends WSW and would have been observed on resistivity profile C4, if profile C4 had been centered adjacent to the sinkhole rather than 200 ft to the north of the sinkhole.

MASW field data were acquired using an RAS 24-channel engineering seismograph, 4.5 Hz geophones spaced at 10-foot intervals, and a sledge hammer source impacted on an aluminum plate placed at a near-offset distance of 30 feet.

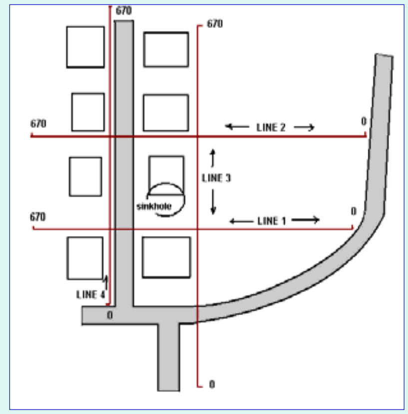

The estimated top of bedrock has been correlated across both MASW profiles.

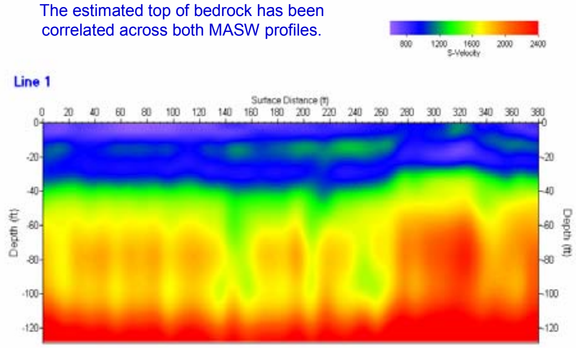

Bedrock, as mapped, is characterized by shear wave velocity values equal to or in excess of 1,600 feet per second (ft/s), whereas soil is characterized by shear wave velocities less than 1,600 ft/s.

MASW and resistivity estimated depths to bedrock are comparable. Resistivity estimates are probably more accurate because MASW data are spatially "smoothed".

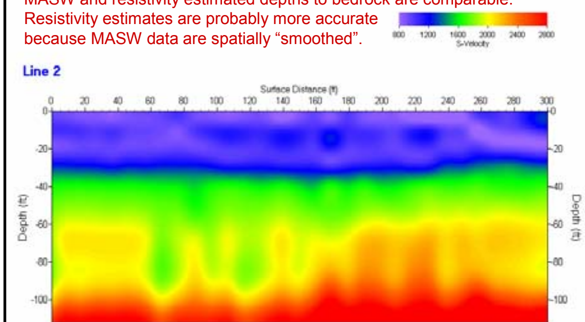

Only one prominent feature is observed on MASW profiles. This low velocity zone correlates well with the NNW-trending anomaly identified on the resistivity profiles.

Conclusions

On the basis of the analyses of the soil borings, electrical resistivity profiles, and MASW profiles, we conclude that the Nixa sinkhole developed near the intersection of two near orthogonal solution widened joint sets. The interpretation of the geophysical data suggests that the rock within the joint sets in proximity to the Nixa sinkhole has been extensively leached and infilled with clays and other fine-grained, low-resistivity sediment. In places, bedrock subsidence appears to have occurred.

There is no evidence that any of the resistivity traverses overly prominent air-filled voids.

CASE STUDY #3:

GEOPHYSICAL PILOT PROGRAM IN TEST AREAS IMMEDIATELY ADJACENT TO THE DRUMANARD ESTATE, LOUISVILLE, KENTUCKY

Drumanard Estate study site: Intersection of Routes 841 and 42

Six independent geophysical data sets were acquired along a total of nine traverses in Louisville, Kentucky as part of a pilot program designed to field-test subsurface imaging technologies in karst terrain.

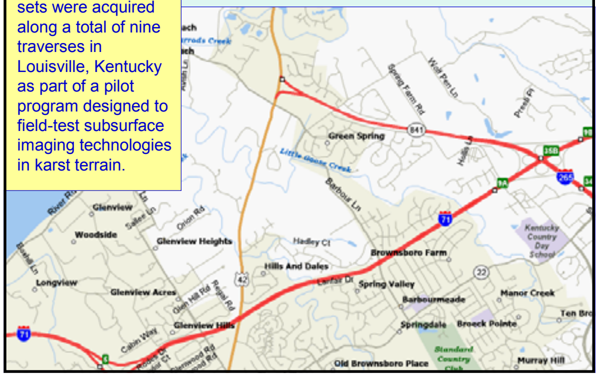

Drumanardville Estates study site

Six geophysical methods were evaluated:

- electrical resistivity
- multi-channel surface wave (MASW)
- conventional seismic refraction
- ground-penetrating radar (GPR)
- self-potential (SP)
- gravity

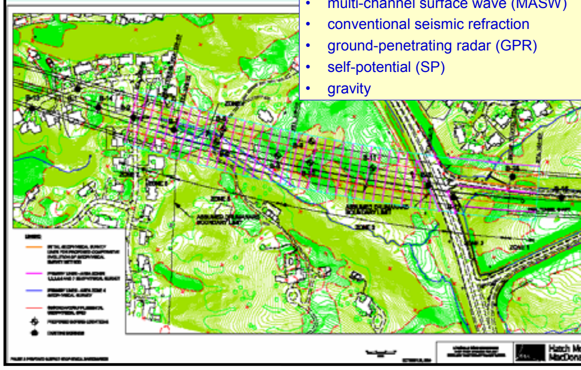

Objective

The primary objective of this pilot study was to evaluate each of these six imaging methods and to recommend which, if any, should be used in any follow-up geophysical investigation of the Drumanard Estate.

Recommendations were based on the following criterion:

- Did the geophysical method provide reliable and useful information about the depth to bedrock?
- Did the geophysical method provide reliable and useful information about the presence of karstic solutioning/identation?
- Did the geophysical method provide reliable and useful information about the depth/base to which the indentations extend?
- Did the geophysical method provide reliable and useful information about karstic indentation in-fill? Are they in-filled with clay or other sediment? Are air-filled voids present?
- Did the geophysical method provide reliable and useful supplemental information about kartsic caves, the depth to the standing water table or the location of active water channels?

Electrical Resistivity Data

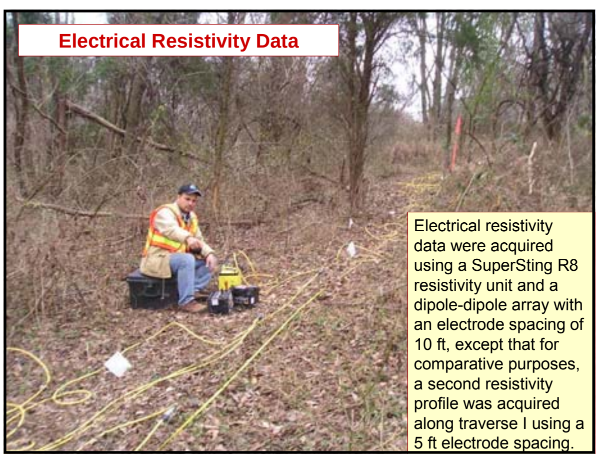

Electrical resistivity data were acquired using a SuperSting R8 resistivity unit and a dipole-dipole array with an electrode spacing of 10 ft, except that for comparative purposes, a second resistivity profile was acquired along traverse I using a 5 ft electrode spacing.

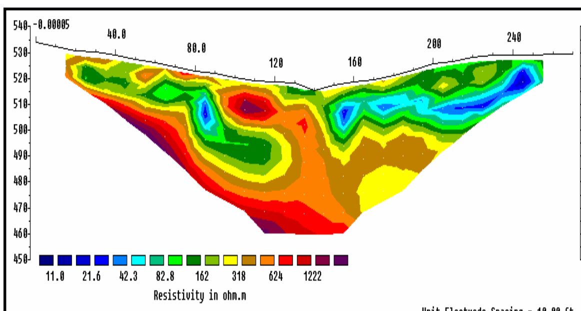

During processing, each resistivity profile was subdivided into 2-D pixels. Each pixel was assigned a specific value of resistivity. Pixel dimensions are a function of electrode spacing and depth of investigation. The pixels on the resistivity profiles acquired using a 10 ft electrode spacing are 10 ft x ~4 ft at surface and 10 ft x ~7 ft at depths on the order of 35 ft.

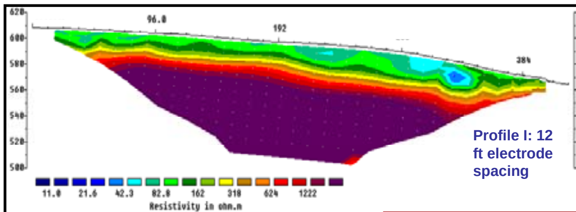

Profile I: 12 ft electrode spacing

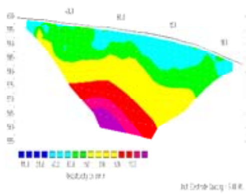

Profile I-2: 5 ft electrode spacing

The pixels on the resistivity profile acquired using a 5 ft electrode spacing are 5 ft x ~2 ft at the surface and 5 ft x ~4 ft at depths on the order of 35 ft. The resolution of the 5 ft spacing data is essentially twice that of the10 ft spacing data.

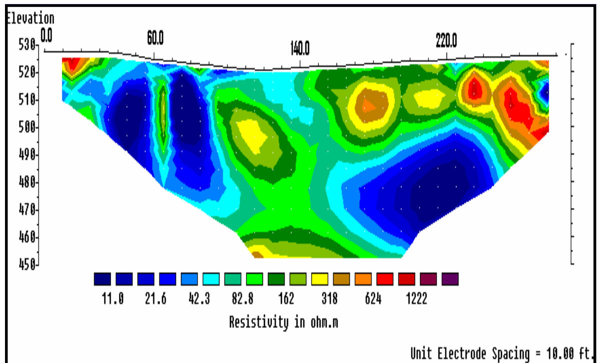

Bedrock is characterized by high resistivities: clay by low resistivities. The complexity of extensively karsted ground is apparent on several of the profiles.

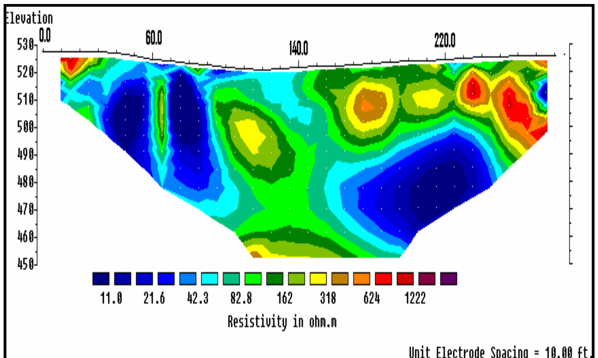

Depths to bedrock were fairly reliable.

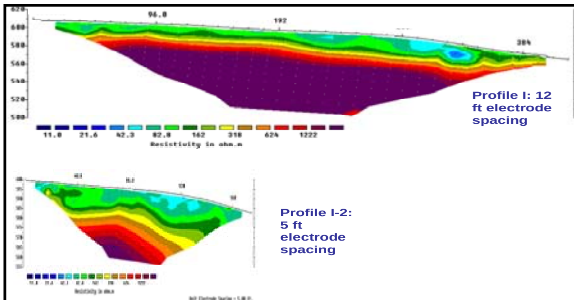

Method	Recommendations
Electrical resistivity	Electrical resistivity data be acquired on the Drumanard Estate site. However, because of the apparent complexity of the bedrock surface, data should be acquired using a 5 ft electrode spacing.

Conventional Seismic Refraction

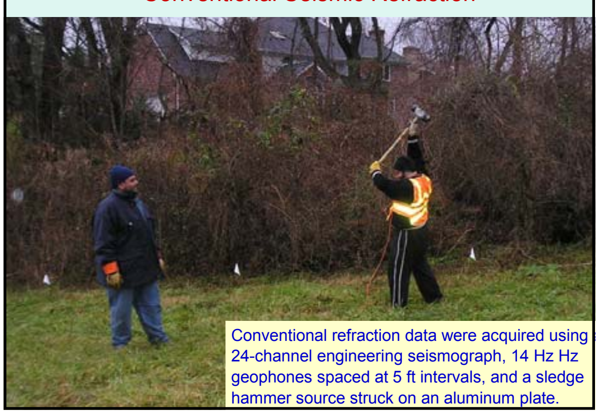

Conventional refraction data were acquired using 24-channel engineering seismograph, 14 Hz Hz geophones spaced at 5 ft intervals, and a sledge hammer source struck on an aluminum plate.

Refraction Surveying

Conventional Seismic Refraction

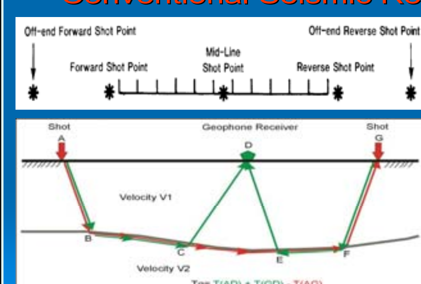

In a typical survey, five sources are discharged along each geophone array. This multiplicity of travel time data allows the depth to bedrock to be estimated with a reasonable degree of precision.

The conventional refraction data were acquired using a 5 ft geophone spacing and a sledge hammer source.

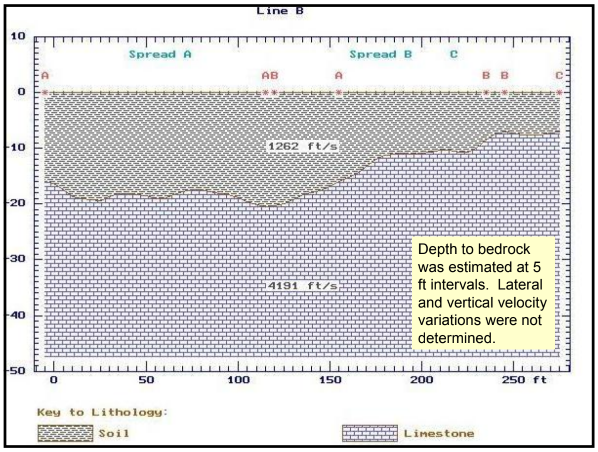

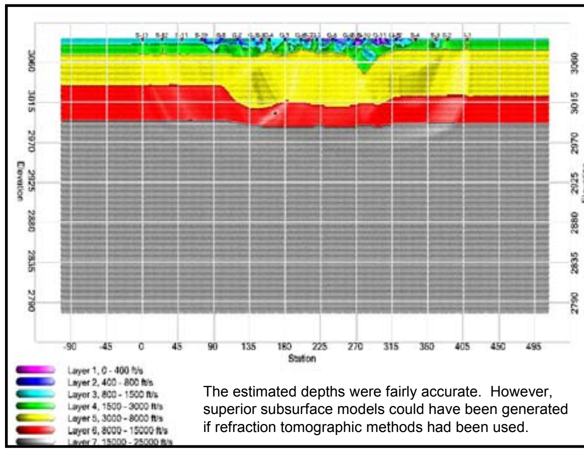

The estimated depths were fairly accurate. However, superior subsurface models could have been generated if refraction tomographic methods had been used.

M3 Velocity "Swath" Model

The result is not simply an image. It's calibrated ground simulation.

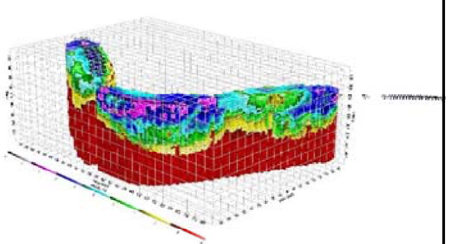

Sources can be discharged off-line, allowing 3-D (swath) images of the subsurface to be generated.

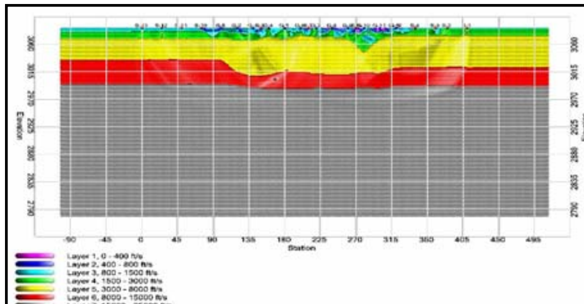

Method	Recommendations
Seismic refraction	Quality refraction data can be acquired in the study area. However, we do not recommend the acquisition of conventional refraction control. Rather, because of the complexity of bedrock, we recommend the acquisition of refraction (surface) tomographic data.

Multi-channel Surface Wave Data (MASW)

MASW field records were acquired using a 24-channel engineering seismograph, 4.5 Hz geophones spaced at 5 ft intervals, and a sledge hammer source struck on an aluminum plate.

Recording of Rayleigh Wave Data

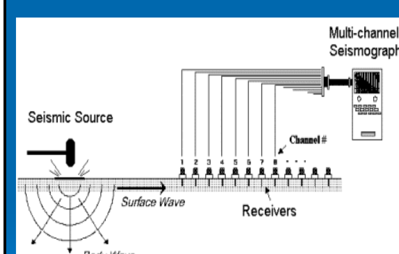

Survey configuration

MASW field records, consisting of 12 seismic traces, were acquired at 20 ft intervals along each traverse

Shot gather

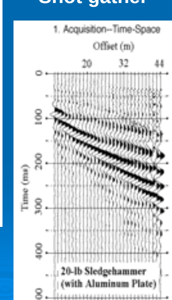

PROCESSING OF 1-D MASW DATA

Two steps: 1) extraction of fundamental-mode dispersion curves and 2) inversion of these curves to obtain 1-D shear-wave depth profiles.

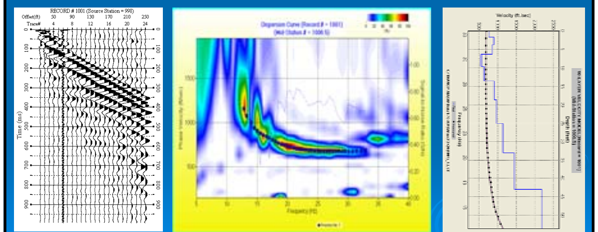

1. Shot Gather   2. Dispersion curves   3. Velocity Inversion

2-D Presentation

1. Acquire multiple MASW records by moving source-receiver array along traverse.
2. Prepare multiple 1-D Vs profiles (one per array).
3. Construct 2-D shear-wave velocity profile.

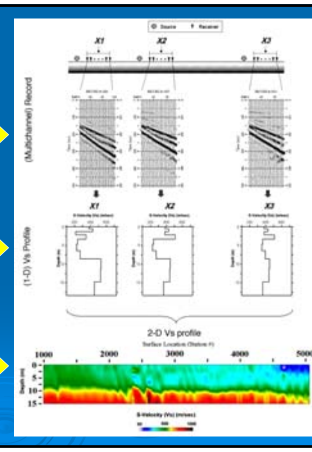

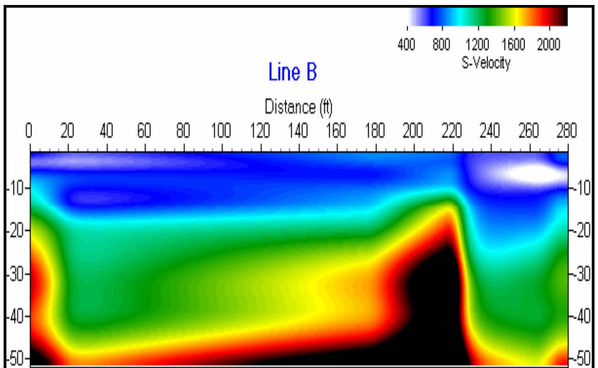

Poor resolution compared to resistivity data, probably because of lateral smoothing.

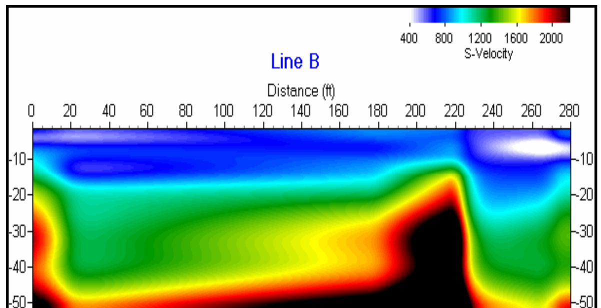

Method	Recommendations
MASW	Electrical resistivity and refraction tomography provide better resolution than MASW. Unless the determination of average shear-wave velocity profiles is critical, we do not recommend the acquisition of additional MASW control.

GPR Data

The GPR data were acquired using a GSSI unit equipped with a 200 MHz ground-coupled antenna.

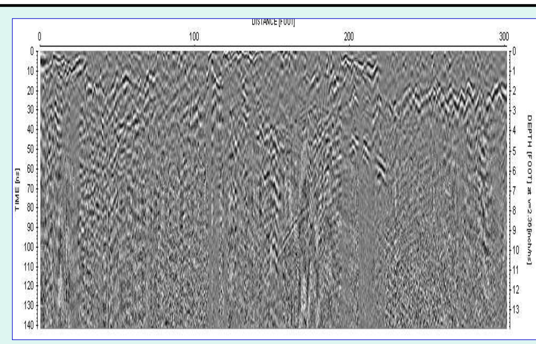

A spatial sampling rate of two radar traces per inch was employed. The GPR data were processed using the commercially available software package Reflexw. Every effort was made to acquire quality data in the field and to enhance any continuous reflections during data processing.

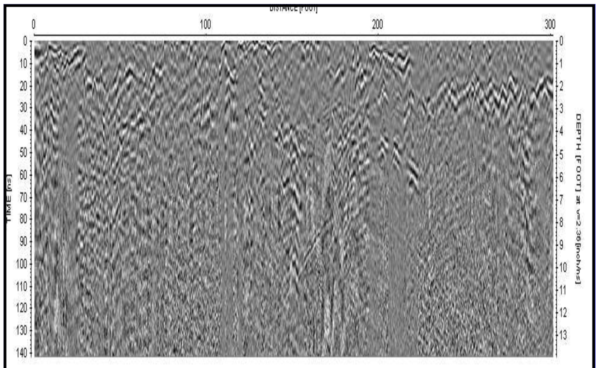

Bedrock could not be imaged on the acquired GPR profiles, except in rear instances where bedrock was extremely shallow. Presumably, the tool was ineffective because of the presence of shallow clay.

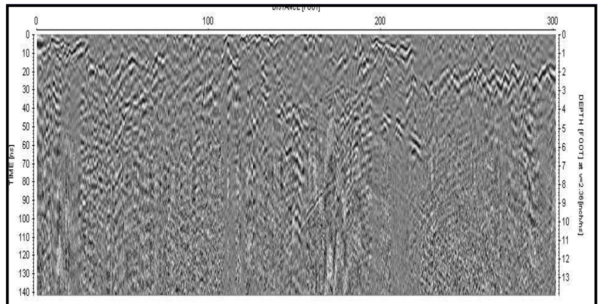

Method	Recommendations
GPR	Conductive clays absorbed the GPR signal and bedrock could not be mapped. It is highly unlikely that significantly superior results would be obtained using a lower frequency source antenna. Therefore we do not recommend that additional GPR data be acquired on the Drumanard Estate site.

SP Data

Two sets of SP data were acquired along each of the traverses using Model #920 023 non-polarizable electrodes and a voltmeter. One set of SP data were acquired along each traverse; a second set was acquired at stations located 5 ft off the traverse. The trailing electrode was coupled to the base station; the lead electrode was moved along the length of the traverses at 10 ft intervals.

Prominent negative anomalies were observed on SP profiles D-1 and D-2. These anomalies are attributed to the flow of water into bedrock at these locations.

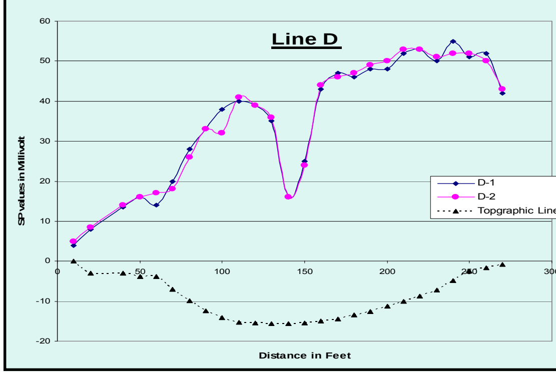

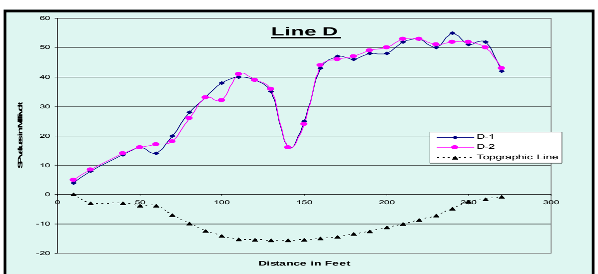

Method	Recommendations
SP	SP data are relatively inexpensive to acquire and process, and can be used to locate zones where water flows into bedrock. If information about the location of fractured conduits is critical, we recommend the acquisition of additional SP data at station spacings of no less than 10 ft, along traverses spaced at intervals of no more than 20 ft.

Gravity Data

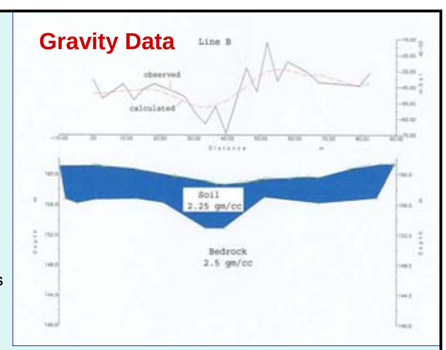

Gravity data were collected using a Lacoste and Romberg model G gravity meter, at station spacings of 10 or 20 ft. At each station, the meter was leveled and at least two readings were recorded to an accuracy of 0.005 gravity meter units. The field data were processed into complete Bouguer gravity anomaly values. This process included removing from the field data instrumental drift variations, earth tide changes, and elevation and latitude variations using values supplied by surveying engineers.

Gravity Data

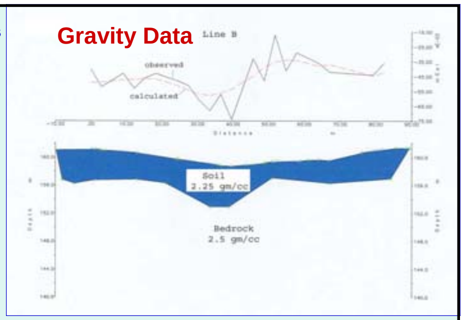

Estimated depths to bedrock were more reliable in some areas and less reliable in others, presumably because gravity readings were also affected by lithologic variations within bedrock. Gravity is of less utility as a reconnaissance tool than either electrical resistivity or refraction tomography, primarily because of the complex nature of bedrock and the bedrock surface. However, the gravity tool could be of significant utility if used to better characterize any anomalies identified on reconnaissance-type geophysical data.

Gravity Method

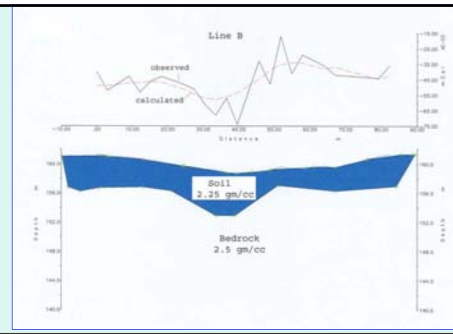

Recommendations

We do not recommend the acquisition of reconnaissance-type gravity data, however we recommend it be acquired as necessary in an effort to delineate anomalies observed on other geophysical data sets.

SUMMARY AND RECOMMENDATIONS

The following six geophysical methods were evaluated:

- electrical resistivity
- multi-channel surface wave (MASW)
- conventional seismic refraction
- ground-penetrating radar (GPR)
- self-potential (SP)
- gravity

Geophysical method	Reliability of estimated depth to bedrock	Horizontal and vertical resolution	Ability to detect and map fractures	Ability to differentiate rock and clay	Ability to locate flowing water	Ability to detect and map air-filled cavities
Electrical resistivity	2	1	1	1	NA	1
Conventional seismic refraction	1	2	2	2	NA	4
Self-potential (SP)	NA	NA	NA	NA	1	NA
Gravity	3	3	3	3	NA	2
Multi-channel surface wave (MASW)	4	4	4	4	NA	3
Ground-penetrating radar (GPR)	∞	∞	∞	∞	NA	∞

Summary of comparative evaluations

Drumanard Estates Site: Conclusions

Based on our analyses, we conclude:

1. Seismic refraction (or refraction tomography) and electrical resistivity control will provide reliable and useful information about the depth to bedrock and the presence of karstic solutioning/indentation, including information about the depth/base to which the indentations extend and the nature of the in-fill sediment.
2. Electrical resistivity control should provide information about the presence and location of any substantive air-filled voids in the subsurface.
3. Self-potential data will provide qualitative information about the location of active water channels.

Drumanard Estates: Recommendations

Recommend that electrical resistivity data, seismic refraction (or refraction tomography) and self-potential data be acquired as part of any subsequent geophysical investigation of the Drumanard Estate site.

Electrical resistivity and seismic refraction (or refraction tomography) imaging technologies will provide cost-effective and useful information about soil lithology and thickness, and the nature of bedrock including the presence of solution-widened joints, karst-related fractures, infill clays and air-filled voids.

Self-potential data will provide useful information about seepage pathways within shallow karsted bedrock.

Questions?

XXXVII Ohio River Valley Soils Seminar
October 27, 2006
Lexington, Kentucky

SETTLEMENTS AND SINKHOLES ASSOCIATED WITH MASSIVE GROUNDWATER LOWERING IN DOLOMITIC AREA

by

Dr. William J. Neely, P.E.
Vice President, Product Development

The Reinforced Earth Company
1660 Hotel Circle North, Suite 304
San Diego, CA 92108

INTRODUCTION

The effects of groundwater lowering in causing settlement are well known. In most cases groundwater lowering does not result in sharp discontinuities in the ground surface but in Karst-type topography the consequences can be catastrophic.

In late 1968, the West Driefontein Gold Mine in South Africa was completely flooded. The mine is located in the Far West Rand region in South Africa where the land surface is old; the most recent rocks belong to the Karroo System, which corresponds to the Carboniferous of the Northern Hemisphere.

In December 1968, the Department of Water Affairs gave permission to dewater the flooded areas of the mine. Dewatering commenced in June, 1969 and early in 1970, cracks were observed in a nearby brickworks which had been in operation for more than twenty years. As the dewatering operations continued, settlements and cracking at the brickworks accelerated, making it increasingly difficult to maintain production. In January 1971, some eighteen months after dewatering operations began, the brickworks was closed.

This paper summarizes the detailed investigations that were undertaken to establish the link between the massive dewatering effort and the operating difficulties at the brickworks. In addition to the settlements that occurred at the brickworks, examples are also given of the massive collapses that took place in the surrounding area associated with enormous solution features in the underlying dolomite bedrock.

GEOLOGIC SETTING

The Far West Rand region is characterized by a series of watertight compartments formed by parallel syenite and diabase dikes through the dolomite; see Fig. 1. A plan showing the Bank and Oberholzer Compartments is provided in Fig. 2. The dikes which form the virtually watertight boundaries between adjacent compartments can be seen as well as the locations of springs which carry groundwater over a dike from one compartment to the next.

The brickworks is located in the Bank Compartment where the weathered shales of the Karroo System outlier are the source of the raw material for the brickmaking activities. The West Driefontein Gold Mine is situated in the adjacent Oberholzer Compartment, immediately west of the Bank Compartment.

In Fig. 3, which is a section through the Bank Compartment, the Witwatersrand System (denoted by W) which contains the gold-bearing conglomerates rests directly on the granite-gneiss basement complex. The younger Transvaal System, which includes the water-bearing dolomite, rests unconformably on an erosion surface that cuts across the older rocks. The Karroo System shales were deposited on the weathered surface of the dolomite (Brink, 1979).

As is typical of dolomitic or limestone areas, there was evidence of depressions in the ground and possible potential sinkholes, well away from the brickworks itself, as early as 1964, well before the dewatering of the West Driefontein Mine.

DESCRIPTION OF BRICKWORKS

The brickworks, referred to as Brickor, was commissioned in 1947. The location of the brickworks within the Bank Compartment is shown in Fig. 4. The general layout of the continuous kiln process is presented in Fig. 5.

The driers and kilns were originally supplied with air heated by single-stage gas producers, which was delivered into two underground flues. While one flue was in operation, the other flue would be cleaned out. In 1968, a two-stage overhead gas producer was installed and use of the underground flues was discontinued.

The bricks to be fired were placed on kiln cars about 7 feet long and 5 feet wide. The cars were initially passed through the driers which were fed with waste hot air at 150°C from the cooling zones of the six kilns. After leaving the driers, the cars entered the kilns. Each kiln was divided into four zones: an approximately 120-ft long drying zone, a pre-heating zone about 80 feet long, a 120-ft long firing zone, and a roughly 100-ft long cooling zone. A maximum temperature of 1100°C was achieved in the firing zone.

Prior to 1970, only normal maintenance was required. One recurring problem was that of kiln rail alignment prior to the commissioning of the overhead gas producer in 1968. It was found that the kiln rails would rise over time; the total upward movement of the rails was about 3 inches between 1947 and 1968. The upward movement was attributed to “dust” collecting under the flue arches when they were heated up, so that the arches did not return to their original position when the flues were cooled after being cleaned out. To deal with this problem, the kilns were shut down and repaired in the vicinity of the underground flues at two-yearly intervals, and the rails were trimmed and lowered about one-half inch at the same time. The problem of upward movement of the rails was no longer experienced after the two-stage overhead gas producer was installed in 1968.

Fundamental to the successful operation of the kilns was the necessity of ensuring that the wheels and axles of the cars were protected from the hot gases in the kilns, particularly in the preheating and firing zones, otherwise the kiln cars would jam on the rails. To ensure that the kiln car axles and wheels were protected, sand or clay seals were used between adjacent cars and between the side walls of the kilns and the cars, as illustrated in Fig. 6; Fig. 7 is a photograph inside tunnel kiln #3 showing the car rails and the longitudinal seals. Fig. 8 shows a detail of the clay seal between adjacent rail cars. A differential settlement of only one and a half inches between the car rails would be sufficient to break the sand seals and the kiln car would foul in the vertical direction. To maintain tolerances for the cars, whenever the kilns were stopped for any reason, the rails were realigned within one-quarter inch and the cars were tested using a template car.

Such tight tolerances were fundamental to the successful operation of the kilns because of the need to avoid ingress of unheated air into the drying, preheating or firing zones. If cold air entered these zones, the temperature of the gases in the kilns would be reduced, adversely affecting the quality of the bricks produced. Also, reduction of the gas temperatures could lead to the temperature falling below the dew point of the gases, resulting in sulfurous gases being deposited on the kiln walls and attacking the brickwork and mortar joints.

FLOODING AND DEWATERING OF THE MINE

On October 26, 1968 the West Driefontein mine was completely flooded by an unexpected outbreak of water in the eastern section of the mine near the dike separating the Oberholzer and Bank compartments, resulting in the loss of substantial areas of the working face. The water inflow was in excess of 100 million gallons per day; clearly, a fissure connecting the two compartments, probably in the dike, had opened up allowing water from the Bank Compartment to flow into the mine workings in the adjacent Oberholzer Compartment. It soon became clear that the only practical way to save the West Driefontein mine, one of the richest gold mines in the world, was to drain the Bank Compartment.

Less than two months after the flooding, permission was given to dewater the Bank Compartment. Dewatering operations were begun early in January 1969 at No. 4 shaft immediately adjacent to the dike separating the two compartments; see Fig. 4. Six months later, in June 1969, pumping started at No. 3 shaft, slightly more than two miles west of the dike.

Records of water levels in a number of boreholes in the Bank Compartment, together with the quantities of water pumped from the mine workings, are shown in Fig. 9. From the beginning of the dewatering operations in January 1969 through November 1969, the water level in the Bank Compartment at Borehole G452 immediately adjacent to the brickworks (see Fig. 4) had dropped less than 15 feet. However, after pumping was started at the East Driefontein Mine, within the Bank Compartment, at the end of January 1970, considerable changes in water level at Borehole G452 (and others) did occur. In fact, as indicated in Fig. 9, Borehole G452 dried up ten months later in October 1970 after the water level there had dropped more than 400 feet. The scale of the dewatering operation can be appreciated from the approximate cone of depletion for the Bank Compartment which indicates measurable water level drops almost six miles from the dike separating the Oberholzer and Bank Compartments; see Fig. 10. The depth of groundwater lowering required to permit mining operations to be resumed was more than 3,000 feet and in the Bank Compartment water levels were lowered during 1969, 1970 and 1971.

EVENTS LEADING TO CLOSURE OF BRICKWORKS

Dewatering of the mine workings began in January 1969 and, a year later, at the East Driefontein mine in the Bank Compartment. By May 1970, ground subsidence was observed at the brickworks railroad siding; a month later an approximately 150-ft diameter sinkhole developed just north of the brickworks. In July, cracks appeared in the ground surface around the brickworks and into the buildings themselves and the conveyor feeding the plant from the claypit settled about 6 inches. Other surface cracks, localized depressions and sinkholes continued to develop through the end of 1970 when, as shown in Fig. 9, pumping rates reached a peak and the drop in groundwater levels was very rapid.

At the same time, there were two recurring problems which gradually made it increasingly more difficult to maintain brick production at economic levels. The first problem was the development of numerous cracks in the brick kilns themselves, which interfered with the flow of hot gases, as well as allowing the ingress of unheated air, in the kilns and adversely affecting the quality of the bricks being produced. The second problem was the repeated failure of the flanges of the kiln car wheels, even though tests showed that there were no defects in the castings.

As settlements continued to increase, problems with subsiding rails, jammed rail cars, rails kicking sideways, local collapses of the tunnel kiln brickwork also became more frequent and serious and it became more and more difficult to operate the facility. In addition, other sinkholes began appearing in areas adjacent to the brickworks, necessitating the closure of an access road close to the facility.

The continuing and accelerating nature of the operating difficulties, as well as larger safety concerns, led to the closure of the brickworks in January 1971, a little more than two years after flooding of the West Driefontein mine.

SETTLEMENT RECORDS

A leveling survey in the area of the brickworks was begun in June 1970, shortly after evidence of subsidence first appeared. Figs. 11 and 12 show the overall pattern of settlement for the two-month period between June and August 1970, and for the roughly seven months from early June through the end of 1970.

Although some of these early measurements may be open to question (e.g., because of the single-loop closure error system used, distance between points in excess of 30 feet, use of contours to show data, and the use of leveling pins on structures resulting in possible distortion of ground movements by tilt of the structure), the overall subsidence pattern is clear. The central area of settlement is located between the driers and the kilns and approximately in the vicinity of the disused underground gas flues.

Surveying methods were improved from January 1971. Fig. 13 shows the overall measurements for the period June 1970 through April 1972. The pattern of the subsidence is broadly similar to those for the earlier surveys in Figs. 11 and 12. It can be seen that the maximum recorded movement reached about 7.5 inches (190 mm) in the vicinity of kiln #6. It is obvious from the contours of settlement that differential movements along the length of the kilns were far greater than the vertical tolerance of 1.5 inches necessary to ensure that the sand seals at the bottom of the kiln cars operate satisfactorily.

SETTLEMENT AND SURFACE STRAIN CALCULATIONS

Attempts to calculate the settlements due to the massive groundwater lowering operation were extremely difficult because of the highly complex sub-surface conditions typical of dolomitic and limestone regions, the presence of unusual materials produced by the weathering of the dolomite and which varied dramatically in extent, thickness and compressibility. Also, the highly irregular bedrock surface made it almost impossible to determine the increases in effective stresses in the most compressible materials because of the ability of the competent Karoo sediments to arch over the large solution features, thereby significantly reducing stress increases in the very much more compressible materials below.

As noted earlier, the geology of the Far West Rand area comprises dolomite bedrock which is overlain to considerable depths by sediments of the Karroo System. The Karroo sediments are of very variable thickness since the weathering of dolomite tends to form deep sub-surface valleys, which are later filled with younger materials. The weathering of dolomite also produces a highly compressible material locally known as wad.

Wad is formed as a result of the chemical decomposition of dolomite by weakly acid ground water. The effectiveness of this chemical action depends on the acidity of the ground water and the chemical composition of the dolomite and, consequently, the extent, thickness and compressibility of the wad are highly variable.

The variation in the geology in the area of the brickworks is illustrated in Figs. 14 and 15. It can be seen that the dolomite rockhead is highly irregular and contains deep slots or subsurface troughs separated by elongated pinnacles. There are two very prominent slots, each more than 500 feet deep, which trend SSW – NNE; one lies east of the kilns and the other directly below the kilns. The model in Fig. 16 shows an oblique view of the dolomite rockhead and the two steep-sided slots underlying the brickworks.

Figs. 14 and 15 show the presence of substantial zones of wad, or manganiferous earth, left after the dolomite had been dissolved by percolating water. The solution of the dolomite took place after the deposition of the Karroo System sediments. There appear to be two areas in which wad has developed to great depth. Exceptionally thick (> 100 feet) occurrences of wad are present below the northern portions of kilns #4 and #6, to the east of kiln #6 and to the west of kiln #1.

The Karroo sediments represent deposition from the melt-waters of the glaciers which moved along the U-shaped slots in the dolomite. The solution of the dolomite and the formation of the highly compressible wad took place after the Karroo sediments were laid down. As pointed out earlier, catastrophic collapses in the form of sinkholes had occurred at a number of locations near the brickworks (including a sinkhole which engulfed the crusher plant at West Driefontein mine in 1962). At the brickworks site, the substantial thickness of more recent Karroo sediments, which had infilled two major solution features in the dolomite at the time of their deposition, was competent enough to arch across the very much weaker and extremely compressible wad produced by additional post-depositional solution, thereby probably preventing the development of a catastrophic sinkhole collapse upon lowering of the groundwater level in the Bank Compartment.

Given the very irregular subsurface geology depicted in Figs. 14 and 15, any agreement between calculated and measured settlements (recognizing that the measurements themselves were begun after kiln operating problems developed and subsidence occurred at the railroad siding) would be largely fortuitous. The situation deteriorates even further once the variability of the wad itself is taken into account. Void ratios for wad typically range from about 3 to as high as 10. Undisturbed sampling of this material from depths of up to 300 feet below ground level is virtually impossible. The compressibility characteristics of the wad were estimated from the results of tests on reconstituted sample. On average, these tests have values for the coefficient of compressibility, m_v, approximately an order of magnitude greater than those for the Karroo sediments from which relatively undisturbed samples were recovered. However, tests on block samples of wad recovered from shallow test pits at other sites suggest that in its relatively undisturbed condition, wad may be as much as 100 times more compressible than the younger Karroo soils.

Estimates of settlements due to the groundwater lowering were made using classical one-dimensional consolidation theory, based on soil profiles in individual boreholes and assuming that the amount of compressible material comprises the thickness of Karroo soils and wad between the original deep water table and the surface of the dolomite bedrock. Using average values of m_v for the Karroo soils and the (reconstituted) wad resulted in fairly good agreement between calculated and measured settlements in some instances but very poor correlation in other instances. Good agreement was not expected given the very considerable difficulties associated with estimating the total amount of settlement at any location from partial time-settlement records, uncertainty about the increase in effective stress due to groundwater lowering because of the ability of the strong Karroo soils to arch around the enormous solution features in the dolomite and the lack of reliable test data for the most compressible material. Subsidence of the ground surface in the brickworks area is three-dimensional in character, with points around the edge of the subsidence bowl experiencing tensile strains while those toward the center are subjected to compressive strains. Calculation of horizontal displacements associated with the observed vertical settlements was done using a finite element analysis in which observed settlements were applied to the surface of the section as fixed vertical displacements. The calculated horizontal strains were in the order of 0.001 in both the longitudinal and transverse directions. Surface horizontal strains of this magnitude were found to be more than sufficient to cause lateral buckling of rails in the kilns. A number of instances of haulage rails tearing loose of their supports were reported in late 1970. Other analyses showed that even relatively small differential settlements along the length of a kiln would be sufficient to cause cracking of the brickwork structure of the kiln itself.

One of the issues that was exploited in an attempt to deflect responsibility for the operating difficulties at the brickworks from the dewatering activities was associated with the underground gas flues.

It will be recalled that from 1947 until 1968 gas was produced in single-stage producers before being fed along two underground flues into the firing zones of the kilns. This system was replaced by an overhead gas main and both underground flues were taken out of service by September 1968, before the West Driefontein mine was flooded.

While the kilns were operating with the underground gas flues there was a continual problem with the kiln car rails in the area of the kiln/flue intersection. The trouble was caused by the rails being moved upwards and this necessitated remedial measures about every two years when the rails were cut down to relevel the track. The total amount of heave over the flues in the period from 1947 to 1968 was about 3 inches.

Relative heave in the area of the flues did go on after the flues were shut down in 1968. This additional heave was most pronounced where the kilns cross over the flues, but some heave also occurred in the haulage ways between the kilns. From the results of shrinkage tests on samples of the soil under the flues it was estimated that the amount of heave associated with the cooling of the ground after the underground flues were abandoned was about an inch.

The overall problem of heave is a complicated thermal, physical and chemical problem and it was not possible to determine its precise nature. However, the heating of the soil in the vicinity of the flues would have suppressed the perched water table. After closure of the underground flues this water table would have been re-established and the drop in temperature would have been favorable to hydration of the sulfate in the mortar and concrete. This probably resulted in expansion in the mortar and concrete, resulting in substantial weakening of the concrete slabs and kiln brickwork.

This expansion due to sulfate attack caused heave of the soil and together with the expansion of the kiln and flue structures would have caused upward movements in the vicinity of the kiln-flue intersection. Between the kilns there is a greater clearance, filled with soil, between the top of the brick arch of the underground flue and the concrete slabs of the kiln superstructure than in those areas where the kilns cross over the flues. This probably accounts for the difference between the amounts of heave in these two areas.

It is quite evident that the problem of local heave in the area of the kiln-flue intersections cannot be attributed to the effects of groundwater lowering. However, this local heave did not play a significant role in the decision to close down the brickworks facility in January 1971.

CONCLUSIONS

The flooding of the West Driefontein mine in late 1968 led to dewatering of an adjacent watertight compartment which was also the site of a major brickworks. About six months after dewatering operations were begun cracks in the ground surface and sinkholes began to develop on the brickworks property. As dewatering continued through 1970, it became increasingly difficult to maintain production because of jammed rail cars in the kilns, ingress of cold air, buckled rails and other factors and the brickworks was eventually closed at the beginning of 1971.

At the brickworks site, dewatering of the flooded mine workings resulted in a drop in groundwater level of more than 400 feet and measured settlements of up to 8 inches.

The complexity of the subsurface geology, arching effects and the inability to obtain realistic compression characteristics for the highly compressible manganiferous earth (wad) made it very difficult to obtain good agreement between measured and calculated settlements, although the settlement profiles approximate the thickness of the deposits that had been dewatered.

ACKNOWLEDGEMENT

The author wishes to recognize the guidance and encouragement he received from the late Dr. David J. Henkel during the course of the work described herein. His teaching, painstaking logic and rigorous approach continue to inspire.

REFERENCES

Brink, A. B. A. (1979). Engineering Geology of Southern Africa, Volume I. Building Publications, Pretoria.

Henkel, D. J. (1982). Geology, geomorphology and geotechnics. Geotechnique 32, No. 3, 175 – 194.

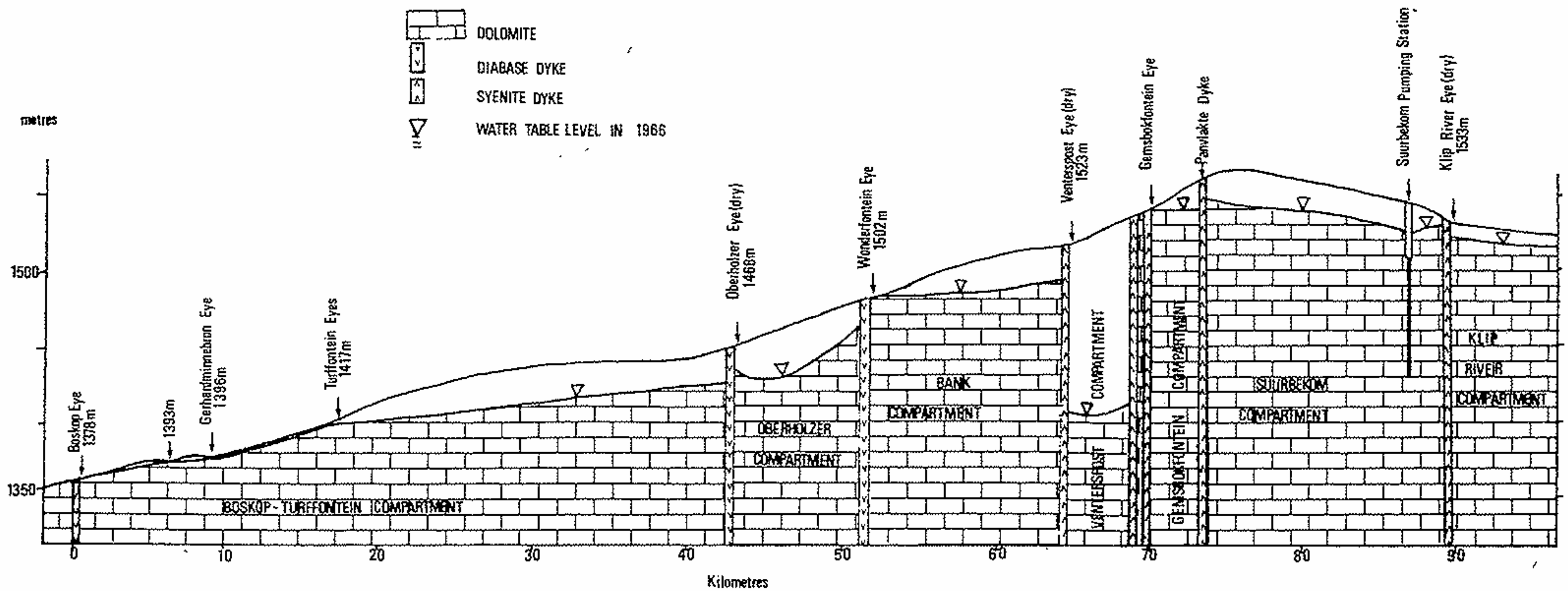

FIG. 1. Geohydrological section through dolomitic compartments of the Far West Rand as in 1966 (After Brink, 1979)

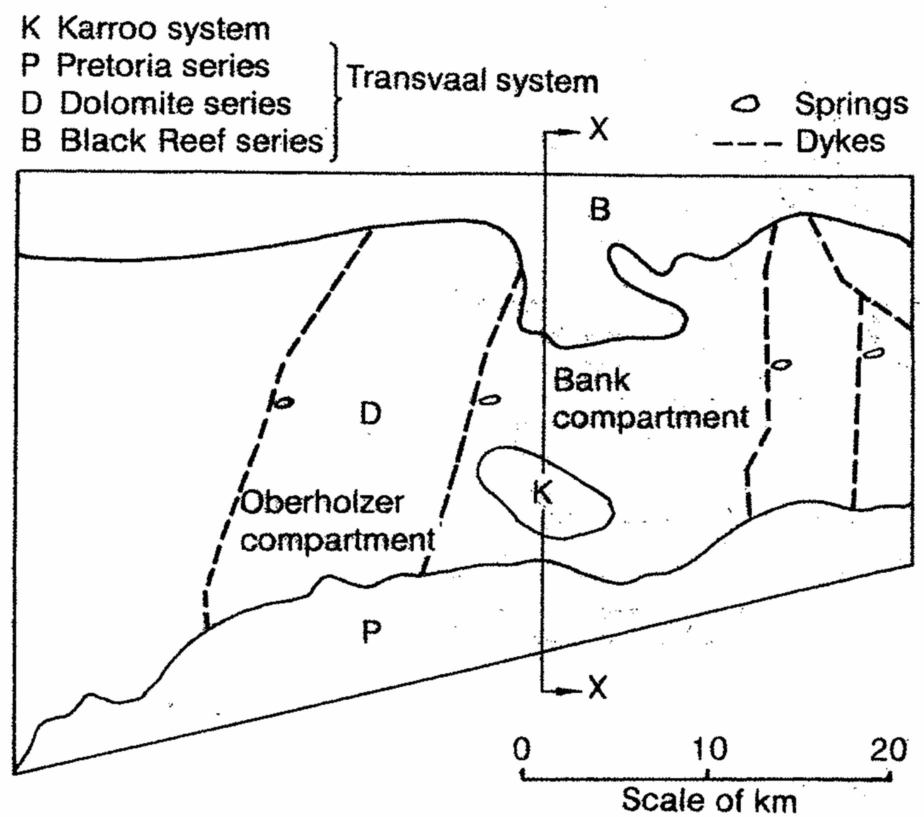

FIG. 2. Plan showing Bank and Oberholzer Compartments (After Henkel, 1982)

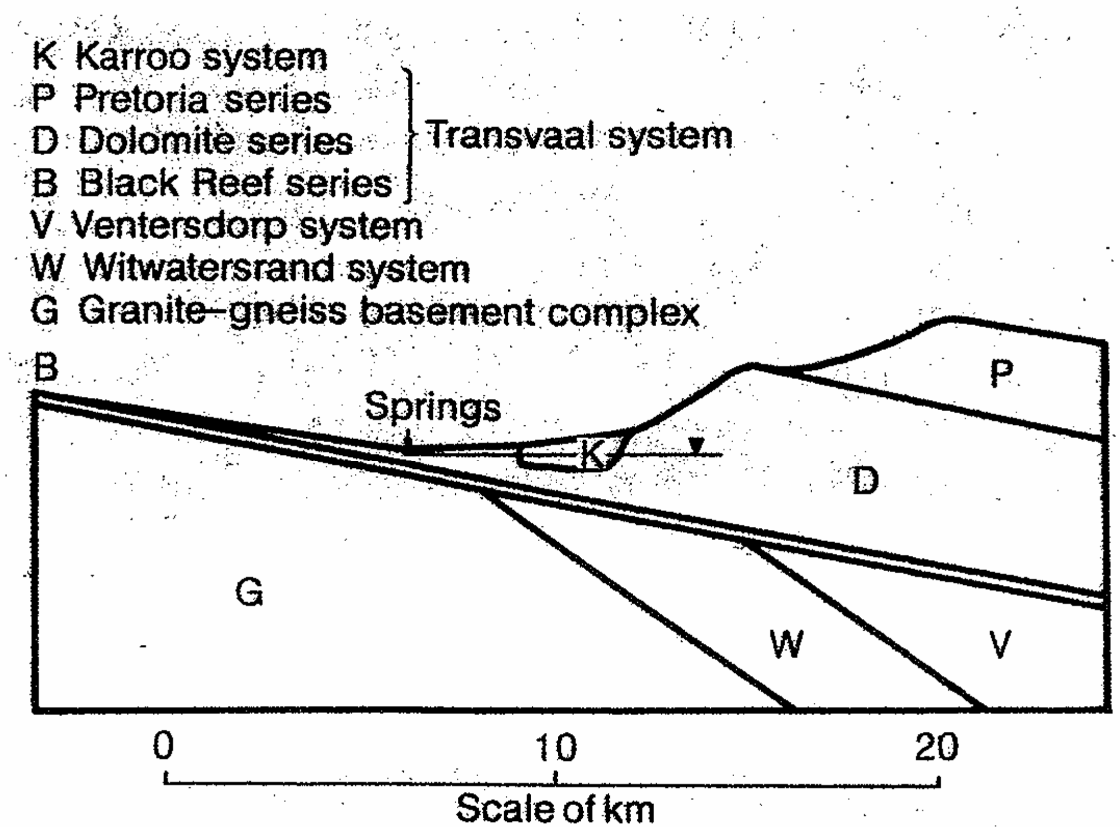

FIG. 3. Section XX through Bank Compartment (After Henkel, 1982)

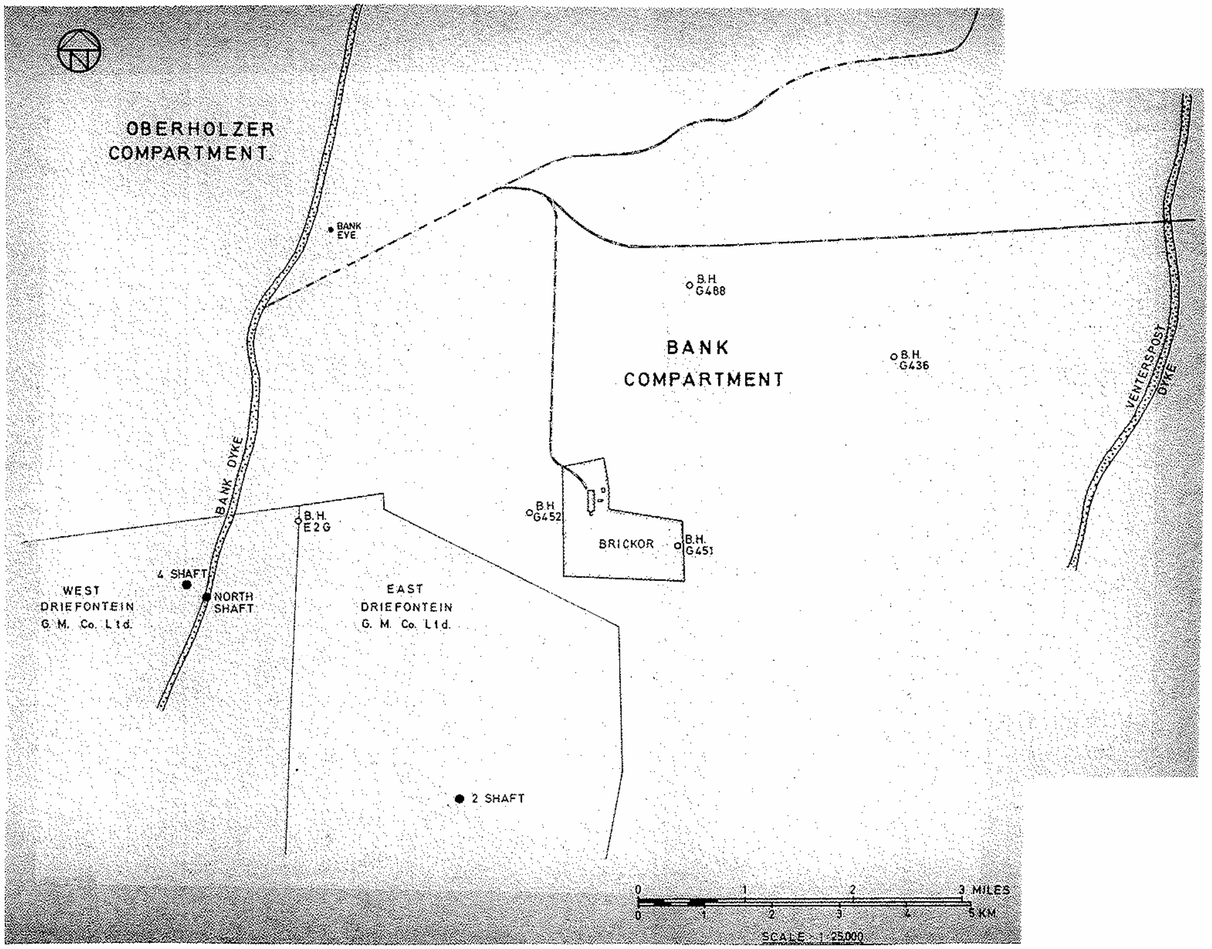

FIG. 4. Location of brickworks within Bank Compartment

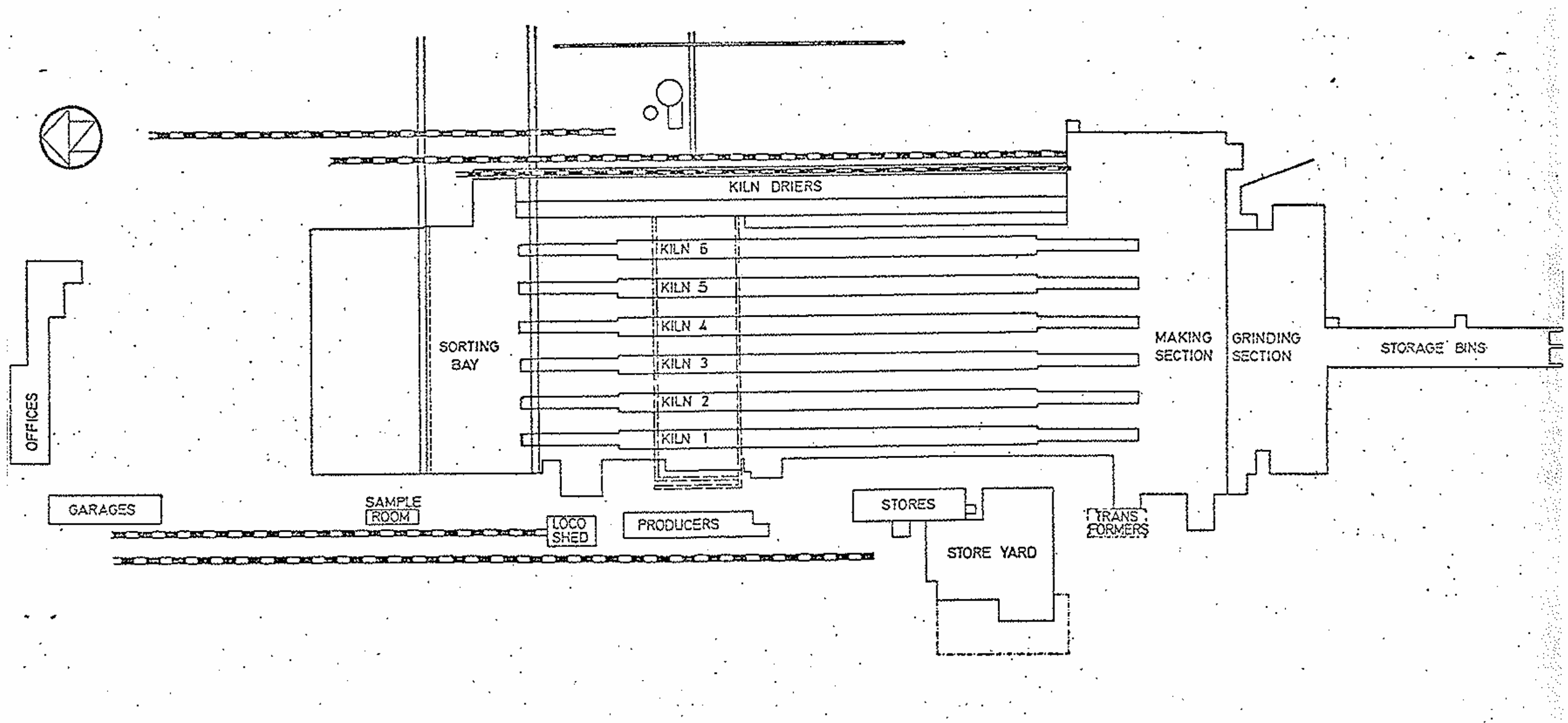

FIG. 5. Layout of tunnel kilns and driers

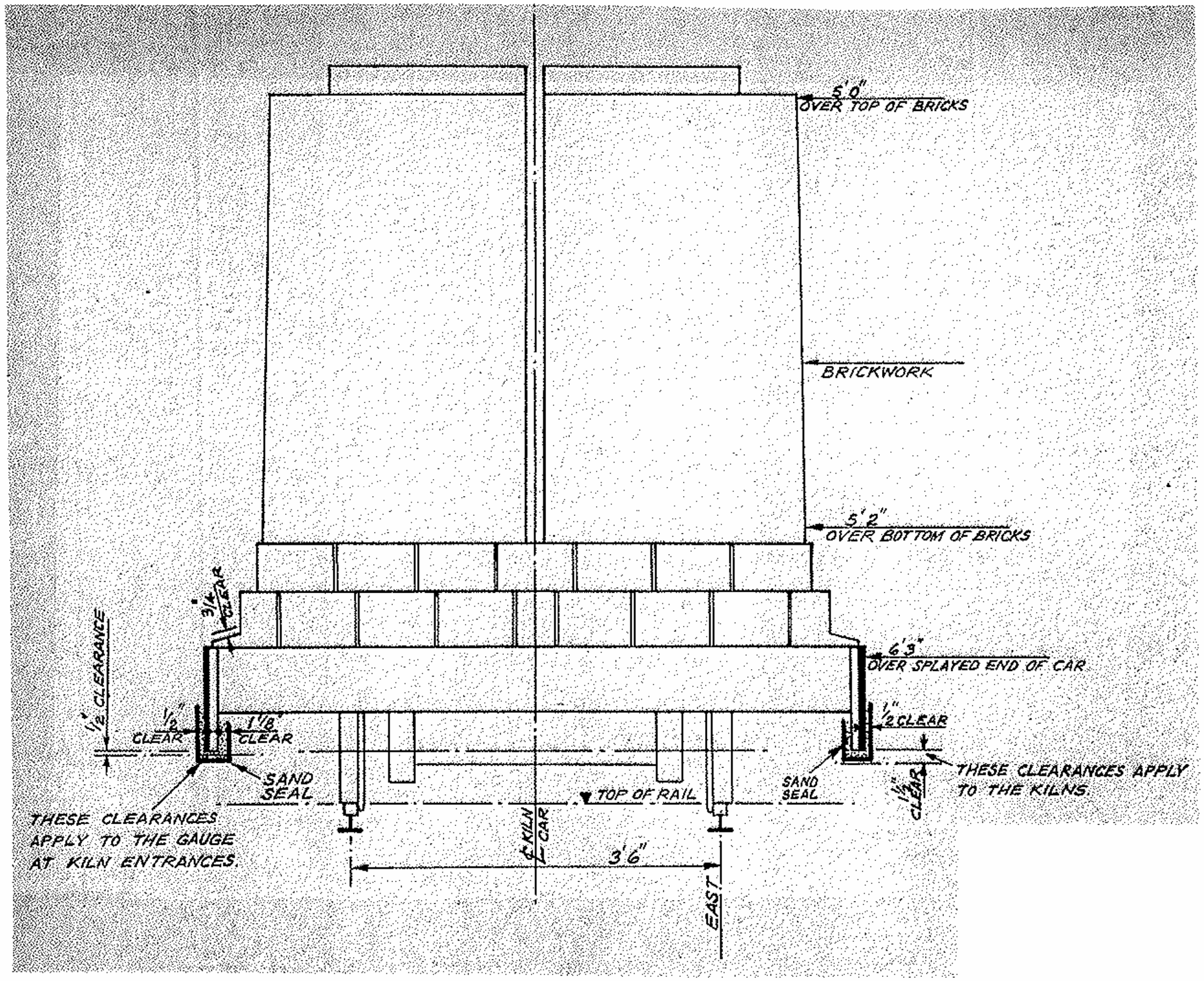

FIG. 6. Sand seals around kiln cars

29

FIG. 7. View of inside of tunnel kiln

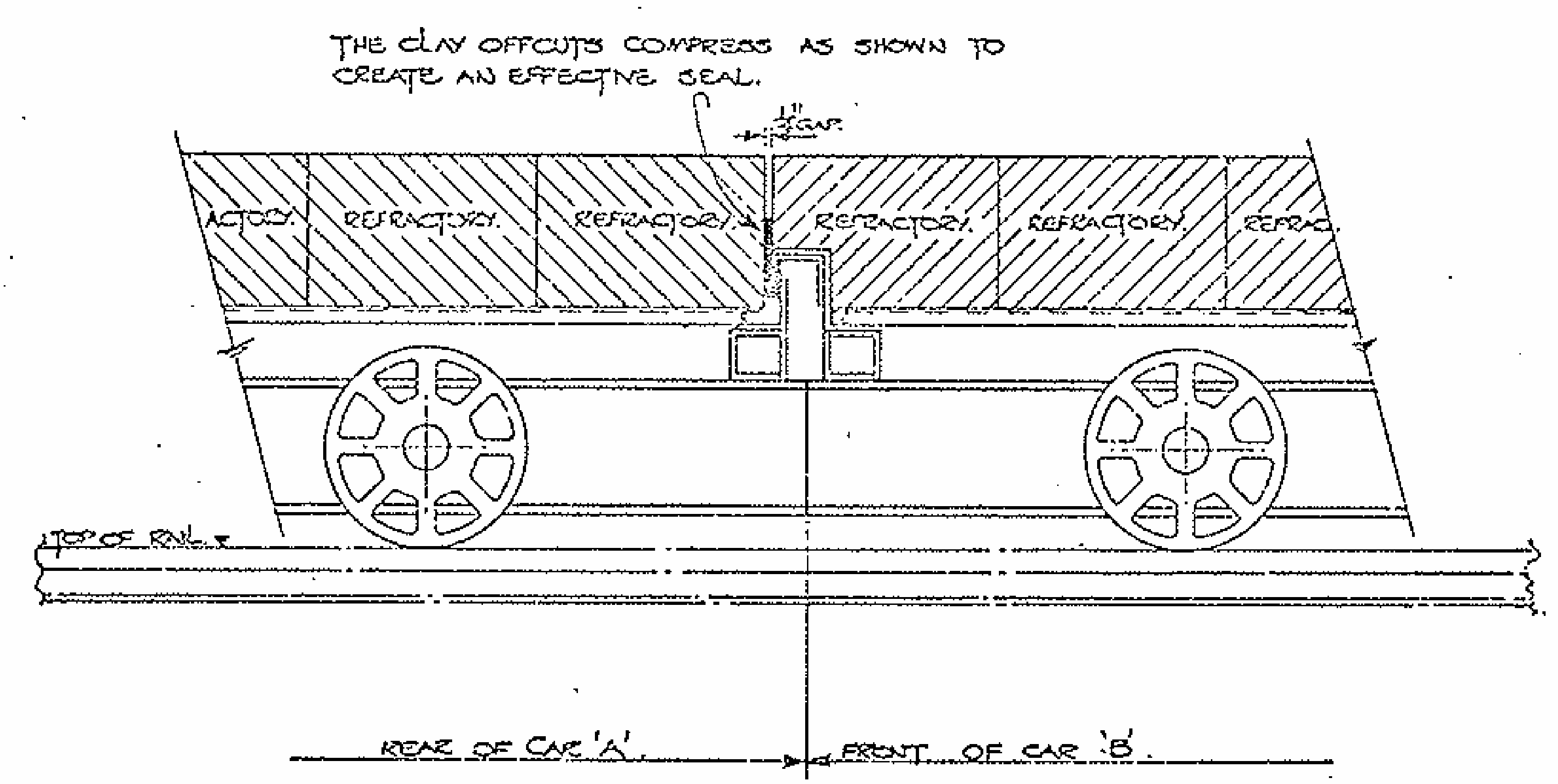

FIG. 8. Detail of clay seal between adjacent rail cars

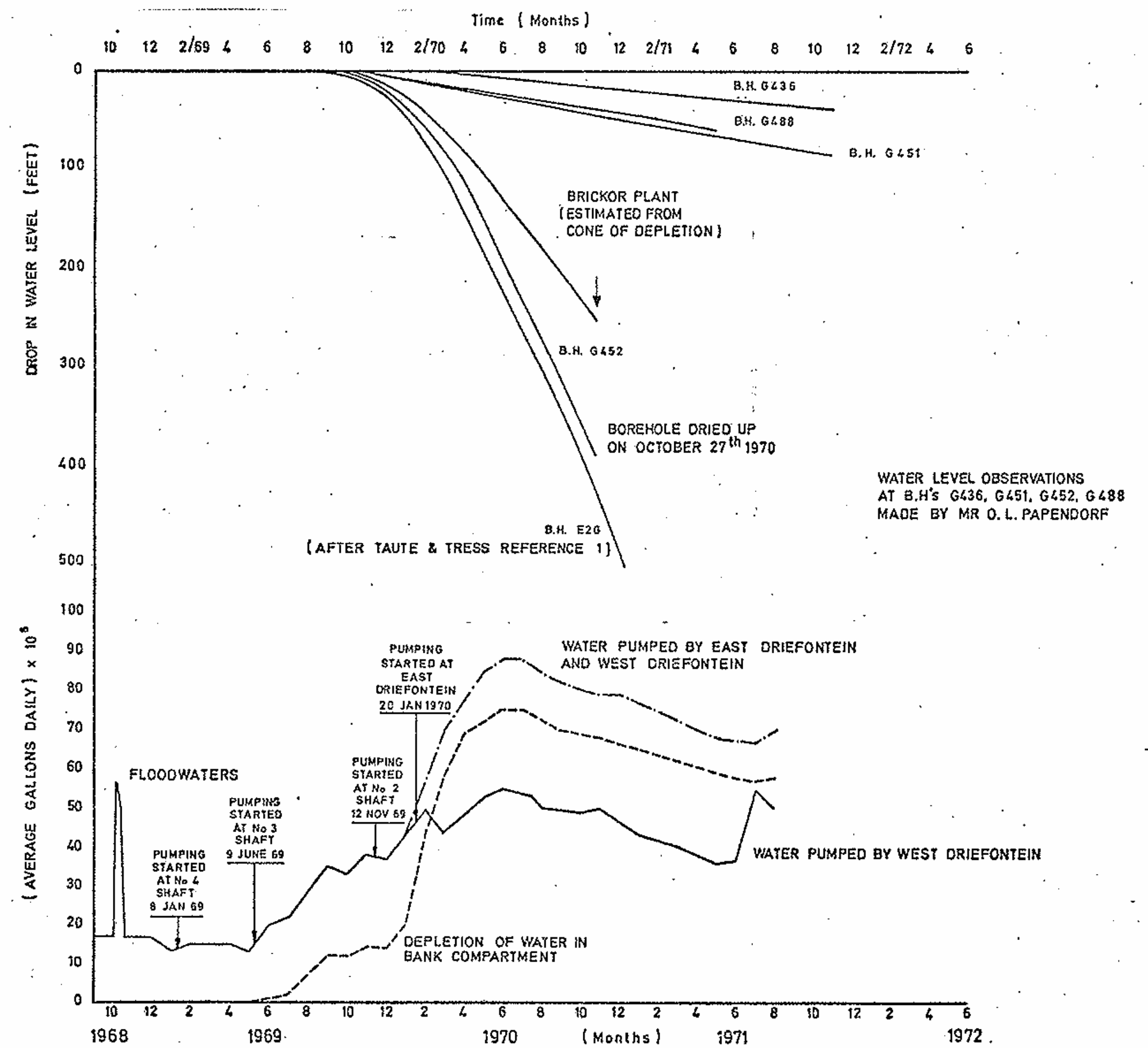

FIG. 9. Water table drop-off rates in Bank Compartment and rates of pumping from flooded mine workings

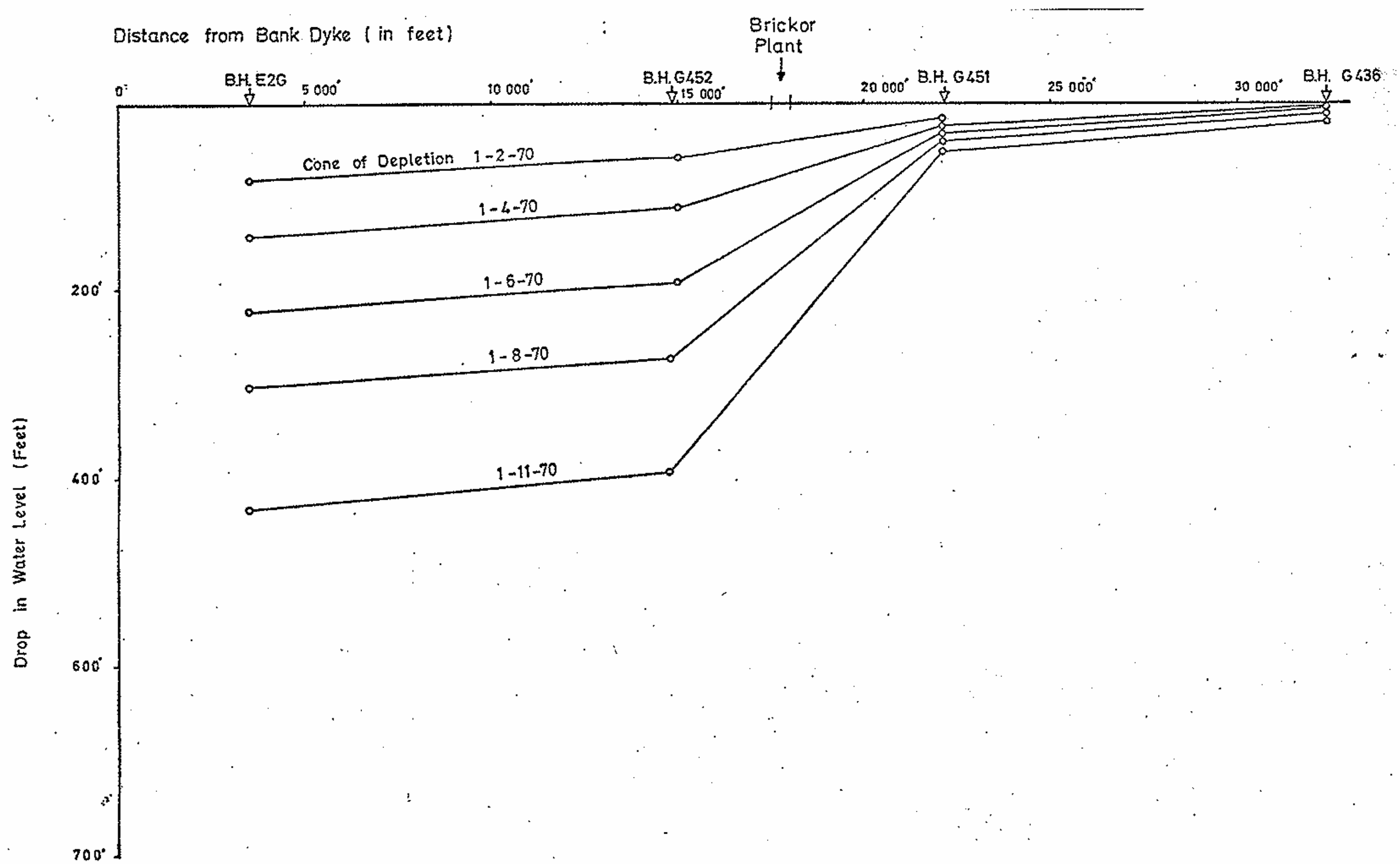

FIG. 10. Cone of depletion for Bank Compartment

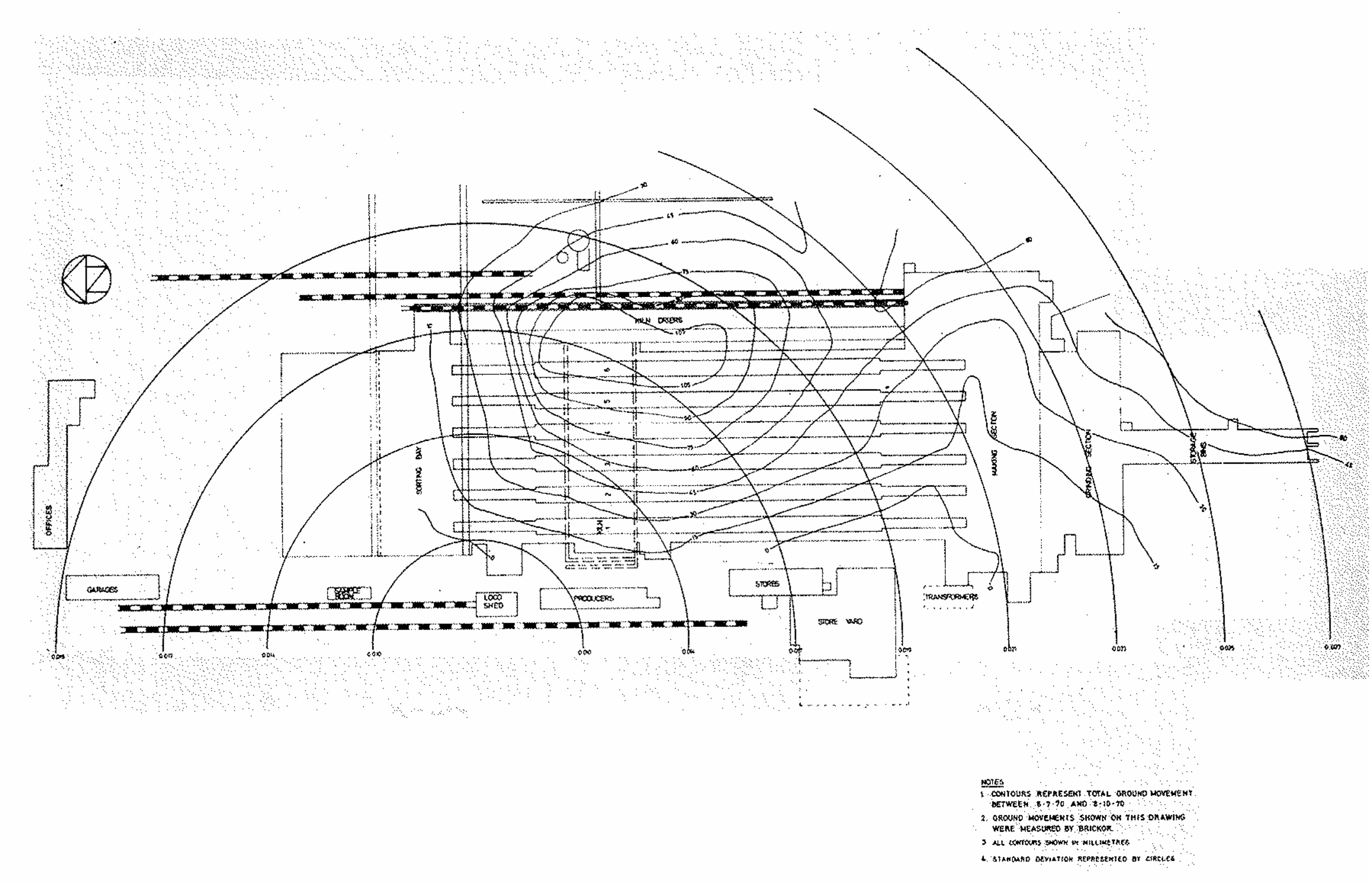

FIG. 11. Measured settlements: June – August 1970

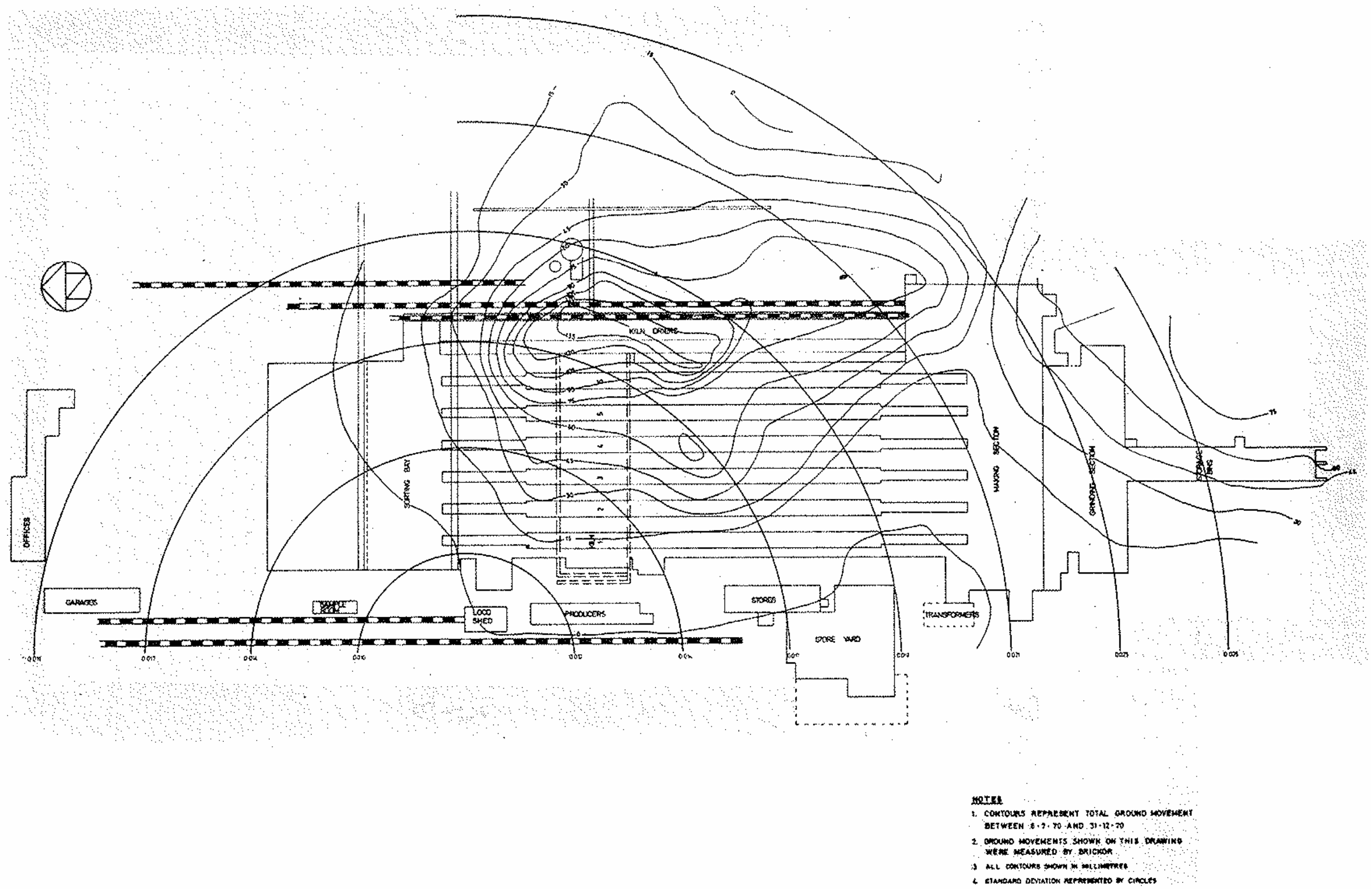

FIG. 12. Measured settlements: June – December 1970

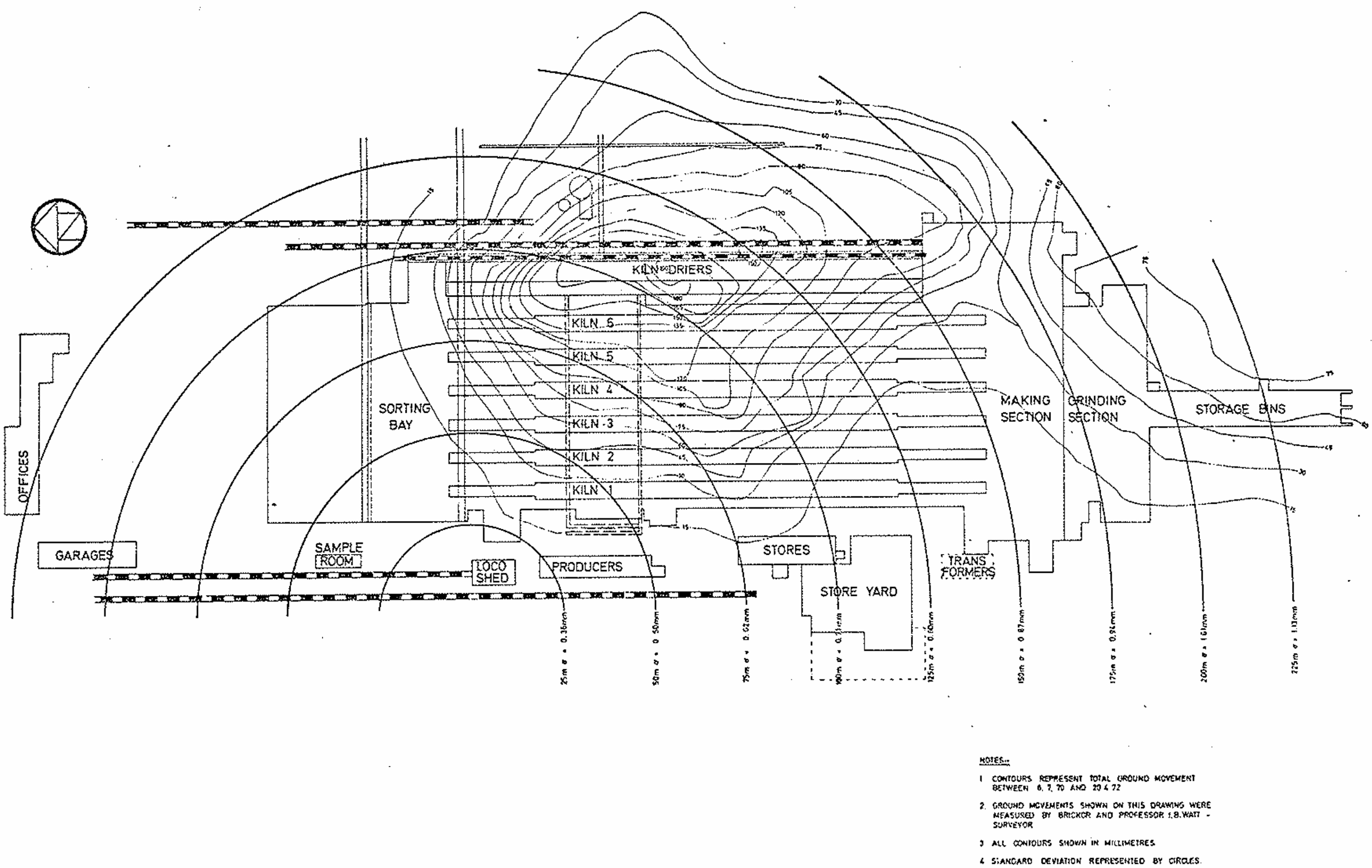

FIG. 13. Measured settlements: June 1970 – April 1972

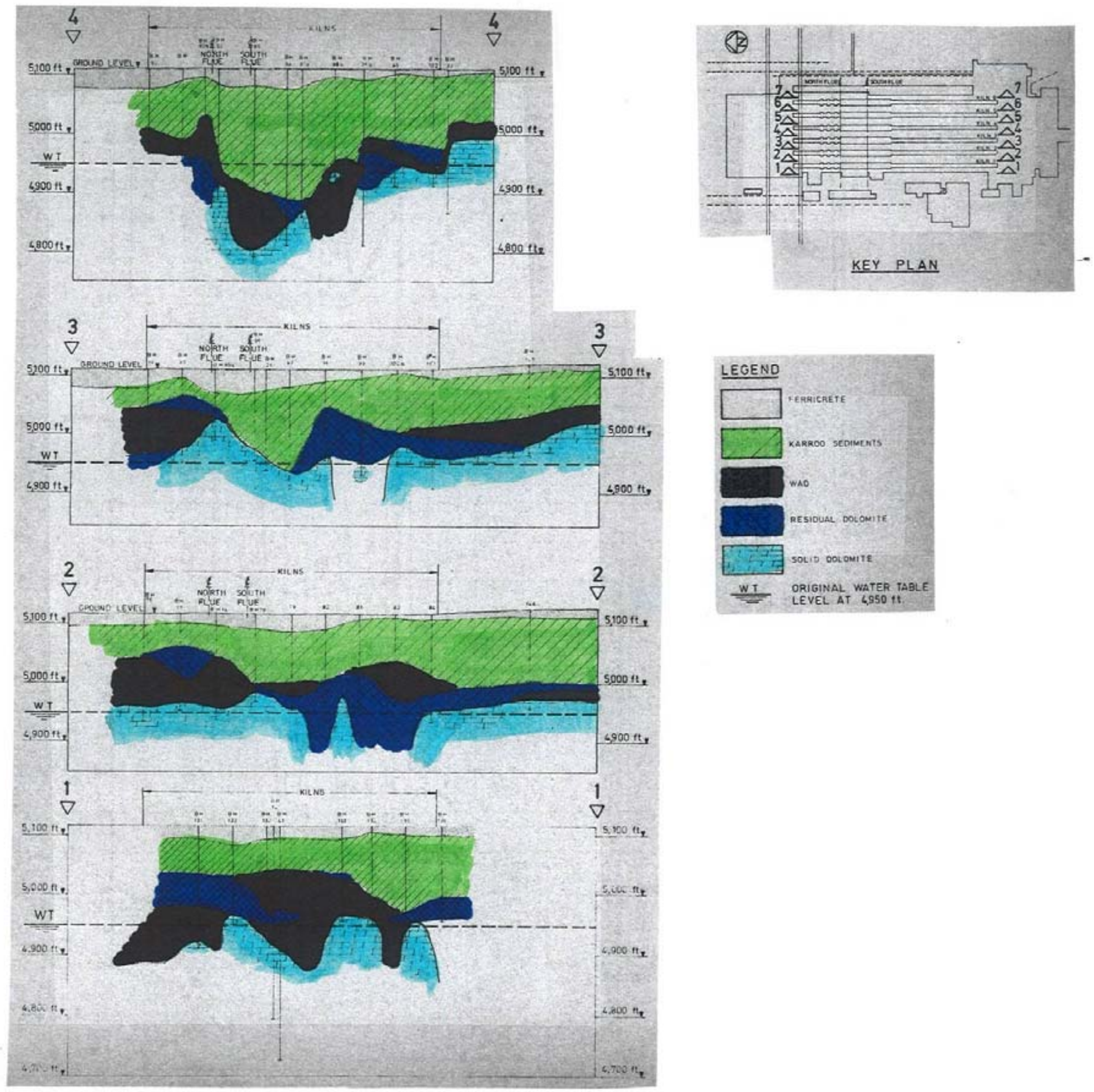

FIG. 14. Geological sections in brickworks area

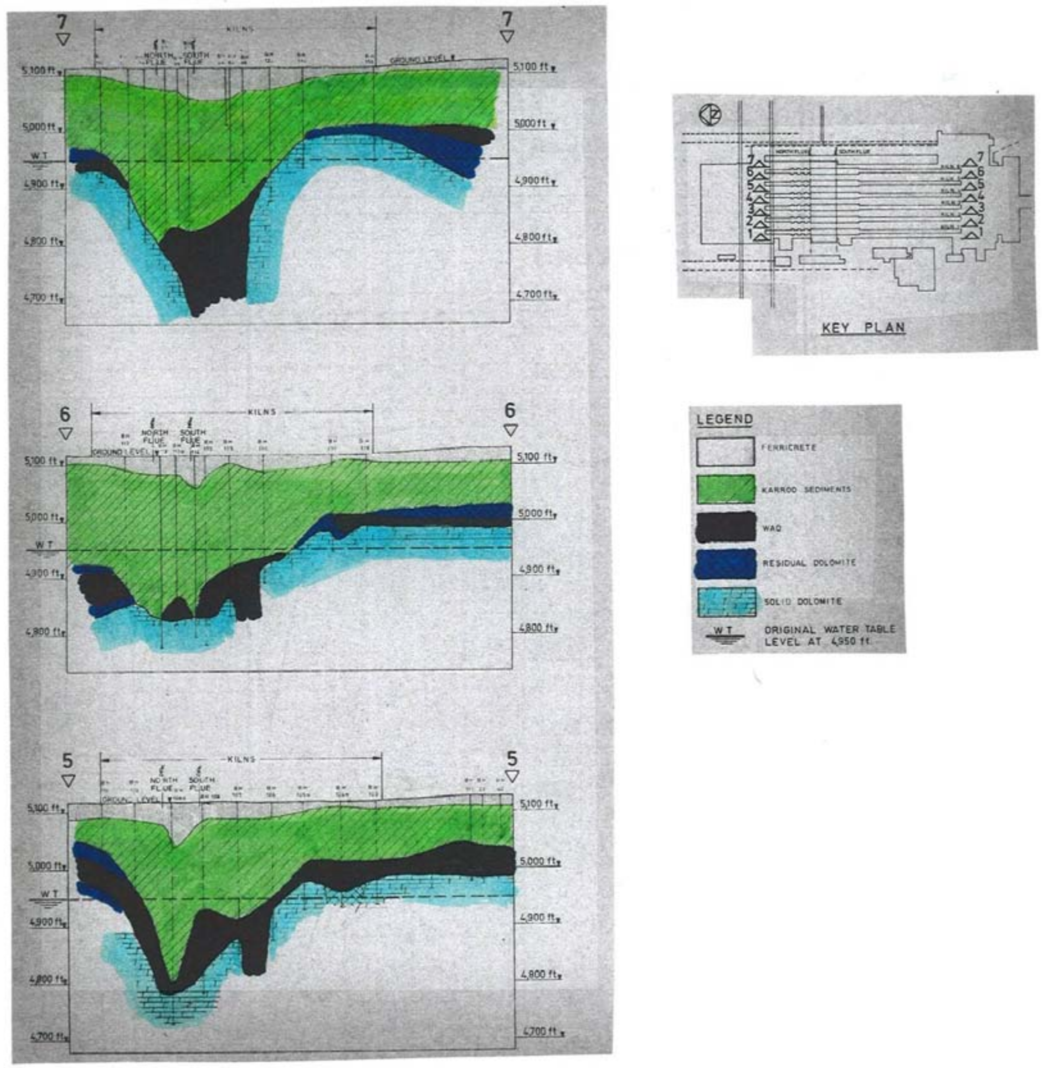

FIG. 15. Geological sections in brickworks area

FIG. 16. Oblique view of model of dolomite rockhead

Ground Penetrating Radar Test Field

J. P. Mohsen
Professor and Chair, Civil and Environmental Engineering, University of Louisville, Louisville, Kentucky, USA.

Tom Rockaway
Assistant Professor, Civil and Environmental Engineering, University of Louisville, Louisville, Kentucky, USA

Claudel NISINGIZWE.
Graduate Student, Civil and Environmental Engineering, University of Louisville, Louisville, Kentucky, USA.

Abstract:

A variety of Non-Destructive Tests (NDT) and Remote Sensing (RS) techniques have been used to identify and assess buried infrastructure without the need of excavation. The underground utility system in of an urban environment is highly congested and is comprised of various utility pipes as well as cables, and other buried features unique to each area.

While many of these NDT and RS techniques have limited success, Ground Penetrating Radar (GPR) appears to have demonstrated capabilities that will enable it to work effectively in an urban environment. Even though using the GPR and generating field data is not very difficult and can be achieved by receiving basic training, the interpretation of the data and locating the position of the utilities and identifying the types and dimensions require much more high level training and accurate interpretation of the signals and field data requires extended experience. A test field has been designed and will be constructed on the campus of the University of Louisville in order to provide training opportunity for engineers who wish to learn how to operate the GPR equipment and be able to effectively interpret the data. The test field will be used for training of personnel and for calibration of equipment.

The test field will simulate an urban intersection with buried sub-structures highlighting water, sewer, gas, and fiber optics features as well as common defects such as voids and sinkholes.

1. INTRODUCTION

While many NDT and RS methods have been unable to operate in this environment, GPR has been successful in detecting underground heterogeneities. A significant amount of progress has been achieved with respect to GPR signal interpretation but it is still difficult to interpret signals obtained from an urban environment. The complexity of the underground environment overlaps signals and increases signal noises such that key features might be obscured. Thus there is need of more work to fully apply GPR to urban environments. However, it is very difficult to gather GPR data in urban settings due to;

- Traffic consideration.
- Access from local government.
- Variety of unknown objects and conditions.
- Poorly known target locations…

In order to provide a mechanism to gather research data and to train practitioners on the GPR technique, the University of Louisville's Center for Infrastructure Research is developing a test field that models an urban intersection environment. A half-acre site has been designated for the development of this facility. Initially the test field will focus on GPR capabilities but will later serve as an exploratory field for other NDT and RS methods.

2. GPR TECHNOLOGY

GPR uses electromagnetic wave propagation and scattering. It images, locates and quantitatively identifies changes in dielectric constants in the subsurface soil.

An electromagnetic trigger pulse (A very short burst of radio-frequency energy) is generated and sent to the antenna. Then the transmitted pulse is radiated into the subsurface and reflected at interfaces with materials that posses different dielectric constants. The reflected portion of the electromagnetic signal travels back to the antenna. The portion of the pulse not reflected continues through the medium until different dielectric properties are encountered which causes further reflections. The reflected portions form a series of pulses known as waveform, the series of waveform recorded produce images. The time delay and amplitude of the waves on the image are related to the location and properties of the interfaces and subsurface structures.
.
GPR systems are basically made of a control unit, an antenna, a data cable, a battery and a survey wheel.

3. SIGNIFICANCE OF THE TEST FIELD

Two important components of a successful GPR survey are; a) calibration of the equipment for use in a specific environment and location and b) the proper interpretation of the acquired field data. A test field with known buried features and soil properties can very well serve as a training ground for both calibration of the equipment and also data interpretation. A literature search conducted within the last three years showed that three such test fields exist in the US, however, neither one is available for use by civilians and there are all located in military installations with very limited access. The test field designed for construction on the campus of the University of Louisville will be much needed facility that will allow any user of GPR equipment access for calibration of equipment and training of personnel.

This test field is designed to specifically model a common urban intersection with a congested system of underground utilities. It is intended that this field will serve as a research and testing facility for both academics and practitioners active in GPR and other NDT techniques.

4. TEST FIELD DESIGN

The University of Louisville test field has been designed and will be constructed modeling the conditions of a street intersection in an urban area.

The test field is subdivided into two distinct sections. The first section is a paved T-section with typical dimensions of an urban street. The second section is an area designated for clean targets of various types and sizes. The intent of the intersection is to provide an opportunity to assess GPR capabilities to locate subsurface utilities and the intent of the second section is to provide an orderly array of common buried infrastructure so the signals from specific materials buried at a specific depth and orientation can be explored with minimal surrounding interference.

The intersection models a T intersection. The streets will be one lane two way direction. The buried infrastructures consist of:

- gas line
- Copper fiber cables
- 24” drain pipe
- Secondary 8” drain pipes with a set drain assemblies of 6” PVC pipes
- 8” water pipe with different off takes at different locations.

Surface structures such as manhole covers are also present.

The second section is found adjacent to the T-intersection. In this section different known targets will be buried with known depths and known characteristics. Several voids will be simulated and a variation of host materials will also be included.

5. CONCLUSION

Assessing the location and conditions of buried infrastructure within an urban environment with NDT and RS techniques is not an easy endeavor. However, new GPR techniques and analysis routines properly calibrated to field conditions show significant promises for effective work within the urban environment. Compiling and cataloging GPR signals is an important step towards pattern recognition of GPR responses and will be done as part of this project.

The designed test field will help the two objectives and the catalogue of images will be continuously upgraded. This work is anticipated to be a significant resource to GPR practitioners and researchers for the development of GPR equipments and capabilities.

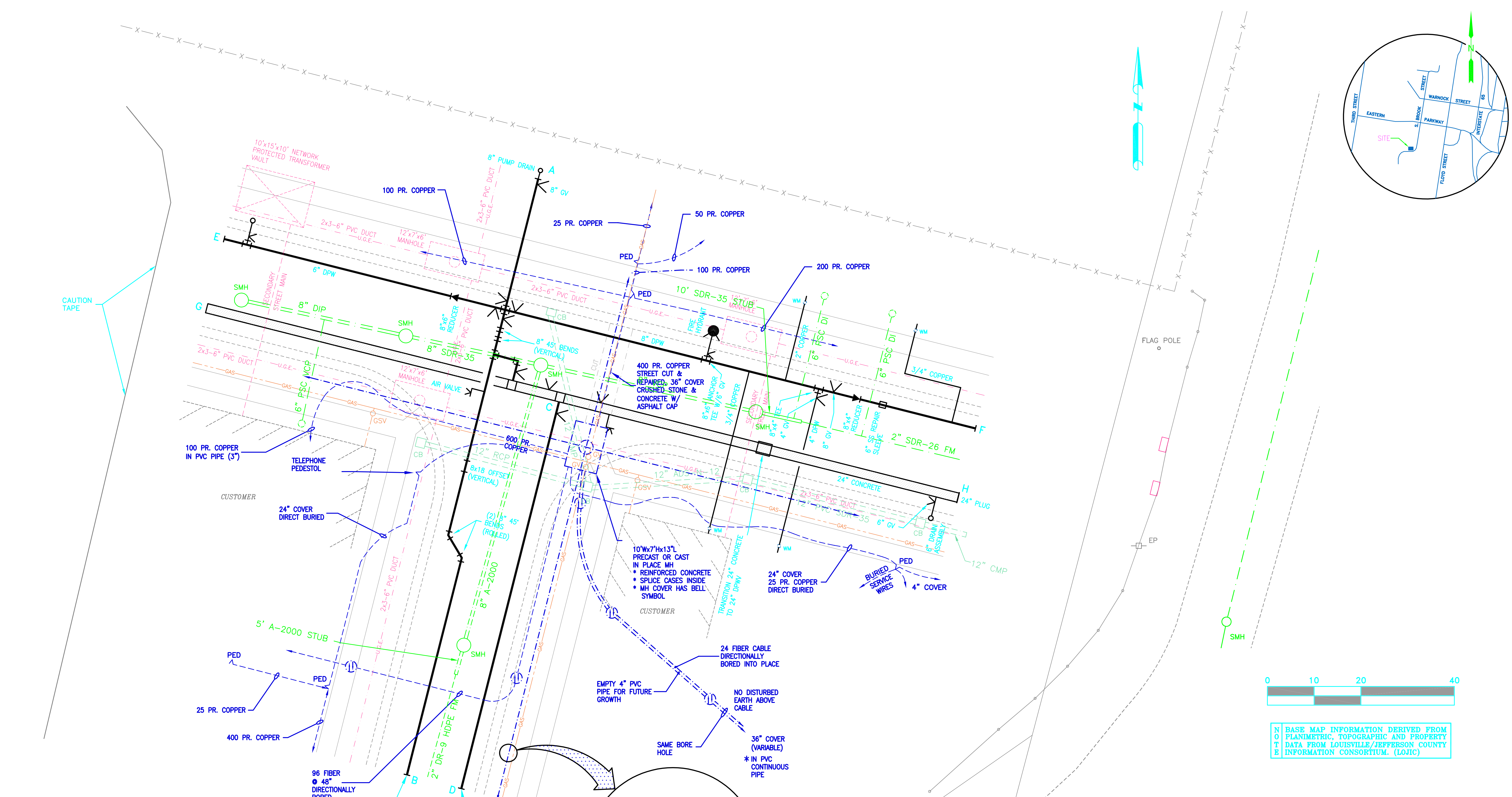

NOTE: BASE MAP INFORMATION DERIVED FROM PLANIMETRIC, TOPOGRAPHIC AND PROPERTY DATA FROM LOUISVILLE/JEFFERSON COUNTY INFORMATION CONSORTIUM. (LOJIC)

University of Louisville

LOUISVILLE WATER COMPANY

550 S. 3RD STREET • LOUISVILLE, KENTUCKY 40202 • (502) 569-3600

JOHN L. HUBER – PRESIDENT

GREGORY C. HEITZMAN – SENIOR VICE PRESIDENT/CHIEF ENGINEER

UNIVERSITY of LOUISVILLE

TEST FIELD

DATE	JULY 2006	SCALE	GRAPHIC SCALE	MAP NO.	XXXXX
DRAWN BY	XXX	CHECKED BY	XXX	ENGR.	XXX
PROJECT NUMBER	XXXXX	SHEET	1 OF 1		
TASK NUMBER	XX				

PRUR – WSMITH Z:\acad\Pipeline Design and Construction\Main Replacement Projects\2006\UofL field\ XXXXX.dwg DATE: JUL 18, 2006 TIME: 6:36 AM